A Dense Gas Model of Combined Transports and Distributions of Solutes in the Interstitium including Steric and Electrostatic Exclusion Effects, and Comparison with Experimental Data

Master of Science Thesis in Applied and Computational Mathematics

Sigrid Ravnsborg Justad

Department of Mathematics
University of Bergen

May 27, 2010

Acknowledgements

I would like to thank especially my supervisor Alf Øien for invaluable help and cooperation during the work with this thesis. I would also like to thank my co-supervisors Helge Wiig and Olav Tenstad for a constructive and including dialog.

To Rune Djurhuus, Morten Nome and Anders Thomassen, thank you for all help and feedback. Thanks to family, friends and fellow students for their support. A special thanks to my Øystein for keeping up with me and for being there all the way.

And finally, thank you Peder, for knowing just when to arrive!

Contents

List of Figures

Chapter 1

Introduction

Physiological research of the circulatory system is highly based on experimental *in vitro* and *in vivo* studies and the analysis of such. However, mathematical modeling of physiological fluid systems is regarded as an important tool for further understanding of circulatory properties. In later years there has been a need for more detailed modeling contributions to this field of research.

Interstitial flow is one field of circulatory research. The interstitium is a fluid filled space outside the cells in the body, and all transport of substances in and out of cells must pass through the interstitium. It is therefore of great interest to obtain a better understanding of this fluid flow.

The interstitial flow is hindered by structural molecules in the interstitium. The structural molecules are mainly a network of fibers which the fluid must flow through. Large substances, e.g. proteins and some therapeutic agents, are hindered to an even larger extent due to their molecular size. They are excluded from a certain fraction of the fluid volume, and thus have a lower distribution volume in the interstitium. The excluded volume will in general vary for different macromolecules, however, may be of considerable size.

The molecular size obviously affect the excluded volume for different substances. However, recent articles by Wiig et al. [1] have shown that the molecular charge may have a strong influence on the exclusion phenomenon. This recent discovery has been the motivation for the modeling in this thesis.

The object for this thesis has first been to derive a set of equations appropriate for modeling fluid flow through the interstitium. Second, a thorough study of electrostatic properties of the interstitium has been performed. The aim has been to obtain a platform for further studies of the interstitial flow, and hopefully obtain some useful benchmarks regarding the electrostatic properties.

The exclusion phenomenon is only relevant for large or charged substances. Therefore, the interstitial fluid may be regarded as *solutes* evolving in a *solvent*. The 'gas' of solutes might be quite dense, and certain *dense gas effects* may come in to force.

The study of the electrostatic properties of the interstitium concerns molecular interactions of charged molecules on a microscopic level. It has therefore been of great interest to retrieve these microscopic properties in our set of modeling equations. Thus we have derived *solute equations* on a microscopic level and used these equations to obtain solute equations on a macroscopic level. Microscopic solute equations are known as Boltzmann type equations. In this thesis certain dense gas corrections to these equations are presented, which are suggested by Øien [1]. The macroscopic solute equations are further used to obtain a compartment model for fluid flow through the interstitium. In this manner we may follow effects on a microscopic level up to, first, a macroscopic level, and second, a compartment level.

In Chapter 2 a thorough description of the interstitium and the exclusion phenomenon is given.

In Chapter 3 we describe collision frequencies in a gas on a microscopic level, that will be used in the solute equations. First collision frequencies for a rare gas is obtained, and second dense gas effects are included.

In Chapter 4 the solute equations are obtained. First a derivation of a general Boltzmann type equation is given. This equation is further used to obtain macroscopic solute equations. Secondly, to account for multicomponent gases and dense gas effects, corrections to the Boltzmann type equation, and hence the macroscopic equations, are successively given. Finally, a background solvent is introduced to the set of macroscopic equations.

In Chapter 5 the set of macroscopic equations obtained in Chapter 4 are used to derive a compartment model for fluid flow through the interstitium. The model is inspired by a similar Starling model in an article by Bert et al. [2].

In Chapter 6 basic electrostatic theory is reviewed. Solutions for the electrostatic potential in a spherical geometry are obtained, as well as an expression for the electrostatic potential energy on a microscopic level. Moreover, electrostatic shielding and dipole effects are discussed.

In Chapter 7 the expression for the potential energy obtained in Chapter 6 is further applied to a study of the electrostatic effects in the interstitium. In addition, some results and observations are presented and compared to experimental findings.

In Chapter 8 the set of macroscopic equations obtained in Chapter 4, and further the compartment model obtained in Chapter 5, are expanded to also include some charge effects on the macroscopic level.

[1] Alf Øien, Professor emeritus, Department of Mathematics, University of Bergen, Norway. Private communication

Chapter 2

Physiological Background - The Interstitium

The interstitium is a fluid filled space which surrounds all the cells in the body. It holds most of the extracellular fluid, and all substances going in and out of the cells must transport through the interstitium. It is therefore important to understand *which* properties that affect the fluid flow, and *how* it is affected. Flow-affecting properties of the interstitium has been the topic of several scientific papers, and is still an active field of research. In this chapter a basic description of the interstitium is given.

2.1 Physiological function

Arteries transport water, salts and nutrients from the heart to the tissue. The arteries divide into thinner vessels, arterioles, and in the thinnest vessels (capillaries) the substances can leave the circulation. Selected substances leave the capillaries through the capillary wall and enter the interstitium, see Figure 2.1. The transport of substances into the interstitium is *selective*. This means that the capillary wall permits a high rate of fluid filtration while at the same time it restricts the passage of macromolecules [3].

In the interstitium there is an exchange of nutrients and waste products from the cells. Water, salts and waste products are reabsorbed by the capillaries and by small veins called venules, and thus returned to the circulation. Venules drain to larger veins that return blood to the heart. Under normal conditions there is a net filtration of fluid from the capillaries, and this excess fluid in the interstitium is drained back to the circulation by the lymphatic system. Lymphatic capillaries are dead-ends of thin lymphatic vessels, and they drain into collecting lymphatics that eventually drain into lymphatic trunks.

The basic structure of the interstitium is similar in all tissues. However, the composition of structural elements varies between tissues. In the following section the basic structure of the interstitium is reviewed briefly.

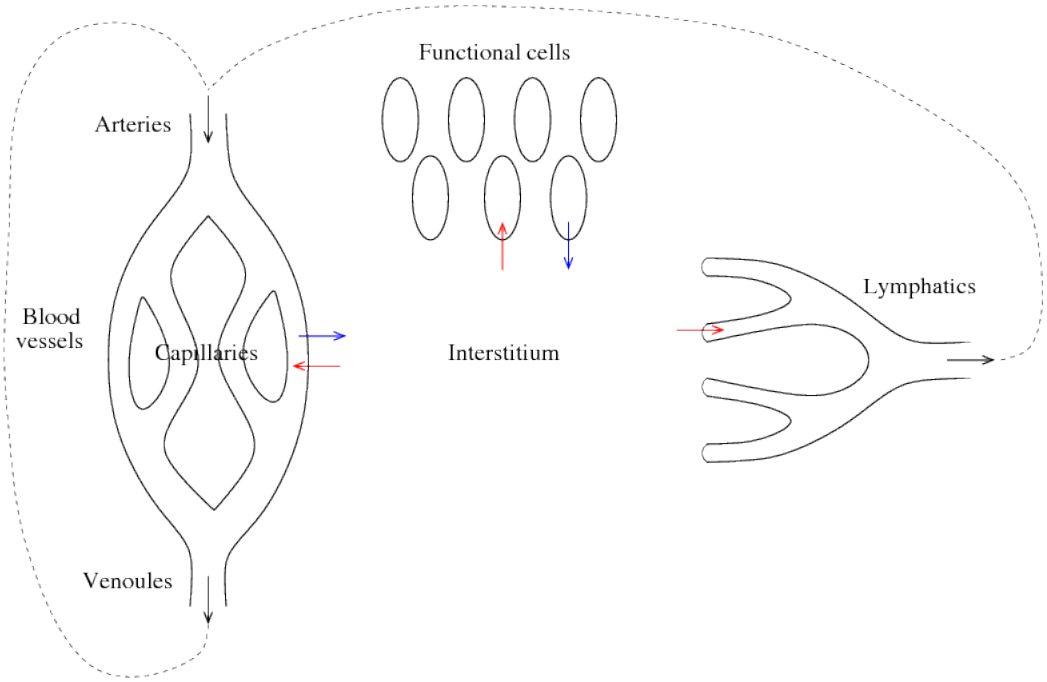

Figure 2.1: Arteries transport water, salts and nutrients to the tissue. There is an exchange of fluid and nutrients in the thinnest vessels, called capillaries, to the interstitium. In the interstitium there is an exchange of fluid, nutrients and waste products from tissue cells. This implies that all substances entering (or leaving) the cells must pass through the interstitium. The net filtrate in the interstitium is drained back to the circulation by the lymphatic system.

2.2 Structure

The interstitium can roughly be split up into two elements; fluid and the structural matrix. The basic structure of the interstitial matrix, also known as the extracellular matrix or ECM, is a network of large protein fibers (collagens). In between the fibers there are large sugar polymers (glycosaminoglycans) which are entrapped in the network. For an illustration see Figure 2.3.

2.2.1 Collagens

Long chains of amino acids are called polypeptides, and they differ by the sequence and number of amino acids in the chain. A collagen molecule is a protein which consists of three long polypeptide chains coiled together in a triple helix [4]. While some polypeptides, called globular proteins, wind up to form spherical structures, fibrous proteins, such as collagens, do not. Instead, several collagen molecules are packed together to form thin

collagen threads, called *fibrils*. These threads can subsequently assemble to form even larger structures; collagen *fibers*. The size of collagen fibers varies between tissues. E.g. in tendons, which connect muscles to bone, the diameter of collagen fibers varies from 30 to 300 nm [1].

The collagen fibers organize in a three dimensional network in the interstitium, and is the major structural element of the interstitial matrix. They, in some sense, span out and support the interstitial space. In this manner they create a space between the fibers which the fluid can flow through.

2.2.2 Glycosaminoglycans

This section is based on [5].

Glycosaminoglycans, or GAGs, are long, chained molecules made up of repeating sugar units that contain amino groups. In the same manner as for polypeptides, the different types of glycosaminoglycans are characterized by the type and number of sugar units in the chains. The sugar units carry carboxylic acid groups that will dissociate into a proton (H^+) and a negatively charged carboxylate group as the pH increases. At physiological pH all of these groups will be negatively charged resulting in the characteristic high negative charge of GAG molecules in the interstitium.

Due to the negatively charged groups (anionic sites) most glycosaminoglycans also bind covalently to protein. The composition of a protein backbone and glycosaminoglycans is called proteoglycan. Subsequently, proteoglycans can form even larger structures where several proteoglycans bind to one specific glycosaminoglycan; hyaluronan.

Hyaluronan is a much longer sugar chain than other glycosaminoglycans. While most glycosaminoglycans are built up of less than 100 sugar units, each hyaluronan molecule may contain around 100000 units. Hyaluronans do not bind covalently to proteins, but exist in the interstitium as single chains or in large aggregates together with proteoglycans as described above. Single hyaluronans have the quaternary structure of a random coil. Therefore, the molecule will occupy a domain that is much larger than the molecule itself [6]. Hyaluronan constitutes a major part of glycosaminoglycans, at least in some tissues [1].

Since glycosaminoglycans are large coils (hyaluronans) or bottle brush-like (proteoglycans) molecules they are entrapped, and hence immobilized, in the collagen network. Together they constitute the main parts of the interstitial matrix.

2.2.3 Fluid

In between the collagen fibers and GAGs there is a fluid filled space. Interstitial fluid consists mainly of water and small ions, e.g. sodium Na^+, chloride Cl^-, potassium K^+ and calcium Ca^{2+}. Ionic density is a measure of the amount of ions present in the fluid. At normal physiological conditions the ionic density in interstitial fluid is 150 mM/L. The pH in the fluid at normal conditions is 7.4, and is referred to as *physiological pH*.

In the fluid there are also several types of proteins derived from blood plasma. They vary in both size and shape, and in general these properties are well defined. E.g. globular proteins have a well defined radius.

The fluid 'fills up' and flow through all the gaps in the matrix. Thus, the interstitial matrix constitute a great hindrance for fluid flow through the interstitium. An interesting point of view is therefore to which extent the flow of different proteins is hindered by the interstitial matrix.

2.3 Excluded volume

The interstitial matrix restricts the available fluid volume or distribution volume for the proteins. Since proteins are large molecules, their center can not come closer to the matrix elements than their radius, i.e. for globular proteins. This is called *steric exclusion*.

Due to the negatively charged elements of the matrix, particularly glycosaminoglycans, recent articles have concluded that negatively charged proteins are excluded to an even larger extent, see [1] and references therein. This phenomenon is called *electrostatic exclusion*, or charge exclusion. In Figure 2.2 an illustration of the two exclusion phenomena is given.

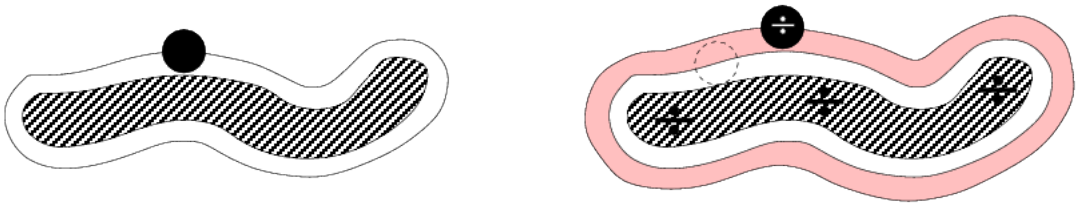

(a) Steric exclusion **(b)** Electrostatic exclusion

Figure 2.2: Proteins are excluded from a certain fraction (white) of the volume surrounding structural matrix components (shaded) due to their size, as shown in 2.2a. This is called *Steric exclusion*. Additional exclusion (pink) due to protein charge is called *electrostatic exclusion*, see 2.2b.

The exclusion phenomenon is only relevant for large molecules, such as proteins. Small molecules, ions and water are assumed to distribute in the entire extracellular fluid volume. Therefore the total *excluded volume* can be measured by comparing the distribution volume for a protein to the distribution volume for another, much smaller, molecule that distributes in the entire extracellular fluid volume. In Figure 2.3 an illustration of the interstitium and the exclusion phenomenon is given. In the figure the *available volume* for a protein is indicated, which is the total fluid volume minus the excluded volume.

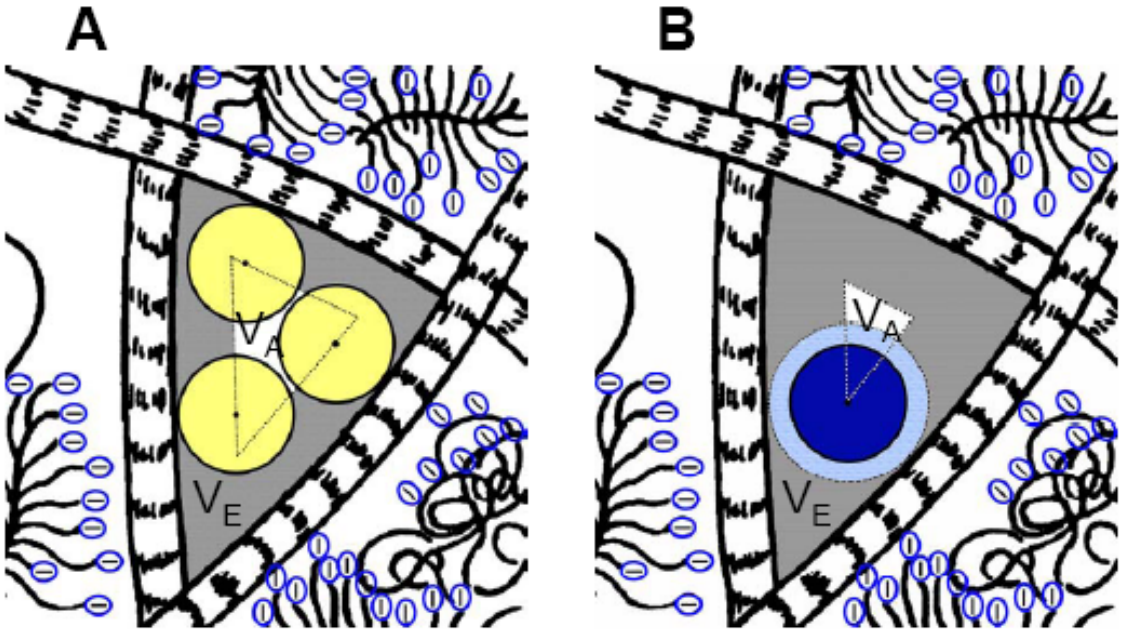

Figure 2.3: Macromolecules (yellow and dark blue) are excluded from a certain fraction of the total interstitial fluid volume due to their molecular size. Glycosaminoglycans have a high negative charge at physiological pH. Thus, negatively charged macromolecules may be excluded to an even larger extent. The available volume V_A, which is the total fluid volume minus the excluded volume, is indicated in both Figures. During physiological experiments negatively charged macromolecules appear to have a larger *effective* radius than their molecular radius, which is indicated in Figure B (light blue). The Figure is reproduced from the article by Wiig et al. [1].

The amount of excluded volume is clearly dependent on the surface-to-volume ratio. Proteins can not be excluded from a surface that is not in contact with the fluid. The total excluded volume around thin collagen fibrils is larger than if all the fibrils were packed together in a bundle. Therefore, the exclusion effect of collagen molecules is less than the exclusion effect of GAG molecules. However, the amount of collagen in the interstitium is large compared to the amount of GAGs, and both exclusion effects must be accounted for [7].

2.4 Drug related motivation for studying exclusion effects

The exclusion phenomenon has been studied extensively, and collagens have been assumed to account for a major part of the exclusion effect. However, more recently, the electrostatic exclusion effect has been given a larger role. It has been shown that the negatively charged elements of the matrix, particularly glycosaminoglycans, give a significant contribution to

the excluded volume for negatively charged proteins [1].

The interstitium in tumor tissues represents a major barrier to drug delivery. In addition some types of tumors contain an increased amount of glycosaminoglycans [1]. According to recent results this may imply a significantly increased excluded volume, which again may affect the drug uptake in tumors. It is therefore of great interest to study the electrostatic exclusion effect thoroughly.

Chapter 3

Collision Frequencies

Particles in a gas constantly collide with each other. The average number of collisions per unit time and particle is called the *collision frequency*. During each collision there is a transfer of molecular properties, i.e. energy and momentum, between the two colliding particles. The collision frequency is thus a 'measure' of the molecular transfer in a gas, and thus is an important quantity in gas kinetics.

In this chapter we will first derive a simple expression for the collision frequencies in a gas. Furthermore, we make necessary corrections for an increased desity of the gas, in accordance with theory by Chapman and Cowling [8]. The collision frequencies derived in this chapter enter into the solute equations to be derived in Chapter 4.

3.1 Collision frequency - a first approach

For simplicity we consider a gas consisting of rigid spherical molecules, i.e. billiard ball-like particles. We consider a gas consisting of two types of particles; 1-particles and larger 2-particles. For a gas consisting of different types of particles, there are several collision frequencies. In this section we derive an expression for the collision frequency for $1 \rightarrow 2$ collisions. The collision frequencies for other types of collisions are derived in a similar manner.

We let τ represent the average time between two successive collisions a 1-particle undergo with 2-particles in the gas. It follows that the collision frequency is given by

$$\nu_c = \frac{1}{\tau} \quad .$$

The average length a particle travels between two successive collisions is called the *mean free path*. In a rarefied gas the mean free path is much greater than the size of the particles. The volume of all the molecules in the gas is negligible as compared to the total volume of the gas. Thus, one may assume that the volume available for the particles to move in between collisions, is approximately equal to the total volume, and thus their size is negligible. It is therefore sufficient to consider a point-like 1-particle interacting with a larger 2-particle, see Figure 3.1.

Figure 3.1: A point-like particle (blue) interacts with a larger particle (red). If τ is the average time between two collisions, and $\overline{v}$ the velocity, then $\overline{v} \cdot \tau$ is the average distance a particle travels between two collisions. It is assumed that there is approximately one large particle inside the volume $\pi\left(\frac{d_2}{2}\right)^2 \overline{v}\tau$, indicated in the Figure.
d_2 = diameter of 2-particle.

The point-like particle approaches the 2-particle with velocity $\overline{v}$, which is assumed to be the average velocity of all the 1-particles in the gas. It follows that the mean free path is equal to $\overline{v}\tau$. One may assume that there is approximately one large 2-particle inside the volume $\pi\left(\frac{d_2}{2}\right)^2 \overline{v}\tau$. This is the volume of a cylinder with bottom equal the crossection of the 2-sphere, called the collisional crossection, and height equal to the mean free path, see Figure 3.1. This implies that, if n_2 is the molecular density of the larger particle, we have:

$$\pi\left(\frac{d_2}{2}\right)^2 \overline{v}\tau n_2 \approx 1 \qquad \Longrightarrow \qquad \nu_{1\to 2} = \frac{1}{\tau} \approx \pi\left(\frac{d_2}{2}\right)^2 \overline{v} n_2 \quad .$$

Thus we have the following expression for the collision frequency in a rarefied gas:

$$\nu_{1\to 2} = \pi\left(\frac{d_2}{2}\right)^2 \overline{v} n_2 \quad . \tag{3.1}$$

3.2 Some dense gas effects

As the density of a gas increases, the molecules account for a fraction of the total volume which is no longer negligible. The collision frequency (3.1) was derived assuming that the available volume for a 1-particle to move in is approximately equal to the total volume. Thus, corrections to the first approach collision frequency is needed. In this section successive corrections are introduced as the density of the gas increases.

The first correction necessary for dense gases is an increase of the collisional crossection. The particles can no longer be considered point-like. It follows that the collision frequency (3.1) is corrected to

$$\nu_{1\to 2} = \pi \left(\frac{d_2 + d_1}{2} \right)^2 \bar{v} n_2 \quad ,$$

where the molecular size of both particle types, d_2 and d_1, are included.

For a collision to take place, the center of the 1-particle must lie on a sphere encircling the 2-particle with radius equal to the sum of the two different particle radii, $\frac{d_2+d_1}{2}$, see Figure 3.2. This sphere is called the *associated sphere of influence* for a $1 \to 2$ collision. During

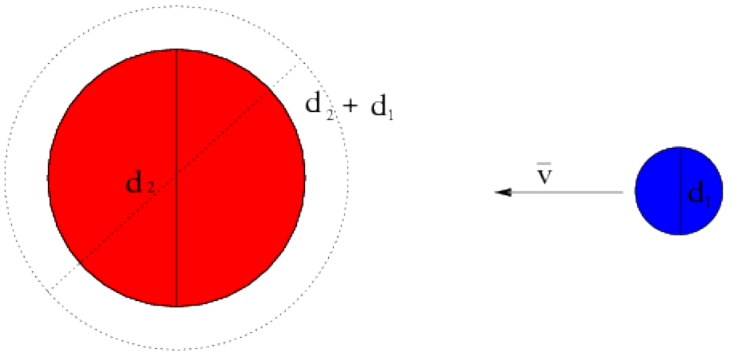

Figure 3.2: Two particles with diameter d_2 (red) and d_1 (blue) interact in a dense gas. The *associated sphere of influence* is the sphere encircling the 2-particle with radius equal to the sum of the particle radii. During a collision the center of the incoming particle must lie on the associated sphere of influence.

a collision with the 2-particle, the center of the 1-particle can never lie on the associated sphere of influence for any other collision. Thus, the 1-particle has a reduced volume to move in, which needs to be accounted for as the density of the gas increases. It is assumed that, during a collision, the volume in which the center of the incoming 1-particle are unable to move in is approximately equal to the volume of all the spheres of influence, associated with $1 \to 2$ collisions, in the gas[1]. It follows that the *available unit volume* for a 1-particle is

$$V_{AV} = 1 - \frac{4\pi}{3} \left(\frac{d_2 + d_1}{2} \right)^3 n_2 \quad ,$$

[1]See remark at the end of this chapter.

where n_2 is the density of 2-particles. This leads to an increased probability of molecular collision, and hence an increased collision frequency, by the factor $\frac{1}{V_{AV}}$ [8]. The resulting collision frequency is then found to be

$$\nu_{1\to 2} = \pi\left(\frac{d_2+d_1}{2}\right)^2 n_2\overline{v}\frac{1}{1-\frac{4\pi}{3}\left(\frac{d_2+d_1}{2}\right)^3 n_2} \quad .$$

If the density of the gas is further increased, we also need to take into account multiple encounters. One may no longer assume that collisions take place undisturbed. Additional particles might partly block the associated sphere of influence for $1 \to 2$ collisions. This effect is called collisional *shielding*. The disturbing particle might both be another 2-particle or 1-particle, however, for generality we assume that it is a 3-particle with diameter d_3.

The associated sphere of influence for a $1 \to 3$ collision covers a part S of the associated sphere of influence for a $1 \to 2$ collision. Thus, the 1-particle is unable to collide with the 2-particle in such a way that its center lies on S, see Figure 3.3. The disturbing 3-particle is placed at position x relative to the center of the 2-particle.

The surface cap S of the associated sphere, which the 3-particle covers, has an area of

$$\text{Area}(S) = 2\pi Rh = 2\pi R(R - \frac{R^2 - r^2 + x^2}{2x}) \quad , \tag{3.2}$$

where h is the height of the surface cap, $R = \frac{d_2+d_1}{2}$ and $r = \frac{d_3+d_1}{2}$, see Figure 3.4. The position for the center of the 3-particle, x, may vary like $\frac{d_2+d_3}{2} \leq x \leq \frac{d_2+d_3}{2} + d_1$. The spherical shell of thickness $\mathrm{d}x$, indicated in Figure 3.3, has an approximated volume of $4\pi x^2\,\mathrm{d}x$. Thus it contains a probable number of $4\pi x^2 n_3\,\mathrm{d}x$ 3-particles, where n_3 is the molecular density of 3-particles. We are able to obtain an expression for the fraction of the associated sphere of influence for a $1 \to 2$ collision probably shielded by a 3-particle. This fraction is called the *Total Shielded Surface* or TSS, and is, in accordance with [8], given by

$$\text{TSS} = \int_{\frac{d_2+d_3}{2}}^{\frac{d_2+d_3}{2}+d_1} \text{Area}(S)\cdot 4\pi x^2 n_3\,\mathrm{d}x \quad .$$

Area(S) is here given by Equation (3.2). If the integration is carried out we obtain the following result for the Total Shielded Surface:

$$\text{TSS}_{1\to 2}(d_3, n_3) = \pi^2 n_3\left(\frac{1}{6}d_2^2d_1^3 + \frac{1}{2}d_2^2d_1^2d_3 + \frac{1}{3}d_2d_1^4 + d_2d_1^3d_3 + \frac{1}{2}d_2d_1^2d_3^2 + \frac{1}{6}d_1^5 + \frac{1}{2}d_1^4d_3 + \frac{1}{2}d_1^3d_3^2\right) \quad . \tag{3.3}$$

The total area of the associated sphere of influence is $4\pi(\frac{d_2+d_1}{2})^2$. It follows that the fractional area of which the center of the incoming 1-particle can lie at during a collision is

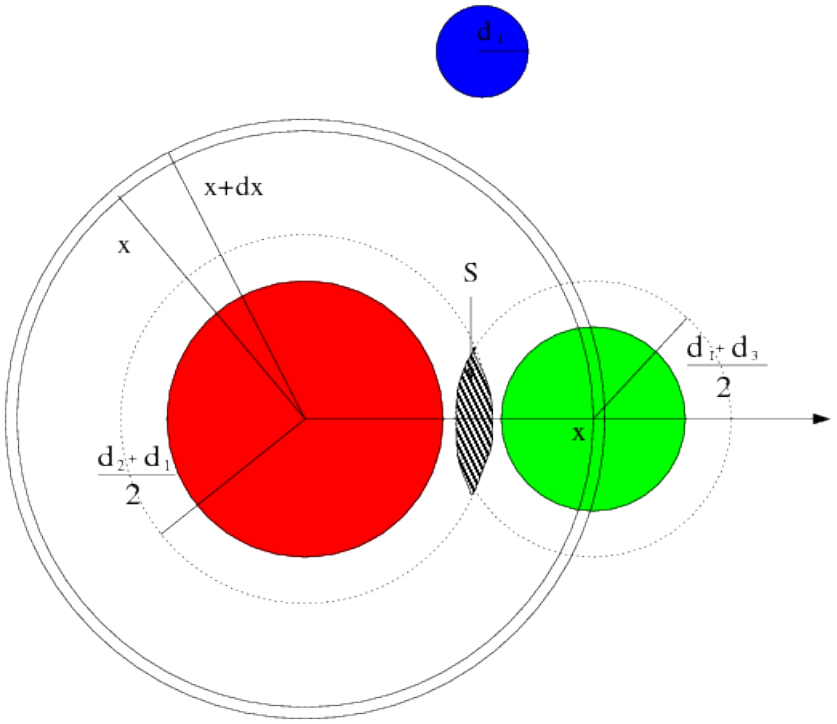

Figure 3.3: In a dense gas there is an additional shielding effect of particle interactions. During an interaction between an incoming 1-particle (blue) and a 2-particle (red) another particle may disturb the collision (green). The disturbing particle may be a third particle type, 3-particles, or another 2- or 1-particle. The associated sphere of influence for the $1 \rightarrow 3$ collision shields a surface cap S of the associated sphere of influence for the $1 \rightarrow 2$ collision, indicated in the Figure (shaded area). The probability of shielding enters into a correction of the collision frequency.
d_1 = diameter of 1-particle.
d_2 = diameter of 2-particle.
d_3 = diameter of 3-particle.
x = position of 3-particle relative the center of the 2-particle.

$1 - \frac{\text{TSS}}{4\pi(\frac{d_2+d_1}{2})^2}$. Thus, the effect of shielding by other molecules is to reduce the probability of a collision in this ratio [8].

Since we consider a two component gas consisting of 1- and 2-particles, there are two possible types of shielding to be accounted for. We may obtain an expression for the TSS for each type of shielding by inserting $d_3 = d_2$, $n_3 = n_2$ and $d_3 = d_1$, $n_3 = n_1$ into the expression (3.3), respectively. The different types of shielding are assumed uncorrelated, and thus we may multiply the two probable fractional areas into the expression for the

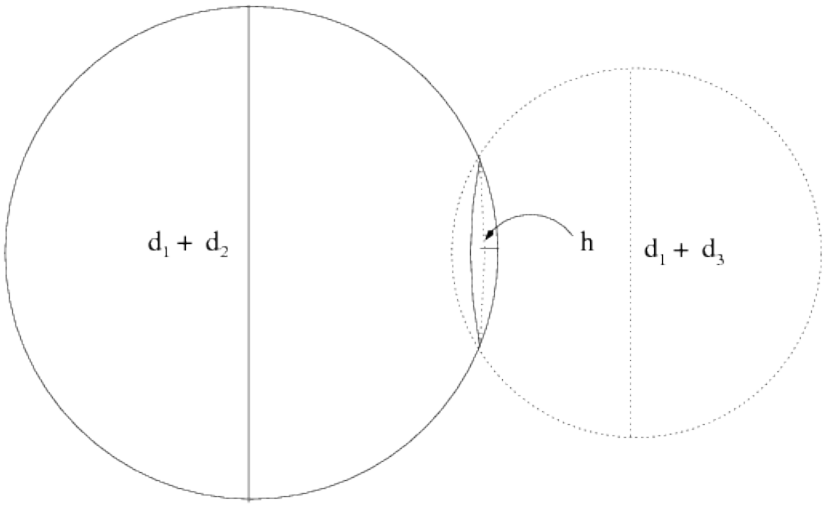

Figure 3.4: The height h of the surface cap S for the shielding of a $1 \rightarrow 2$ collision.
d_1 = diameter of 1-particle.
d_2 = diameter of 2-particle.
d_3 = diameter of 3-particle.

collision frequency. We finally obtain

$$\nu_{1\rightarrow 2} = \pi \left(\frac{d_2 + d_1}{2} \right)^2 n_2 \overline{v} \chi_{1\rightarrow 2} \quad , \tag{3.4}$$

where the *steric factor* χ is given by

$$\chi_{1\rightarrow 2} = \frac{1}{1 - \frac{4\pi}{3}(\frac{d_2+d_1}{2})^3 n_2} \left[1 - \frac{\mathrm{TSS}(d_2, n_2)}{4\pi(\frac{d_2+d_1}{2})^2} \right] \left[1 - \frac{\mathrm{TSS}(d_1, n_1)}{4\pi(\frac{d_2+d_1}{2})^2} \right] \quad . \tag{3.5}$$

If there are several components in the gas, other possible shieldings is accounted for by including similar terms for each component in the steric coefficient.

As the density in a gas increases, the particles collide more often. However, the collisions are increasingly shielded by other particles. One may interpret the effect of shielding as a loss of efficiency in the collisional transfer. Thus, the effect of a dense gas on the steric

factor, and hence the collision frequency, is first an increase in the number of encounters, and second a loss of efficiency in the collisional transfer due to shielding. More complex interaction corrections, and consequent further collision frequency corrections, for even higher densities may be thought of, but will not be discussed here.

The expression (3.4) is an expression for the $1 \rightarrow 2$ collision frequency in a gas consisting of two types of particles. In a similar manner we may obtain collision frequencies for the other possible collision types in the gas, e.g. $\nu_{1\rightarrow 1}$. These expressions will be further used in following chapters.

Remark

We have aimed at developing collision frequencies between particles in a mixture of several different types of particles, and denoted 1- *and* 2*-particles to be of two arbitrary types (which may also be identical types of particles). We have developed the collision frequency between* <u>one</u> 1*-particle and* <u>all</u> 2*-particles from its simplest form, through stepwise refinements. Doing this we consider the* $1 \rightarrow 2$ *collision frequency to be built up independent of the fact that the* 1*-particle also undergo collisions with other types of particles, that build up other collision frequencies.*

The second refinement is due to the excluded volume because of all the spheres of influence of $1 \rightarrow 2$ *collisions. The last refinement is due to other particles of all different types (the shielding effect) that may disturb each of the* $1 \rightarrow 2$ *collisions taking place.*

Particles have been considered as rigid spheres in this scheme. This may be an oversimplification of real molecular (and further, for charged particle) interactions. However, we consider the estimation we have done as relevant as a first attempt in quantifying the interactions. A more thorough analysis of interactions in dense gas systems certainly will modify to some extent our results quantitatively. Such modifications may easily be adopted and used in the equations we develop later, since these are of quite general form regarding collision frequency dependencies.

Chapter 4

Gas- and Fluid Equations

4.1 Equations on a microscopic level

4.1.1 Phase space

To be able to derive equations of motion for a gas from a statistic mechanical point of view we need to describe the motion of all the particles, or molecules in the gas.

If the molecules are small point like particles, the motion of one particle is fully described by six variables, three positional and three velocity variables. If the particle has a defined molecular size we need six additional variables, to describe the orientation of the molecule and the angular velocity. However, if we assume that the molecules are *spherically symmetric*, we do not need to account for their orientation. Furthermore, if we assume that the molecules are *smooth* so that the angular velocity is not influenced by particle collisions, the variables describing their angular velocity can be neglected as well. Under these assumptions the motion of a particle, with a defined molecular size, can be fully described by six variables, which are the same as for point like particles.

Thus, the motion of a particle can be represented by a moving point in a six dimensional hyperspace, which is called *phase space*, see Figure 4.1. Curves in the phase space are called phase trajectories. When two particles in a gas collide their velocity changes. This causes their phase trajectories to 'jump' in the velocity dimensions, see Figure 4.1.

The motion of one large molecule is sufficiently described by the motion of a point like particle. However, when considering several large molecules in a gas, their size will affect the motion. The importance of their size increases with the molecular size and the density of the gas. These effects are called *dense gas effects*, and was studied on a microscopic level in Chapter 3. The dense gas effects act in addition on a macroscopic level, which will be studied thoroughly later in this chapter. For now we restrict ourselves to consider point like particles in a gas.

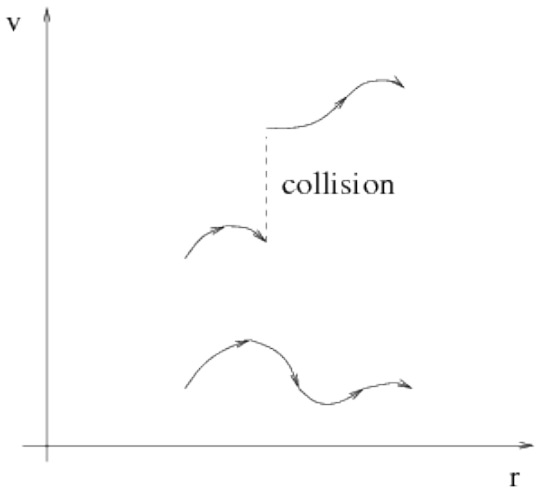

Figure 4.1: The motion of a particle are represented by a trajectory in $(\mathbf{r}, \mathbf{v})$ space. This space is called phase space. Collisions between spherical, rigid particles leads to discontinuous trajectories in velocity dimensions $\mathbf{v}$.
$\mathbf{r}$ = spatial dimensions.
$\mathbf{v}$ = velocity dimensions.

4.1.2 The distribution function

There are a large number of particles present in a gas, and to study the trajectory of each individual particle seems meaningless. We rather represent the particles by a continuous distribution function f in the six dimensional phase space, $f(\mathbf{r}, \mathbf{v}, t)$. The distribution function represents the probable density of molecules per unit volume of phase space. It follows that $f(\mathbf{r}, \mathbf{v}, t)\, \mathrm{d}\mathbf{r}\, \mathrm{d}\mathbf{v}$ is the probable number of particles in the spatial volume element $\mathrm{d}\mathbf{r}$ with a velocity in the range of $\mathrm{d}\mathbf{v}$, and thus, if the gas is sufficiently dense, is a good approximation to the number of particles in the volume element $\mathrm{d}\mathbf{r}\, \mathrm{d}\mathbf{v}$.

4.1.3 Derivation of the Boltzmann equation

In this section an equation of motion on a microscopic level is derived. This equation is known as the *Boltzmann equation*. Later this equation is used to obtain macroscopic solute equations. We will at first derive the collisionless Boltzmann equation from Newton's second law of motion for a single particle. In fact, any one of those equations can be used to derive the other, and hence the two principles are equivalent [9].

First we consider a force dominated system. Particles in such systems are assumed to only be driven by external forces, and the effect of particle collisions are thus neglected.

The motion of a single particle is given by its trajectory in phase space $(\mathbf{r}(t), \mathbf{v}(t))$. The trajectory is given by Newton's second law of motion, i.e.

$$\frac{d\mathbf{r}}{dt} = \mathbf{v} \quad , \quad \frac{d\mathbf{v}}{dt} = \frac{\mathbf{F}(\mathbf{r})}{m} \quad , \tag{4.1}$$

where the forces $\mathbf{F}$ are assumed to be velocity independent, $\mathbf{F} = \mathbf{F}(\mathbf{r})$. Related to appropriate initial conditions the above differential Equation (4.1) provide an initial value problem. Given that the force field $\mathbf{F}$ and the velocity $\mathbf{v}$ are continuous, the IVP has a unique solution [10]; the particle trajectory $(\mathbf{r}(t), \mathbf{v}(t))$.

We consider a small volume element in phase space $d\mathbf{r}d\mathbf{v}$ which transforms into $d\mathbf{r}'d\mathbf{v}'$ during the time interval from t to $t + \Delta t$, see Figure 4.2. Since the Equation of motion

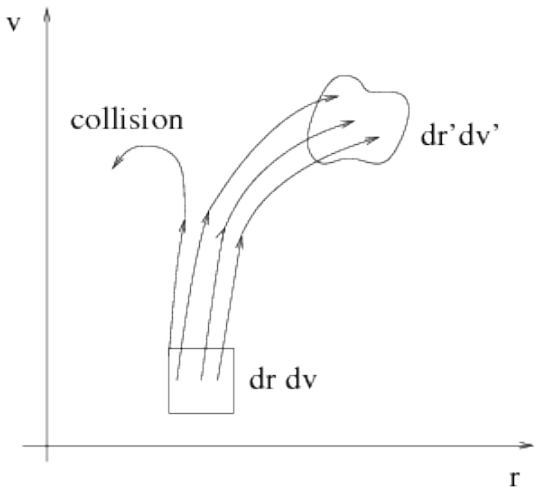

Figure 4.2: A small volume element $d\mathbf{r}d\mathbf{v}$ of particles in phase space transforms into $d\mathbf{r}'d\mathbf{v}'$ during a short time period Δt. If particle interactions are neglected the number of particles inside the volume element is conserved during transformations.
$\mathbf{r}$ = spatial dimensions.
$\mathbf{v}$ = velocity dimensions.

(4.1), with appropriate initial conditions, provides unique solutions, this implies that no particle trajectories may intersect each other. It follows that no particle may leave the volume element $d\mathbf{r}d\mathbf{v}$ during Δt. Thus, the number of particles inside the volume element is conserved, i.e.

$$f(\mathbf{r}', \mathbf{v}', t + \Delta t)d\mathbf{r}'d\mathbf{v}' = f(\mathbf{r}, \mathbf{v}, t)d\mathbf{r}d\mathbf{v} \quad . \tag{4.2}$$

The transformation of the volume element is defined mathematically by

$$d\mathbf{r}'d\mathbf{v}' = J(\mathbf{r}', \mathbf{v}')d\mathbf{r}d\mathbf{v} = \begin{vmatrix} \dfrac{\partial \mathbf{r}'}{\partial \mathbf{r}} & \dfrac{\partial \mathbf{r}'}{\partial \mathbf{v}} \\ \dfrac{\partial \mathbf{v}'}{\partial \mathbf{r}} & \dfrac{\partial \mathbf{v}'}{\partial \mathbf{v}} \end{vmatrix} d\mathbf{r}d\mathbf{v} \quad ,$$

where $J(\mathbf{r}', \mathbf{v}')$ is the Jacobi determinant for the transformation. During the short time period Δt, the position $\mathbf{r}(t)$ and velocity $\mathbf{v}(t)$ are transformed into

$$\mathbf{r}' = \mathbf{r}(t + \Delta t) \quad , \quad \mathbf{v}' = \mathbf{v}(t + \Delta t) \quad , \tag{4.3}$$

in accordance with the Equation of motion (4.1). The expressions (4.3) may be linearized to show that the Jacobi determinant is of order $\mathcal{O}(1 + (\Delta t)^2)$.

$$\mathbf{r}' \approx \mathbf{r}(t) + \Delta t \mathbf{v}(t) + \mathcal{O}((\Delta t)^2) \quad , \quad \mathbf{v}' \approx \mathbf{v}(t) + \Delta t \frac{\mathbf{F}(\mathbf{r}(t))}{m} + \mathcal{O}((\Delta t)^2) \quad .$$

If we insert for the Jacobi determinant in the expression for number conservation (4.2), it follows that the time derivative of f is 0:

$$\frac{df}{dt} = \lim_{\Delta t \to 0} \frac{f(\mathbf{r}', \mathbf{v}', t + \Delta t) - f(\mathbf{r}, \mathbf{v}, t)}{\Delta t} = 0 \quad .$$

If we write out the derivative $\frac{df}{dt}$ we obtain the *collisionless Boltzmann equation*

$$\frac{\partial f}{\partial t} + \mathbf{v} \cdot \frac{\partial f}{\partial \mathbf{r}} + \frac{\mathbf{F}}{m} \cdot \frac{\partial f}{\partial \mathbf{v}} = 0 \tag{4.4}$$

If particle collisions are accounted for, the Conservation Equation (4.2) breaks down. Collisions allow particles to 'jump' out of, or in to, the volume element during Δt, and the derivative of f is no longer zero. This net 'leakage' is accounted for by adding a term on the right hand side of Equation (4.4). The collision term is denoted $\left(\frac{\partial f}{\partial t}\right)_{coll}$, and may be interpreted as the number of incoming particles to a volume element $d\mathbf{r}d\mathbf{v}$ during Δt minus outgoing particles.

Various collision terms have been derived with a different degree of complexity, however, we will not go into details on this. In this thesis we will use the *Bhatnagar-Gross-Krook* collision term [1], or BGK term for short.

$$\left(\frac{\partial f}{\partial t}\right)_{coll} = \left(\frac{\partial f}{\partial t}\right)_{BGK} = \nu_c (f_M - f)$$

Here ν_c is the collision frequency (3.1), which was described in Chapter 3, and f_M is the Maxwellian distribution, described below.

Due to particle collisions, energy and momentum are transferred between particles, i.e. collisional transfer. If there are no external forces acting on the gas, collisional transfer relax any initial distribution f towards the Maxwell distribution f_M.

$$f_M = n \left(\frac{m}{2\pi\kappa T} \right)^{3/2} \exp\left(- \frac{m(\mathbf{v} - \mathbf{U})^2}{2\kappa T} \right) \quad , \tag{4.5}$$

where n is the number density of the gas, m is the molecular mass, κ is the Boltzmann constant, T is the temperature and $\mathbf{U}$ is the particle velocity in the mean, which together with the number density n and temperature T is a macroscopic quantity of the gas. We will return to these macroscopic quantities later.

[1] See e.g. [11] for a short description of the BGK approximation, or the article by Bhatnagar et al. [12] where the BGK term was first presented.

The BGK term is a rather simple collision term, nevertheless, it expresses the main effect of collisions, namely that the distribution function relaxes towards a Maxwellian distribution, i.e $f \to f_M$ as $t \to \infty$.

We have then obtained the *Boltzmann equation* with a BGK collision term.

$$\frac{\partial f}{\partial t} + \mathbf{v} \cdot \frac{\partial f}{\partial \mathbf{r}} + \frac{\mathbf{F}}{m} \cdot \frac{\partial f}{\partial \mathbf{v}} = \nu_c (f_M - f) \quad . \tag{4.6}$$

The second term in the Boltzmann equation is the particle velocity and the spatial density gradient. Thus, this term expresses how diffusional processes acts on the gas. Furthermore, the third term expresses the effect of external forces on the gas. We will refer to them as *diffusion term* and *force term* respectively.

4.2 Equations on a macroscopic level

4.2.1 Macroscopic quantities

When we presented the Maxwell distribution f_M (4.5), it included several macroscopic quantities which we had not yet defined. In this section we briefly define several macroscopic quantities of a gas to be used in the macroscopic equations.

The distribution in velocity space may be of little interest when describing macroscopic systems. We are interested in physical quantities which do not depend on the velocity of each particle but rather express an averaged quantity for particles, regardless of their velocity. We may obtain a macroscopic quantity by integrate the wanted quantity, weighted by the distribution function, over the entire velocity space.

In this section we give a brief definition of relevant macroscopic quantities.

$n(\mathbf{r}, t)$ **number density** of particles at a space point $\mathbf{r}$ and time t

$$n(\mathbf{r}, t) = \int f(\mathbf{r}, \mathbf{v}, t) \, \mathrm{d}\mathbf{v} \quad , \tag{4.7}$$

where the integration is over the entire velocity space. If m is the molecular mass of the components in the gas, it follows that the mass density is

$$\rho(\mathbf{r}, t) = n(\mathbf{r}, t) m \quad .$$

$\mathbf{U}(\mathbf{r}, t)$ **velocity in the mean**

$$\mathbf{U}(\mathbf{r}, t) = \frac{1}{n(\mathbf{r}, t)} \int \mathbf{v} f(\mathbf{r}, \mathbf{v}, t) \, \mathrm{d}\mathbf{v} \quad . \tag{4.8}$$

$\mathbf{P}(\mathbf{r}, t)$ **Pressure tensor**

$$\mathbf{P}(\mathbf{r}, t) = \int m(\mathbf{v} - \mathbf{U})(\mathbf{v} - \mathbf{U}) f(\mathbf{r}, \mathbf{v}, t) \, \mathrm{d}\mathbf{v} \quad , \tag{4.9}$$

from which the scalar pressure is defined

$$p(\mathbf{r},t) = \frac{1}{3}\int m(\mathbf{v}-\mathbf{U})\cdot(\mathbf{v}-\mathbf{U})f(\mathbf{r},\mathbf{v},t)\,\mathrm{d}\mathbf{v} \quad .$$

$T(\mathbf{r},t)$ **Temperature**

$$T(\mathbf{r},t) = \frac{1}{3n(\mathbf{r},t)\kappa}\int m(\mathbf{v}-\mathbf{U})\cdot(\mathbf{v}-\mathbf{U})f(\mathbf{r},\mathbf{v},t)\,\mathrm{d}\mathbf{v} \quad . \tag{4.10}$$

When a gas is in thermodynamic equilibrium locally, the distribution function f equals the Maxwell distribution f_M and the *ideal gas law*

$$p = n\kappa T \quad ,$$

is valid [13]. Here κ is the Boltzmann constant and T is the absolute temperature. This relation is used to describe the temperature of a gas away from thermodynamic equilibrium.

$\mathbf{q}(\mathbf{r},t)$ **Heat flux**

$$\mathbf{q}(\mathbf{r},t) = \frac{1}{2}\int m(\mathbf{v}-\mathbf{U})\cdot(\mathbf{v}-\mathbf{U})(\mathbf{v}-\mathbf{U})f(\mathbf{r},\mathbf{v},t)\,\mathrm{d}\mathbf{v} \quad . \tag{4.11}$$

4.2.2 Moment equations

From the Boltzmann equation one may derive a set of macroscopic equations. This is done by computing certain velocity moments of the Boltzmann equation. A velocity moment is obtained by multiplication of the velocity $\mathbf{v}$, of increasing order, into the equation and integrate over the entire velocity space. We compute the zeroth, first and second velocity moment of the Boltzmann equation to obtain a continuity equation, equation of motion and temperature equation, respectively.

Continuity equation - zeroth order moment

We integrate the Boltzmann Equation (4.6) term by term over the entire velocity space.

$$\int \frac{\partial f}{\partial t}\,\mathrm{d}\mathbf{v} + \int \mathbf{v}\cdot\frac{\partial f}{\partial \mathbf{r}}\,\mathrm{d}\mathbf{v} + \int \frac{\mathbf{F}}{m}\cdot\frac{\partial f}{\partial \mathbf{v}}\,\mathrm{d}\mathbf{v} = \int \nu_c(f_M - f)\,\mathrm{d}\mathbf{v} \quad ,$$
$$\frac{\partial}{\partial t}\int f\,\mathrm{d}\mathbf{v} + \nabla\cdot\int \mathbf{v}f\,\mathrm{d}\mathbf{v} + \int \frac{\partial}{\partial \mathbf{v}}\cdot\left(\frac{\mathbf{F}}{m}f\right)\mathrm{d}\mathbf{v} = \nu_c(n-n) \quad ,$$

where we let $\nabla = \frac{\partial}{\partial \mathbf{r}}$ represent the spatial del operator. In the computation of the force term the divergence theorem is applied, and the integration is then over the limiting values

of $\mathbf{v}$. The distribution function must tend to zero as $\mathbf{v}$ becomes infinite [8], and given that the force field $\mathbf{F}$ is finite, it follows that the integral is zero. We obtain

$$\frac{\partial}{\partial t}\int f\,\mathrm{d}\mathbf{v} + \frac{\partial}{\partial \mathbf{r}}\cdot\int \mathbf{v} f\,\mathrm{d}\mathbf{v} + \int\limits_{\Sigma_\mathbf{v}} \left(\frac{\mathbf{F}}{m} f\right)\cdot \mathrm{d}S_\mathbf{v} = \nu_c(n-n) \quad ,$$

$$\frac{\partial}{\partial t} n + \nabla\cdot(n\mathbf{U}) + 0 = 0 \quad .$$

Thus, if we multiply the molecular mass m into the equation, the zeroth order velocity moment of the Boltzmann equation provide the following *continuity equation*

$$\frac{\partial \rho}{\partial t} + \nabla\cdot(\rho\mathbf{U}) = 0 \quad . \tag{4.12}$$

Equation of motion - first order moment

First order velocity moment of the Boltzmann equation is obtained multiplying the velocity $\mathbf{v}$ into the equation and integrate over the velocity space. We present a brief summary of the computations here, and the details are left to the Appendix A.1.

Time derivative:

$$\int \mathbf{v}\frac{\partial f}{\partial t}\,\mathrm{d}\mathbf{v} = \frac{\partial}{\partial t}(n\mathbf{U}) \quad .$$

Diffusion term:

$$\int \mathbf{v}\left(\mathbf{v}\cdot\frac{\partial f}{\partial \mathbf{r}}\right)\mathrm{d}\mathbf{v} = \nabla\cdot(n\mathbf{U}\mathbf{U}) + \frac{1}{m}\nabla\cdot\mathbf{P} \quad .$$

Force term:

$$\int \mathbf{v}\left(\frac{\mathbf{F}}{m}\cdot\frac{\partial f}{\partial \mathbf{v}}\right)\mathrm{d}\mathbf{v} = -\frac{1}{m}n\mathbf{F} \quad .$$

Collision term:

$$\int \mathbf{v}\nu_c(f_M - f)\,\mathrm{d}\mathbf{v} = 0 \quad .$$

We multiply the molecular mass m into the equation, and apply the Continuity Equation (4.12). The *equation of motion* is found to be

$$\rho\left[\frac{\partial \mathbf{U}}{\partial t} + \mathbf{U}\cdot\nabla\mathbf{U}\right] = -\nabla\cdot\mathbf{P} + n\mathbf{F} \quad . \tag{4.13}$$

Temperature equation - second order moment

We now multiply $(\mathbf{v}-\mathbf{U})^2$ into the Equation (4.6) and perform the velocity integration. This corresponds to the trace of the tensor $(\mathbf{v}-\mathbf{U})(\mathbf{v}-\mathbf{U})$, and thus is the trace of the second order moment. Again, details are left to the Appendix A.1.

Time derivative:

$$\int (\mathbf{v}-\mathbf{U})^2 \frac{\partial f}{\partial t}\,\mathrm{d}\mathbf{v} = \frac{1}{m}\frac{\partial}{\partial t}(3n\kappa T) \quad .$$

Diffusion term:

$$\int (\mathbf{v}-\mathbf{U})^2 \left(\mathbf{v}\cdot\frac{\partial f}{\partial \mathbf{r}}\right)\mathrm{d}\mathbf{v} = \frac{2}{m}\nabla\cdot\mathbf{q} + \frac{1}{m}3n\kappa T\nabla\cdot\mathbf{U} + \frac{1}{m}\mathbf{U}\cdot\nabla(3n\kappa T) + \frac{2}{m}\mathbf{P}\colon\nabla\mathbf{U} \quad .$$

Force term:

$$\int (\mathbf{v}-\mathbf{U})^2 \left(\frac{\mathbf{F}}{m}\cdot\frac{\partial f}{\partial \mathbf{v}}\right)\mathrm{d}\mathbf{v} = 0 \quad .$$

Collision term:

$$\int (\mathbf{v}-\mathbf{U})^2 \nu_c (f_M - f)\,\mathrm{d}\mathbf{v} = 0 \quad .$$

We sum up all terms, multiply $\frac{m}{2}$ into the equation and apply the continuity equation. Finally, we obtain the *temperature equation*

$$\frac{3}{2}n\kappa\left[\frac{\partial T}{\partial t} + \mathbf{U}\cdot\nabla T\right] + \nabla\cdot\mathbf{q} + \mathbf{P}\colon\nabla\mathbf{U} = 0 \quad . \tag{4.14}$$

4.3 Dense gas effects

4.3.1 Corrections to microscopic equation

The Boltzmann Equation (4.6) in Section 4.1.3 was derived under the assumption that the molecules in the gas were point like particles. If the molecules are large and the density increases, Equation (4.6) is strictly no longer valid. The molecules in the gas occupy a certain fraction of the total volume which is no longer negligible.

We recall from Chapter 3 some of the properties of dense gases. In a dense gas the molecules are packed closer together and the mean free path is comparable to the molecular size. On a collisional level this means that we no longer can assume that particle collisions take place undisturbed. A correction to the collision frequency ν_c for dense gases (3.4) was derived in Chapter 3. This correction accounts for dense gas effects on a microscopic level. However, dense gas effects also appear on a macroscopic level. It is clear that an additional correction to the collision term is needed to account for macroscopic effects, or non-uniformities.

The correction term for the Boltzmann Equation (4.6) has been suggested by Øien [2], in correspondence with previous and similar correction terms by [8] and [14].

$$\frac{\partial f}{\partial t} + \mathbf{v} \cdot \frac{\partial f}{\partial \mathbf{r}} + \frac{\mathbf{F}}{m} \cdot \frac{\partial f}{\partial \mathbf{v}} = \nu_c(f_M - f) + \frac{\partial}{\partial \mathbf{r}} \cdot \left[\frac{2\pi}{3} d^3 n \chi (\mathbf{U} f_M - \mathbf{v} f) \right] \quad , \tag{4.15}$$

where χ is the steric coefficient described in section 3. In Equation (4.15) r is now the position of the center of the particles. The idea behind the correction term is that the incoming particles, with velocity $\mathbf{v}$, is distributed according to $f(\mathbf{v})$ and the deflected particles, with velocity $\mathbf{U}$ in the mean, is distributed according to $f_M(\mathbf{v})$.

The collision term, first term on the right hand side of Equation (4.15), is essentially the same as before. However, in accordance with the dense gas expansion in Chapter 3, Equation (3.4), the collision frequency is modified to

$$\nu_c = \pi d^2 n v_{rel} \chi \quad .$$

If we compare the size of the collision and correction term in Equation (4.15), we observe that the correction term is negligible for a rare gas.

$$\begin{aligned} &\nu_c(f_M - f) \sim d^2 \chi v_{rel} n f \quad , \\ &\frac{\partial}{\partial \mathbf{r}} \cdot \left[\frac{2\pi}{3} d^3 n \chi (\mathbf{U} f_M - \mathbf{v} f) \right] \sim \frac{1}{L} d^3 \chi (\|\mathbf{U}\| + \|\mathbf{v}\|) n f \sim \frac{d}{L} d^2 \chi v_{rel} n f \quad , \end{aligned}$$

where L is a characteristic length scale for non-uniformities in the gas, and d is the molecular size. In a rare gas L is obviously much bigger than d, and the correction term vanishes. If d and L are comparable sizes, however, the correction term is no longer negligible.

To sum up, dense gas effects in Equation (4.15) is expressed through the χ factor in the collision term, and through the correction term.

4.3.2 Correction to macroscopic equations

To account for the dense gas effects in the macroscopic equations, it is sufficient to compute velocity moments of the new correction term and add the resulting quantities to the Continuity Equation (4.12), Equation of motion (4.13) and Temperature Equation (4.14), respectively.

Zeroth order:

$$\int m \frac{\partial}{\partial \mathbf{r}} \cdot \left[\frac{2\pi}{3} d^3 n \chi (\mathbf{U} f_M - \mathbf{v} f) \right] \mathrm{d}\mathbf{v} = 0 \quad .$$

The dense gas effects do not affect the continuity equation.

[2] Alf Øien, Professor emeritus and advisor, Department of Mathematics, University of Bergen, Norway. Private communication

First order:

$$\int m\mathbf{v}\frac{\partial}{\partial \mathbf{r}}\cdot\left[\frac{2\pi}{3}d^3n\chi(\mathbf{U}f_M-\mathbf{v}f)\right]\mathrm{d}\mathbf{v}=-\nabla\cdot\left[\frac{2\pi}{3}d^3n\chi\mathbf{P}\right] \quad .$$

The dense gas effects is expressed through a correction of the pressure tensor $\mathbf{P}$.

Second order:

$$\begin{aligned}\int \frac{1}{2}m(\mathbf{v}-\mathbf{U})^2\frac{\partial}{\partial \mathbf{r}}\cdot\left[\frac{2\pi}{3}d^3n\chi(\mathbf{U}f_M-\mathbf{v}f)\right]\mathrm{d}\mathbf{v}\\ =-\nabla\cdot\left(\frac{2\pi}{3}d^3n\chi\mathbf{q}\right)-\frac{2\pi}{3}d^3n\chi\mathbf{P}\colon\nabla\mathbf{U} \quad .\end{aligned}$$

The dense gas effects is expressed through a correction of the heat flux $\mathbf{q}$ and the $\mathbf{P}\colon\nabla\mathbf{U}$ term.

Thus, the continuity equation, equation of motion and temperature equation for dense gases are found to be

$$\frac{\partial\rho}{\partial t}+\nabla\cdot(\rho U)=0 \quad , \tag{4.16}$$

$$\rho\left[\frac{\partial\mathbf{U}}{\partial t}+\mathbf{U}\cdot\nabla\mathbf{U}\right]=n\mathbf{F}-\nabla\cdot\left(1+\frac{2\pi}{3}d^3n\chi\right)\mathbf{P} \quad , \tag{4.17}$$

$$\frac{3}{2}n\kappa\left[\frac{\partial T}{\partial t}+\mathbf{U}\cdot\nabla T\right]+\nabla\cdot\left(1+\frac{2\pi}{3}d^3n\chi\right)\mathbf{q}+\left(1+\frac{2\pi}{3}d^3n\chi\right)\mathbf{P}\colon\nabla\mathbf{U}=0 \quad . \tag{4.18}$$

These equations are almost in accordance with Chapman and Cowling [8].

4.4 Multicomponent fluids

The equations in the previous section were derived for a gas containing only one type of particles, i.e. a *one component gas*. The interactions in such a gas is always between similar particles. However, if a gas contain several types of particles, all possible particle interactions must be accounted for. In this section we will extend the equations to apply for a *multicomponent gas*.

We restrict ourselves to consider a two component gas. Further extensions will follow the same principles, and is easily accounted for. The two components of the gas is referred to as i-particles and j-particles. Both components are represented by distribution functions, $f_i(\mathbf{r}_i,\mathbf{v}_i,t)$ and $f_j(\mathbf{r}_j,\mathbf{v}_j,t)$, which both follow the Boltzmann equation. Each particle interacts with both similar particles, ii- collisions, and particles of the different type, ij-collisions. We first consider the particles as point like particles. Later we account for the dense gas effects, in accordance with one component gases.

4.4.1 Corrections to microscopic equations - collisional transfer

The distribution functions f_i og f_j follow the Boltzmann Equation (4.6), however, the collision term on the right hand side in the equation only accounts for interactions with similar particles. As described in Section 4.1.3, this collision term expresses that the distribution function f relaxes towards the Maxwell distribution f_M. During molecular encounters there is an exchange of both momentum and energy between the particles. The collisional transfer for one particle, after several encounters, 'drag' the particle towards the mean particle velocity and energy. Thus, a collision dominated system, from whatever initial distribution, eventually distributes according to the Maxwell distribution (4.5).

The additional collision term, to account for ij-collisions, therefore expresses a drag towards a Maxwell distribution with the mean velocity and temperature of the other particle type. The Maxwell distributions are given as

$$f_{ii,M} = n_i \left(\frac{m_i}{2\pi\kappa T_i} \right)^{3/2} \exp\left(- \frac{m_i(\mathbf{v}_i - \mathbf{U}_i)^2}{2\kappa T_i} \right) \quad , \tag{4.19}$$

$$f_{ij,M} = n_i \left(\frac{m_i}{2\pi\kappa T_j} \right)^{3/2} \exp\left(- \frac{m_i(\mathbf{v}_i - \mathbf{U}_j)^2}{2\kappa T_j} \right) \quad , \quad i \neq j \quad . \tag{4.20}$$

Thus, the extension to the Boltzmann Equation (4.6) is found to be

$$\boxed{\frac{\partial f_i}{\partial t} + \mathbf{v}_i \cdot \frac{\partial f_i}{\partial \mathbf{r}_i} + \frac{\mathbf{F}_i}{m_i} \cdot \frac{\partial f_i}{\partial \mathbf{v}_i} = \nu_{ii}(f_{ii,M} - f_i) + \nu_{ij}(f_{ij,M} - f_i) \quad ,} \tag{4.21}$$

where the collision frequencies ν_{ii} and ν_{ij} are similar to (3.1).

Collisional transfer generally happens on different time scales [15]. Lighter particles move around with high velocities in the mean, and thus have a correspondingly high collision frequency. Therefore they reach a self-Maxwellian rapidly. Heavier particles reach a self-Maxwellian later, due to their lower velocities. The two components also interact and reach an equilibrium with each other. However, if e.g. i-particles are much lighter than j-particles, at most a fraction $\frac{m_i}{m_j}$ of the energies involved can be transferred in each encounter [15]. Thus, one may assume that the changes in energies (temperature equation) are small as compared to the changes in momentum (equation of motion).

In the following we assume that we have a mass difference between the two components in the gas, i.e. $m_i \ll m_j$ which is most relevant for our later studies. Furthermore, we neglect the changes in temperatures, and assume that the two temperatures are equal, $T_1 = T_2 = T$, for the same reason.

4.4.2 Corrections to macroscopic equations

We need only evaluate the contribution from the new collision term due to ij-collisions.

Zeroth order moment:

$$\int m_i \nu_{ij}(f_{ij,M} - f_i)\, \mathrm{d}\mathbf{v}_i = 0 \quad .$$

The presence of additional components in gas does not affect the continuity equation. This was expected since the continuity equation expresses conservation of mass. The continuity equation applies component-wise.

First order moment:

$$\int m_i \mathbf{v}_i \nu_{ij}(f_{ij,M} - f_i)\,\mathrm{d}\mathbf{v}_i = \nu_{ij}\rho_i(\mathbf{U_j} - \mathbf{U_i}) \quad .$$

In a multicomponent gas a component experience a 'frictional drag' from the other component. It follows from Newton's third law of motion that $\nu_{ij}\rho_i$ equals $\nu_{ji}\rho_j$.

The continuity equation and equation of motion for each component is then found to be

$$\frac{\partial \rho_i}{\partial t} + \nabla \cdot (\rho_i \mathbf{U}_i) = 0 \quad , \tag{4.22}$$

$$\rho_i \left[\frac{\partial \mathbf{U_i}}{\partial t} + \mathbf{U_i} \cdot \nabla \mathbf{U_i} \right] = n_i \mathbf{F}_i - \nabla \cdot \mathbf{P_i} - \nu_{ij}\rho_i(\mathbf{U_i} - \mathbf{U_j}) \quad . \tag{4.23}$$

Extension of the Equations (4.22) and (4.23) is a straight forward addition of several interaction terms, $ij, ik, il, ...$

Dense gas effects

The inclusion of dense gas effects for a multicomponent gas is, however, not straight forward. We make a simplifying assumption that one component, e.g. the j-component, is considered immobilized due to their large mass as compared to i-particles. It follows that $\mathbf{U}_j$ is set to zero, and thus, the equations for that component is dropped.

Again a correction term is needed to the Boltzmann equation, this time to express the dense gas effects on interactions between the two components. And again, the correction term has been suggested by Øien [3]. The final extension to the Boltzmann equation reads

$$\begin{aligned} \frac{\partial f_i}{\partial t} + \mathbf{v}_i \cdot \frac{\partial f_i}{\partial \mathbf{r}_i} + \frac{\mathbf{F}_i}{m_1} \cdot \frac{\partial f_i}{\partial \mathbf{v}_i} =& \nu_{ii}(f_{ii,M} - f_i) + \frac{\partial}{\partial \mathbf{r}} \cdot \left[\frac{2\pi}{3} d_i^3 n_i \chi_{ii} (\mathbf{U}_i f_{ii,M} - \mathbf{v}_i f_i) \right] \\ &+ \nu_{ij}(f_{ij,M} - f_i) - \frac{\partial}{\partial \mathbf{r}} \cdot \left[\frac{2\pi}{3} \left(\frac{d_i + d_j}{2} \right)^3 n_j \chi_{ij} \mathbf{v}_i f_{ij,M} \right] \quad . \end{aligned} \tag{4.24}$$

[3] Alf Øien, Professor emeritus, Department of Mathematics, University of Bergen, Norway. Private communication

A computation of the velocity moments give the following corrections

Zeroth order moment:

$$\int m_i \frac{\partial}{\partial \mathbf{r}} \cdot \left[\frac{2\pi}{3} \left(\frac{d_i + d_j}{2} \right)^3 n_j \chi_{ij} \mathbf{v}_i f_{ij,M} \right] \mathrm{d}\mathbf{v}_i = 0 \quad .$$

No corrections of the continuity equation.

First order moment:

$$\int m \mathbf{v}_i \frac{\partial}{\partial \mathbf{r}} \cdot \left[\frac{2\pi}{3} \left(\frac{d_i + d_j}{2} \right)^3 n_j \chi_{ij} \mathbf{v}_i f_{ij,M} \right] \mathrm{d}\mathbf{v}_i$$
$$= -\frac{2\pi}{3} \left(\frac{d_i + d_j}{2} \right)^3 \nabla (n_i \kappa T n_j \chi_{ij}) \quad .$$

In case of a Maxwell distribution, which follows from assuming a local thermodynamic equilibrium, we have a diagonal pressure tensor $\mathbf{P}_i = n_i \kappa T \mathbf{I}$ [13]. Thus, the additional term may be interpreted as a correction of the pressure tensor.

The continuity equation and equation of motion for a two component gas, including on immobilized component, is found to be

$$\frac{\partial \rho_i}{\partial t} + \nabla \cdot (\rho_i \mathbf{U}_i) = 0 \tag{4.25}$$

$$\rho_i \left[\frac{\partial \mathbf{U_i}}{\partial t} + \mathbf{U_i} \cdot \nabla \mathbf{U_i} \right] = n_i \mathbf{F}_i - \nabla \cdot \left(1 + \frac{2\pi}{3} d_i^3 n_i \chi_{ii} \right) \mathbf{P_i}$$
$$- \nu_{ij} \rho_i \mathbf{U_i} - \frac{2\pi}{3} \left(\frac{d_i + d_j}{2} \right)^3 \nabla (n_i \kappa T n_j \chi_{ij}) \tag{4.26}$$

4.5 Introduction of a background continuum

To obtain a set of equations suitable for modeling interstitial flow, we introduce a *background continuum*. This implies that we have a system mainly consisting of a continuum, or a solvent, which our 'gas' evolves in. The solvent we may, without loss of generality, describe using classical hydrodynamic equations, i.e Navier-Stokes like fluid equations. The gas particles is referred to as 1-particles and 2-particles (immobile). They interact with each other, as described in previous sections, and they also interact with the solvent. To be able to relate the equations to each other, the solvent is referred to as s-particles.

The solvent is assumed to have velocity field $\mathbf{U}_s$. This gives rise to a $1s$ friction drag term in the equation of motion for particle 1. In accordance with Newton's third law of motion a friction term is added to the Navier-Stokes equation for the solvent. Furthermore, this also applies for a $s2$ friction drag term, due to solvent interactions with the immobile 2-particles.

We have the following set of fluid equations for the solvent and 1-particles:

$$
\begin{aligned}
&\frac{\partial \rho_1}{\partial t} + \nabla \cdot (\rho_1 \mathbf{U}_1) = 0 \\
&\rho_1 \left[\frac{\partial \mathbf{U}_1}{\partial t} + \mathbf{U}_1 \cdot \nabla \mathbf{U}_1 \right] = n_1 \mathbf{F}_1 - \nabla \cdot \left(1 + \frac{2\pi}{3} d_1^3 n_1 \chi_{11} \right) \mathbf{P}_1 - \nu_{12} \rho_1 \mathbf{U}_1 \\
&\qquad\qquad - \frac{2\pi}{3} \left(\frac{d_1 + d_2}{2} \right)^3 \nabla (n_1 \kappa T n_2 \chi_{12}) - \rho_1 \nu_{1s} (\mathbf{U}_1 - \mathbf{U}_s) \\
&\frac{\partial \rho_s}{\partial t} + \nabla \cdot (\rho_s \mathbf{U}_s) = 0 \\
&\rho_s \left[\frac{\partial \mathbf{U}_s}{\partial t} + \mathbf{U}_s \cdot \nabla \mathbf{U}_s \right] = n_s \mathbf{F}_s - \nabla p_s + \nabla \cdot \mu \left[\nabla \mathbf{U}_s + (\nabla \mathbf{U}_s)^T - \frac{2}{3} \nabla \cdot \mathbf{U}_s \mathbf{I} \right] \\
&\qquad\qquad - \rho_s \nu_{s1} (\mathbf{U}_s - \mathbf{U}_1) - \rho_s \nu_{s2} \mathbf{U}_s
\end{aligned}
\tag{4.27}
$$

where $\rho_s \nu_{s1} = \rho_1 \nu_{1s}$ obviously. This set of equations will be used in the following chapters.

It should be remarked that the 'collision frequencies' ν_{1s}, ν_{s1} and ν_{s2} are not given in accordance with (3.4). They rather express the magnitude of the friction drag on the solvent, and should be interpreted as such. E.g. a large ν_{1s} in express that the solute is tightly bound to the solvent. The notation could be misleading, however, is chosen for simplicity in further work.

Chapter 5

Compartment Model

In this chapter we will use the set of Equations (4.27) derived in Chapter 4 to derive a compartment model for fluid flow through the interstitium. Compartment models are coarse fluid models, where all spatial variations in the fluid system are neglected. These models are used extensively to model fluid flow in physiological literature.

The compartment model derived in this chapter is in compliance with the Starling Model from [2].

5.1 Model adaptation

In a compartment model the fluid system is divided into several compartments. Inspired by Bert et al. [2], we define a closed fluid system composed of three compartments; interstitium, circulation (blood) and lymph. As described in Chapter 2, fluid enters the interstitium from the capillaries, and excess fluid is drained to the lymphatics. The lymphatic system leads the fluid back to circulation, see Figure 5.1. We neglect the transport of fluid in and out of tissue cells.

The composition of the fluid must be defined properly for our solute equations, derived in Chapter 4, to apply. As a first attempt we let the fluid be composed of a solvent and a solute. The solute is a larger substance, e.g. a type of protein. In the interstitial compartment there are additional fixed macromolecules. The presence of these macromolecules is an attempt to represent the hindrance by the interstitial matrix.

The solute and the solvent are in constant interaction with each other. In addition they interact with the fixed macromolecules in the interstitial compartment. For an illustration of the fluid composition in the interstitial compartment see Figure 5.2. In Chapter 8 the fluid composition is expanded to also include ions and charged components of the interstitial matrix.

Hindrance of the flow by the interstitial matrix are hopefully represented by interactions with the fixed macromolecules. In accordance with the notation used in Chapter 4, the subscript s refers to the solvent, 1 refers to the solute and 2 refers to the fixed macromolecules.

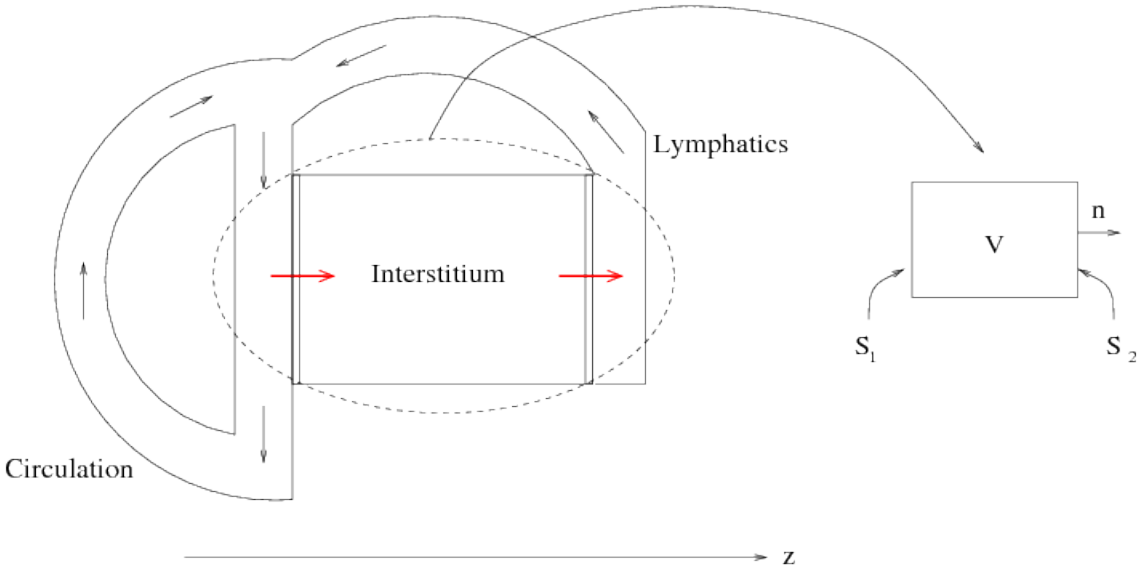

Figure 5.1: A schematic compartment model of the fluid system: The fluid system is divided into three compartments; interstitium, circulation (blood) and lymph. Inside each compartment all variables are assumed constant in space. There is an exchange of fluid across the membranes, indicated in the figure.
V = volume.
S = surface.
$\mathbf{n}$ = outer unit normal.
z = flow direction.

5.1.1 General compartment equations

Compartment models are based on the assumption that all components of a compartment are well mixed at all times. This implies that no physical quantities can vary in space inside a compartment, and thus only vary with time. Several compartments are coupled and there is an exchange of fluid between them, see Figure 5.1. If the fluid system is closed, exchange of fluid can only occur at common boundaries between two compartments. These boundaries are called *membranes*.

Equations describing flow in a compartment fluid system are called *compartment equations*. These equations are constructed to satisfy an important physical principle; the *conservation of mass* in a closed system. This principle is stated as follows

$$\boxed{\text{Accumulated mass inside V}} \quad = \quad \boxed{\text{Mass flux into V through S}} \quad ,$$

where V is the volume and S is the boundary of a compartment. Mathematically the mass conservation reads

$$\frac{d}{dt}M = -\int_S \rho \mathbf{U} \cdot \mathbf{n} \, \mathrm{d}S \quad , \tag{5.1}$$

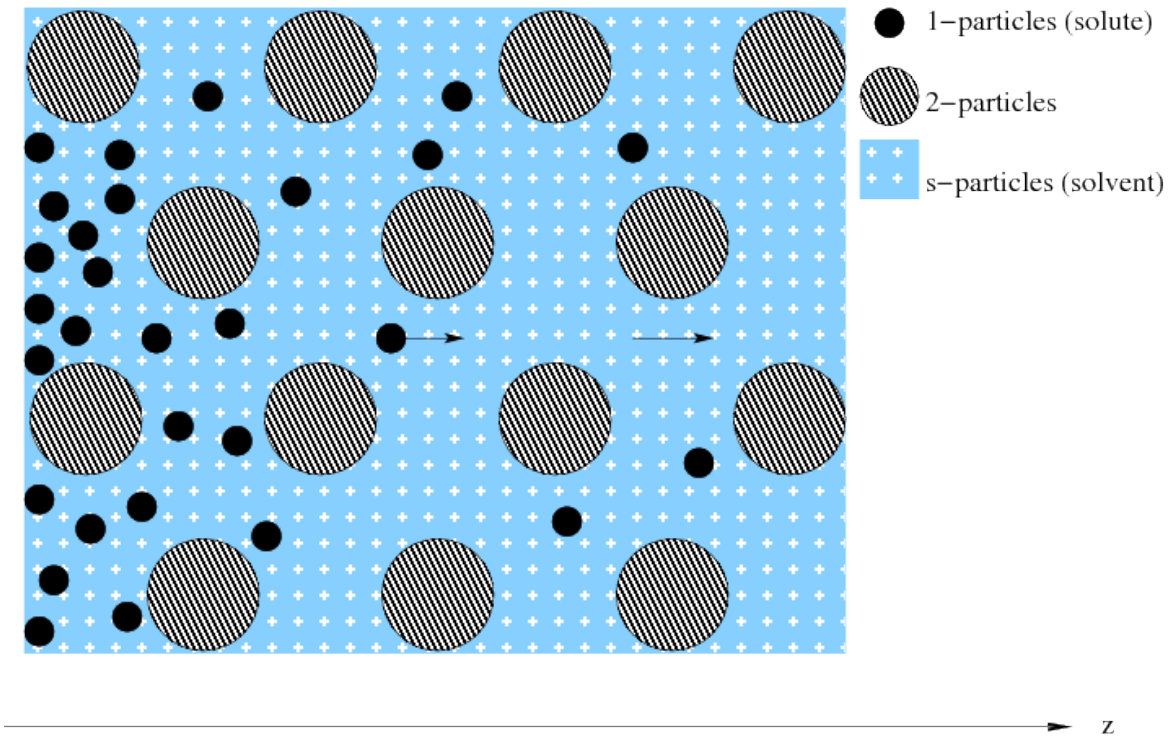

Figure 5.2: The interstitial compartment is composed of fixed macromolecules (shaded), moving macromolecules or solute (black) and a solvent (light blue). The solute interacts with both the solvent, which accounts for water and small ions, and the fixed macromolecules, which account for the interstitial matrix.
z = flow direction.

where ρ is the mass density of the fluid, $\mathbf{U}$ is the fluid velocity and $\mathbf{n}$ is the outer unit normal of S, see Figure 5.1. The mass conservation Equation (5.1) is valid for each compartment. In case of a multi component fluid, the equation is valid for each component of the fluid.

In a compartment model it is more relevant to include fluid fluxes, rather than velocity fields. The evaluation of the integral on the right hand side in Equation (5.1) depends obviously on the complexity of the integrand and the surface S. However, for a simple geometry, as in Figure 5.1, the integral can be evaluated as follows

$$\frac{d}{dt}M = mJ_zS_1 - mJ_zS_2 \quad , \tag{5.2}$$

where J_z is the *number molecular flux* of the fluid per unit area, and is defined to be

$$J_z = \int_0^1 \int_0^1 nU_z \, \mathrm{d}A \quad , \tag{5.3}$$

where $\mathrm{d}A$ is a small surface fraction, the integral is over a unit area, n is the number density and U_z is the flow component in z-direction.

The fluxes in Equation (5.2) must be evaluated. A set of governing equations for the fluid system is applied for this purpose. In general, the fluxes will contain information from both interfacing compartments, and from the membrane between them. The set of Equations (4.27) derived in Chapter 4 will be the governing equations for our fluid system. We will assume that this set of equations, with minor modifications, also apply for flow through the membranes, i.e. pore flow. The modifications are only briefly described. In Section 5.2 we will derive local flux expressions based on the set of equations (4.27), further the fluxes are modified to apply for pore flow, and averaged over the membranes.

5.2 Evaluation of averaged membrane fluxes

We will use the set of Equations (4.27) derived in Chapter 4 for a solute evolving on a solvent background in constant interaction with each other and fixed macromolecules. We will assume that the system is in a

- Quasi steady state

A *quasi steady state system* is essentially a system 'close to' an equilibrium state. The quasi steady state assumption implies a balance of forces in the equations of motion, since acceleration terms are assumed small and negligible.
In addition following simplifying assumptions are made:

- Flow is directed in the z-direction
- No x- or y-dependency in any variables
- Constant viscosity μ
- Constant solvent mass density ρ_s
- Diagonal pressure tensor $\mathbf{P}_1$
- External forces are absent

There is a net flow from capillaries to lymph, as described in Chapter 2. Thus, assuming that the flow is in the z-direction, see Figure 5.2, seems justified. The assumptions on μ and ρ_s follows from assuming that the solvent is a homogeneous and incompressible newtonian fluid. A local thermodynamic equilibrium is assumed. It follows that the pressure tensor is diagonal with $\mathbf{P}_1 = n_1 \kappa T \mathbf{I}$, where n_1 is the number density of the solute, κ is the Boltzmann constant and T is the temperature [13]. For now we restrict our model to apply for systems in which there are no external forces. From the above assumptions we obtain the following flow fields

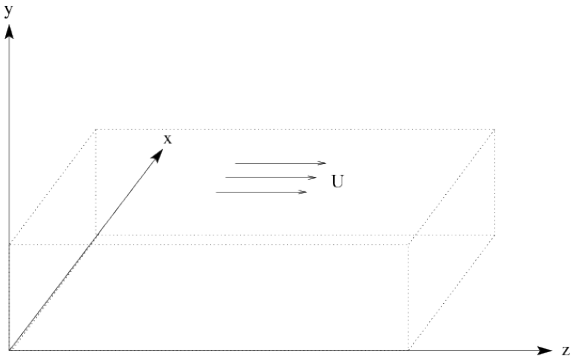

Figure 5.3: The flow is directed in the z-direction. It is assumed no variations in any variables in both the x- and y-direction. $\mathbf{U}$ = flow field.

$$\mathbf{U}_1 = U_1(z)\mathbf{e}_z \quad , \quad \mathbf{U}_s = U_s \mathbf{e}_z \quad . \tag{5.4}$$

With all of the assumptions put into the Equations of motion in (4.27), we arrive at the following equations, which are equations of motion for the solute and the solvent in z-direction.

$$\begin{aligned} 0 &= -\kappa T \frac{d}{dz}\left\{\left[1 + \frac{2\pi}{3}\left(\frac{d_1+d_2}{2}\right)^3 \chi_{12} n_2 + \frac{2\pi}{3} d_1^3 \chi_{11} n_1\right] n_1\right\} \\ &\quad - \rho_1 \nu_{12} U_1 - \rho_1 \nu_{1s}(U_1 - U_s) \quad , \\ 0 &= -\frac{dp_s}{dz} - \rho_s \nu_{s1}(U_s - U_1) - \rho_s \nu_{s2} U_s \quad . \end{aligned}$$

A small rearrangement of the terms then gives us the following expressions for the velocities:

$$\rho_1 U_1 = -\frac{1}{\nu_{12} + \nu_{1s}} \kappa T \frac{d}{dz}(X n_1) + \rho_1 \frac{\nu_{1s}}{\nu_{12} + \nu_{1s}} U_s \quad , \tag{5.5}$$

$$\rho_s U_s = -\frac{1}{\nu_{s1} + \nu_{s2}} \frac{dp_s}{dz} + \rho_s \frac{\nu_{s1}}{\nu_{s1} + \nu_{s2}} U_1 \quad , \tag{5.6}$$

where we have defined

$$X \quad \stackrel{\text{def}}{=} \quad 1 + \frac{2\pi}{3}\left(\frac{d_1+d_2}{2}\right)^3 \chi_{12} n_2 + \frac{2\pi}{3} d_1^3 \chi_{11} n_1 \quad . \tag{5.7}$$

We can now use the defined flux (5.3) to obtain an expression for the fluxes. However, a small adjustment is done for the solvent flux, since it is more convenient to relate to the

solvent *volume flux* rather than the molecular flux. In accordance with (5.3) we have the following fluxes

$$J_1 = \int_0^1\int_0^1 n_1 U_1 \,\mathrm{d}A \quad , \quad J_s = \int_0^1\int_0^1 U_s \,\mathrm{d}A \quad , \tag{5.8}$$

where J_1 is a molecular flux and J_s is a volume flux.

The solvent flux J_s is constant. This follows from (5.4). We recall that $\rho = mn$, and insert Equations (5.5) and (5.6) into the expressions for the fluxes. The calculation is straight forward, and we are left with two coupled expressions for the fluxes

$$J_1 = -\frac{1}{m_1}\frac{1}{\nu_{12}+\nu_{1s}}\kappa T\frac{d}{dz}(Xn_1) + n_1\frac{\nu_{1s}}{\nu_{12}+\nu_{1s}}J_s \quad , \tag{5.9}$$

$$J_s = -\frac{1}{\rho_s}\frac{1}{\nu_{s1}+\nu_{s2}}\frac{dp_s}{dz} + \frac{1}{n_1}\frac{\nu_{s1}}{\nu_{s1}+\nu_{s2}}J_1 \quad . \tag{5.10}$$

By inserting Equation (5.9) into Equation (5.10) we are able to relate the solvent volume flux, J_s, to well known, and measurable, pressures; the *hydrostatic pressure* P and the *osmotic pressure* Π. The hydrostatic pressure is the sum of the partial pressures of the solvent and solute, and is therefore the total pressure of the fluid as a whole [8]. The partial pressure of the solute is the diagonal element in the pressure tensor plus the steric correction terms. For the solvent flux we obtain

$$J_s = -K\frac{d}{dz}\Big[P - \sigma\Pi\Big] \quad , \tag{5.11}$$

where

$$\begin{aligned}
\Pi &= \kappa T X n_1 \quad , \\
P &= p_s + \Pi \quad , \\
K &= \frac{1}{\left(1 - \frac{\nu_{s1}}{\nu_{s1}+\nu_{s2}}\cdot\frac{\nu_{1s}}{\nu_{12}+\nu_{1s}}\right)}\frac{1}{\rho_s}\frac{1}{(\nu_{s1}+\nu_{s2})} \quad , \\
\sigma &= \frac{\nu_{12}}{\nu_{12}+\nu_{1s}} \quad .
\end{aligned}$$

Here K is called a local *filtration coefficient* and σ is called a local *reflection coefficient*. Equation (5.11) expresses that the solvent flux is driven by gradients in the hydrostatic and osmotic pressure.

Equation (5.9) and (5.11) express the local fluxes through a unit surface area (cross section) in the interstitial compartment. However, with minor adjustments, they also apply for local fluxes through a unit surface area of the pores in the membrane. We neglect all terms due to interactions with 2-particles in the equations, and further add similar terms due to interactions with the pore wall.

Solvent and solutes are transported through pores in the membrane. The capillary membrane is a semipermeable membrane, as described in Chapter 2. Since the transport is restricted to small pores in the capillary membrane, the hindrance of flow varies for different components of the fluid. The pore wall hindrance gives rise to similar friction terms as for the structural molecules. Thus, for a simple adaptation of the flux equations, we change all terms in Equation (5.9) and (5.11) due to matrix interaction into similar terms due to interactions with the pore walls. This implies that ν_{12} and ν_{s2} is changed into ν_{1pw} and ν_{spw}, where the subscript pw refer to porewall obviously. However, it should be remarked that ν_{1pw} and ν_{spw} no longer are collision frequencies in accordance with (3.4). They rather express the magnitude of a friction force due to the pore walls.

A modified set of local fluxes, which apply through a membrane, is given by

$$J_1 = -\frac{1}{m_1}\frac{1}{\nu_{1pw}+\nu_{1s}}\kappa T\frac{d}{dz}(Xn_1) + n_1\frac{\nu_{1s}}{\nu_{1pw}+\nu_{1s}}J_s \quad , \tag{5.12}$$

$$J_s = -K\frac{d}{dz}\Big[P - \sigma\Pi\Big] \quad , \tag{5.13}$$

where

$$K = \frac{1}{\left(1-\frac{\nu_{s1}}{\nu_{s1}+\nu_{spw}}\cdot\frac{\nu_{1s}}{\nu_{1pw}+\nu_{1s}}\right)}\frac{1}{\rho_s}\frac{1}{(\nu_{s1}+\nu_{spw})} \quad ,$$

$$\sigma = \frac{\nu_{1pw}}{\nu_{1pw}+\nu_{1s}} \quad .$$

The parameter K is a local filtration coefficient. The 'collision frequencies' in K represent the magnitude of a friction force, e.g. ν_{1s} represents how tight the solute is bound to the solvent. σ is a local reflection coefficient.

We now average the expressions for the fluxes along the pores in the membrane. The flux expressions (5.12) and (5.13) are integrated from the pore entrance to the pore end, and divided by the pore length l. The 'collision frequencies', and hence the local filtration coefficient K and local reflection coefficient σ, are taken to be the average values along the pores, and are thus constant.

It is assumed that the pressure P and (Xn_1) are continuous at the pore ends. We thus obtain

$$(J_s)_m \approx \left(\frac{K}{l}\right)_m\Big[\Delta_m P - \sigma_m\kappa T\Delta_m(Xn_1)\Big] \quad ,$$

$$(J_1)_m \approx \frac{1}{m_1}\left(\frac{1}{\nu_{1pw}+\nu_{1s}}\frac{1}{l}\right)_m\kappa T\Delta_m(Xn_1) + \overline{n}_{1,m}(1-\sigma_m)(J_s)_m \quad ,$$

where the subscript m refers to membrane, and $\overline{n}_{1,m}$ is the average number density of solutes inside the membrane. The operator Δ_m is the difference operator over the membrane, e.g. $\Delta_m P = P|_{z=0} - P|_{z=l}$.

The fluid transport through the lymph capillary membrane is somewhat less rigid than through the blood capillary membrane. The lymph membrane is more permeable to larger molecules so the transport of macromolecules through this membrane is mainly by filtration [2]. Since the collision frequency ν_{1s} is a measure of how tight the solute is bound to the solvent through the membranes, we will approximate this effect by letting $\nu_{1s} \to \infty$ for the lymph capillary membrane. It follows that the reflection coefficient σ_{ly} goes to zero, and the local filtration coefficient K_{ly} reduces to $\frac{1}{\rho_s \nu_{spw}}$. We thus evaluate the flux terms for the lymph capillary in this limit. The membrane specific fluxes are thus found to be

$$
\begin{aligned}
(J_s)_{cap} &= \left(\frac{K}{l}\right)_{cap,m} \left[\Delta_{cap,m} P - \sigma_{cap,m} \kappa T \Delta_{cap,m}(X n_1)\right] \quad , \qquad (5.14)\\
(J_s)_{ly} &= \left(\frac{K}{l}\right)_{ly,m} \Delta_{ly,m} P \quad ,\\
(J_1)_{cap} &= \frac{1}{m_1}\left(\frac{1}{\nu_{1pw}+\nu_{1s}}\frac{1}{l}\right)_{cap,m} \kappa T \Delta_{cap,m}(X n_1) + \overline{n}_{1,cap,m}(1-\sigma_{cap,m})(J_s)_{cap} \quad ,\\
(J_1)_{ly} &= \overline{n}_{1,ly,m}(J_s)_{ly} \quad ,
\end{aligned}
$$

We observe that fluxes through the membranes are related to pressure differences over the membranes, and in addition specific membrane parameters. The expression (5.14) can be recognized as the *Starling equation*, which is a well known equation in membrane physiology.

5.3 Excluded volume

In the interstitium solute molecules are excluded from a fraction of the total fluid volume V due to their size. This was described in Chapter 2. The exclusion phenomenon also applies for the pore volume, see Figure 5.4. The excluded volume V_E is indicated in the figure. The solute density n_1 is the number of solute molecules per unit volume. If the excluded volume is accounted for, the effective density increases. This gives rise to a definition of an additional solute density. The density in the available volume, $V_{AV} = V - V_E$, is called the *available density* $n_{1,AV}$. We will define this density as

$$
n_{1,AV} \stackrel{\text{def}}{=} X n_1 \quad . \qquad (5.15)
$$

Since X is equal to or larger than 1, the available density is obviously equal to or larger than n_1. It follows that the excluded volume is

$$
V_E = \left(1 - \frac{1}{X}\right) V \quad , \qquad (5.16)
$$

where V is the total fluid volume. We observe that when the dense gas effects are neglected, i.e. $X \to 1$, the excluded volume goes to zero, as we would expect. And as the dense gas effects increase, the excluded volume approaches the total fluid volume V.

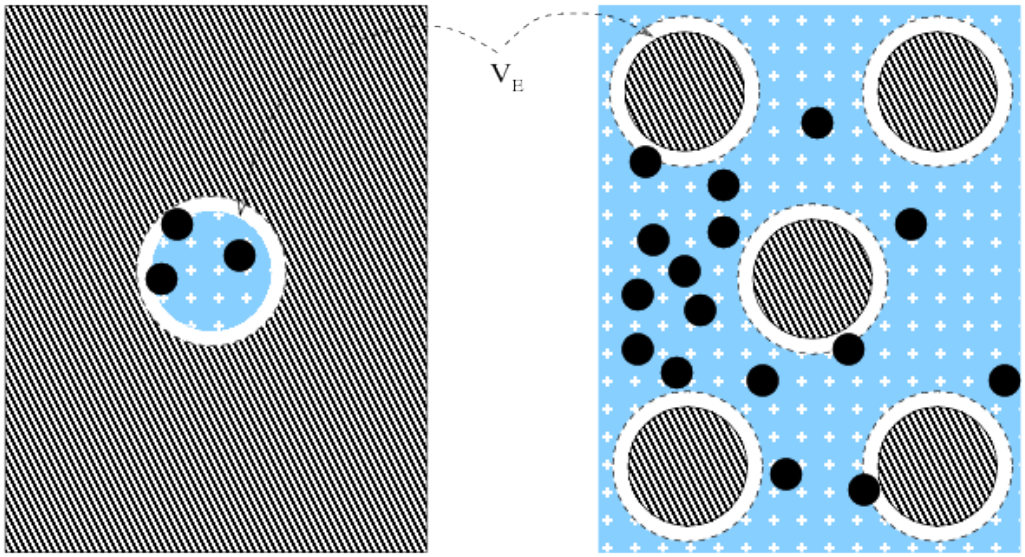

Figure 5.4: The solute is excluded from a certain fraction of the total fluid volume due to its molecular size. This volume is referred to as the *excluded volume* V_E. In a membrane pore (left) the excluded volume is the volume of a cylindrical shell, and in the interstitial compartment (right) the excluded volume is the volume of several spherical shells.

5.3.1 The X factor

We now briefly recall the origin of the X factor (5.7)

$$X = 1 + \frac{2\pi}{3}\left(\frac{d_1 + d_2}{2}\right)^3 \chi_{12} n_2 + \frac{2\pi}{3} d_1^3 \chi_{11} n_1 \quad .$$

The two last terms is due to corrections of the pressure tensor for dense gases. They therefore express *dense gas effects* on the pressure. These effects arose when we accounted for the molecular size of the solute in the derivation of the macroscopic equations in Chapter 4. Since the solute molecules are assumed large, as compared with water molecules or ions, their size is no longer negligible during particle interactions. The second term in X is due to $1-2$ (protein-matrix) interactions and the last term is due to $1-1$ (protein-protein) interactions. Without the dense gas effects the X factor is 1, i.e. no corrections to the pressure tensor.

5.4 A compartment model

In Section 5.1.1 we derived a general compartment equation. We will now use the evaluated flux expressions from Section 5.2 to obtain a compartment model for interstitial flow. A small adjustment for the solvent equation is needed, in accordance with the definitions of the fluxes (5.8). This implies an easy transfer from accumulated mass to accumulated volume in Equation (5.1.1), as it is assumed that the total solvent volume is almost equal the total volume V.

We then have 7 unknown variables in the system:

$n_{1,int}$	Interstitial solute density
P_{int}	Interstitial hydrostatic pressure
$M_{1,int}$	Total interstitial solute content
V_{int}	Total interstitial fluid volume
$n_{1,cap}$	Capillary solute density
P_{cap}	Capillary hydrostatic pressure
P_{ly}	Lymphatic hydrostatic pressure

The three last variables are assumed known. We are then left with 4 unknowns, and thus need 4 equations to close the system. Equation (5.2), evaluated for the solute and solvent respectively, provide us with two equations. In addition we have the definition of the interstitial mass density which relates $n_{1,int}$ to $M_{1,int}$ and V_{int}. To close the system we adopt an assumption from the article by Bert et al. [2]; interstitial hydrostatic pressure P_{int} is a (known) function of interstitial fluid volume V_{int}. We have thus obtained a compartment model for interstitial fluid flow.

Compartment model

$$
\begin{aligned}
\frac{d}{dt}V &= K'_{cap,m}\Big[\Delta_{cap,m}P - \sigma_{cap,m}\kappa T\Delta_{cap,m}(Xn_1)\Big] \\
&\quad - K'_{ly,m}\Delta_{ly,m}P \\
\frac{d}{dt}M_1 &= \left(\frac{1}{\nu_{1pw}+\nu_{1s}}\frac{S}{l}\right)_{cap,m}\kappa T\Delta_{cap,m}(Xn_1) \\
&\quad + m_1\overline{n}_{1,cap,m}(1-\sigma_{cap,m})(J_sS)_{in} - m_1\overline{n}_{1,ly,m}(J_sS)_{out} \\
m_1n_{1,int} &= \frac{M_1}{V} \\
P_{int} &= F(V)
\end{aligned}
\tag{5.17}
$$

Here $K'_m = \left(\frac{KS}{l}\right)_m$ is a filtration coefficient for the entire membrane, where S is the total membrane surface and l is the membrane thickness.

In Chapter 8 this model is expanded to also account for electrostatic exclusion effects.

Chapter 6

Electrostatics

The physiological composition of the interstitium makes it necessary to take a closer look at the electric properties of the medium. Although we consider the interstitium to be electroneutral, i.e. it does not have a net charge, each charged component of the interstitial matrix possesses a *local electric field*. In addition, the composition of the extracellular fluid will contribute to the effect of such fields. It is clear that certain interstitial properties, such as ionic density and pH-value, will affect how a possibly charged solute interacts with the interstitial matrix. In the present chapter we attempt to analyze the local electric field surrounding charged parts of the ECM. We will derive relevant, but general, equations for the behavior of such electric fields.

6.1 Basic equations

We will now study a simple system of charged particles. The system has a source sphere, or molecule, which is the main source to the electric field. In accordance with the notation used in Chapter 3 we will denote this sphere a 2-particle, or simply refer to *the source*. The source sphere is assumed to be fixed in space. The sphere is surrounded by a fluid which consists of small, point-like ions and water, see Figure 6.1. We assume the *electrostatic approximation* is valid.

The behavior of electrostatic fields are then described by two of Maxwell's equations, i.e. Gauss' law of the electric field

$$\nabla \cdot \mathbf{D} = \rho_f \quad , \tag{6.1}$$

and Faraday's law reduced to

$$\nabla \times \mathbf{E} = 0 \quad , \tag{6.2}$$

where $\mathbf{D}$ is the displacement vector, E is the electric field and ρ_f is the free charge density, which is the sum of all free charges of the system; $\rho_f = \sum_i q_i n_i$. In a homogeneous, linear and isotropic medium the displacement vector $\mathbf{D}$ can be written as $\epsilon_0 \kappa_d \mathbf{E}$, where ϵ_0 is the permittivity in vacuum and κ_d is the dielectric constant. Faraday's law (6.2) states that an electrostatic field is irrotational, which implies that the field is derived from an electric

potential, i.e $\mathbf{E} = -\nabla\phi$. Then Gauss' law (6.1) can be rewritten as the *Poisson equation* for the electric potential ϕ. The behavior of an electrostatic field is thus given by

$$\nabla^2\phi = -\frac{1}{\epsilon_0\kappa_d}\rho_f \quad . \tag{6.3}$$

This equation will consistently be used to find an electrostatic potential, assuming that the Displacement field $\mathbf{D}$ is linear on the entire domain. This implies that the dielectric constant κ_d is indeed constant on the entire domain.

6.2 Model equations

To find the electrostatic potential surrounding the source sphere we need to solve the Poisson Equation (6.3). First we assume that the source charge is uniformly distributed throughout the sphere. A spherical symmetry of the system with the origin placed in the source sphere center is therefore justified. This implies that the free charge ρ_f of the system is given by

$$\rho_f(r) = \begin{cases} \rho_{f,vol} & \text{for } r \leq a \\ (n_+ - n_-)e & \text{for } r > a \end{cases} \quad ,$$

where a is the radius of the sphere, n_+ and n_- is the density of positively and negatively charged (monovalent) ions respectively, and e is the elementary charge. The volume charge density $\rho_{f,vol}$ is constant and given in unit charges per unit volume.

Since the free charge ρ_f is a discontinuous function of r in general, we will solve for the two domains separately.

6.2.1 Internal solution

We solve for the internal domain where $r \leq a$. With the Laplacian operator written in spherical coordinates, the governing equations is

$$\frac{1}{r^2}\frac{d}{dr}\left(r^2\frac{d}{dr}\phi\right) = -\frac{1}{\epsilon_0\kappa_d}\rho_{f,vol} \qquad , \qquad r \leq a \quad .$$

It is a straight forward procedure to solve the equation. We obtain

$$\phi(r) = -\frac{1}{6\epsilon_0\kappa_d}\rho_{f,vol}r^2 + \frac{C_1}{r} + C_2 \qquad , \qquad r \leq a \quad .$$

6.2.2 External solution

The only free charge outside the source, i.e. for $r > a$, is the ionic charges. We will assume the ionic densities are given by the *Boltzmann distribution*, i.e.

$$n_i(r) = n_{i,0}e^{-\frac{q_i}{\kappa T}\phi(r)} \quad , \quad i = +, - \tag{6.4}$$

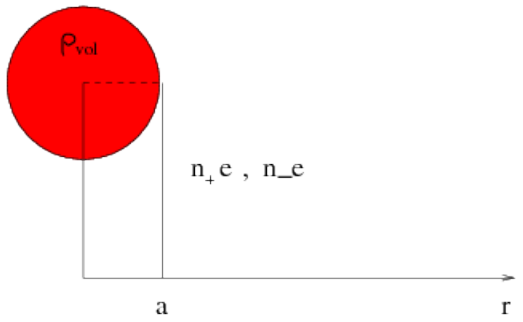

Figure 6.1: The charged source sphere of radius a is surrounded by water and small ions. A spherical symmetry in the electric potential is assumed, and thus, the potential is a function of r. The free charge of the system changes for $r = a$, and the potential must be found on the two domains separately. Inside the source sphere, $0 \leq r < a$, the free charge is uniformly distributed $\rho_{f,vol}$. Outside the source, $r > a$, the free charge is given by the density of anions n_- and cations n_+ times the unit charge e.
r = distance from source center.

where $q_i = \pm e$ for cations and anions respectively, and $n_{i,0}$ is a reference value where the potential $\phi = 0$. The reference value is taken to be far away from the source sphere. This assumption implies *local thermodynamic equilibrium* in the fluid. The Boltzmann distribution relates the ionic densities to the electric potential ϕ. A derivation of Boltzmann distribution from the equation of motion for ions is given in the Appendix A.3. We are able to solve this equation for large r, i.e. where $\phi \approx 0$. When ϕ is small we may expand the exponentials

$$n_i(r) \sim n_{i,0}\left[1 - \frac{q_i}{\kappa T}\phi(r) + \mathcal{O}(\phi^2)\right] \quad , \quad r \gg a \quad .$$

We apply the linear approximations and substitute for the ionic densities, n_+ and n_-. If we assume that the reference values of the ionic densities are equal, i.e. $n_{+,0} = n_{-,0} = n_0$, we obtain a governing equation

$$\frac{1}{r^2}\frac{d}{dr}\left(r^2\frac{d}{dr}\phi\right) = \frac{1}{\Lambda_d^2}\phi \quad , \tag{6.5}$$

where

$$\Lambda_d^2 = \frac{\epsilon_0\kappa_d\kappa T}{2n_0e^2} \quad . \tag{6.6}$$

The length Λ_d is called the *Debye length* and is a characteristic screening length for the medium. Again, it is a straight forward procedure to solve the equation.

$$\phi(r) = C_3\frac{1}{r}e^{-\Lambda_d^{-1}r} + C_4\frac{1}{r}e^{\Lambda_d^{-1}r} \quad , \quad r \gg a \quad . \tag{6.7}$$

6.2.3 Boundary conditions and matching

We have now obtained a solution for the potential on two domains separately. However, the solution for the external domain is only valid for large r. To obtain a solution for the entire domain we stretch the solution for the external domain inwards and match the two solutions at the source sphere interface $r = a$. We require both the potential function ϕ and also the derivative of the potential $r^2 \frac{d}{dr}\phi$, and hence the electric field , to match there. I.e. we require the potential ϕ to be *continuous to second order*:

$$\phi(a) = \lim_{r \to a^+} \phi(r) \quad , \quad a^2 \frac{d}{dr}\phi(a) = \lim_{r \to a^+} r^2 \frac{d}{dr}\phi(r) \quad .$$

In addition we have two boundary conditions. First we must require ϕ to be *finite* when $r \to 0$ and second, when $r \to \infty$ the potential must go to 0. The matching and the boundary conditions determines the coefficients in the solution. The potential on the entire domain is then found to be

$$\phi(r) = \begin{cases} \dfrac{1}{3\epsilon_0\kappa_d}\rho_{f,vol}\left[a^2\left(\dfrac{1}{2} + \dfrac{\Lambda_d}{a+\Lambda_d}\right) - \dfrac{1}{2}r^2\right] & \text{for } r < a \\ \dfrac{1}{3\epsilon_0\kappa_d}\rho_{f,vol}\dfrac{a}{r}\dfrac{a^2\Lambda_d}{a+\Lambda_d}e^{-\Lambda_d^{-1}(r-a)} & \text{for } r \geq a \end{cases} \quad . \tag{6.8}$$

6.3 Screening effect and dipole effect

If the source sphere had been placed in vacuum, or a completely neutral medium, then the free charge ρ_f would be zero on the external domain. The governing equation then reduces to the Laplace equation on this domain, i.e.

$$\frac{1}{r^2}\frac{d}{dr}\left(r^2\frac{d}{dr}\phi\right) = 0 \quad , \quad r > a \quad , \tag{6.9}$$

which has the solution

$$\phi(r) = \frac{A}{r} + B \quad , \quad r > a \quad .$$

It follows that the potential would fall as $\frac{1}{r}$ external to the sphere. The effect of positive and negative ions surrounding the sphere is therefore an *additional exponential fall*. This is known as the **screening effect**; the ions to some extent conceal the electric field from the external surroundings, or screen out the field, see Figure 6.2a. We will refer to the sphere as a *dressed source*[1] when we want to emphasize that the source sphere is placed in a non-neutral medium. The Debye length Λ_d (6.6) is to be interpreted as a measure of how fast (in space) the ions screen out the electric field. This length measure is therefore a property possessed by the medium surrounding the source charge, and is independent of the source charge itself.

[1] A *dressed particle* is a particle which includes the particle charge and its attendant polarization cloud [15]. The concept of dressed particles is used in plasma physics.

Although not carrying free charge, the water molecules also contributes to the electric field. The molecules are net neutral, however, their charge is distributed unevenly inside the molecule. One end of the molecule is carrying slightly more positive charge components than the other. Such molecules are known as *dipoles*. When placed in an electric field the water molecules are *polarized* and in the mean they turn one end pointing towards the source center, in the same manner as a compass needle, see Figure 6.2b. This is known as the **dipole effect**. The dimensionless dielectric constant κ_d is a measure of the dipole effect, for example is $\kappa_d \approx 75$ for water at 37 °C, while for a medium not containing dipoles $\kappa_d = 1$.

The dipole effect is quite complex where elements of the effect act in opposition to each other. This can be observed if we take a closer look at the electric potential (6.8) obtained above. By studying the Debye length Λ_d (6.6) we observe that

$$\uparrow \kappa_d \quad \Longrightarrow \quad \uparrow \Lambda_d \qquad , \qquad \Lambda_d \sim \sqrt{\kappa_d} \quad .$$

An increased Debye length implies both an increase in the ratio $\frac{\Lambda_d}{a+\Lambda_d}$ and an increase in the exponential $e^{-\Lambda_d^{-1}(r-a)}$. The potential range increases. As a consequence the dielectric effect can be interpreted as a weakening of the exponential damping of the potential, which act in opposition to the screening effect. However, at the same time the magnitude of the potential is reduced through the factor $\frac{1}{\kappa_d}$ in Equation (6.8). Hence, we can conclude that the dielectric effect to some extent levels out, or smooths the screening effect.

From the Debye length Λ_d (6.6) we also observe

$$\uparrow n_0 \quad \Longrightarrow \quad \downarrow \Lambda_d \qquad , \qquad \Lambda_d \sim \frac{1}{\sqrt{n_0}} \quad .$$

An increased ionic density leads to a decrease in the Debye length, which implies an intensified shielding of the source.

We have created a model of the source sphere to indicate how we interpret the screening effect and dipole effect on a microscopic level, see Figure 6.2. We choose the source charge to be negative in the model. In the region immediately outside the surface of the sphere there will be an excess of cations since the negative source charge attracts cations, as well as repels anions. There is established a diffuse layer of ions outside the source sphere where the distribution of ions is governed by the Boltzmann distribution (6.4). This approach may be seen in accordance with the Gouy-Chapman model from the theory of electric double layers EDL[2], to some extent.

6.4 Charge distributions

6.4.1 Surface charge

The total source charge Q is found by multiplying the volume charge density $\rho_{f,vol}$ with the volume of the source sphere $\frac{4\pi}{3}a^3$. Thus, assuming the charge is uniformly distributed

[2]see e.g. J. Cross [16]

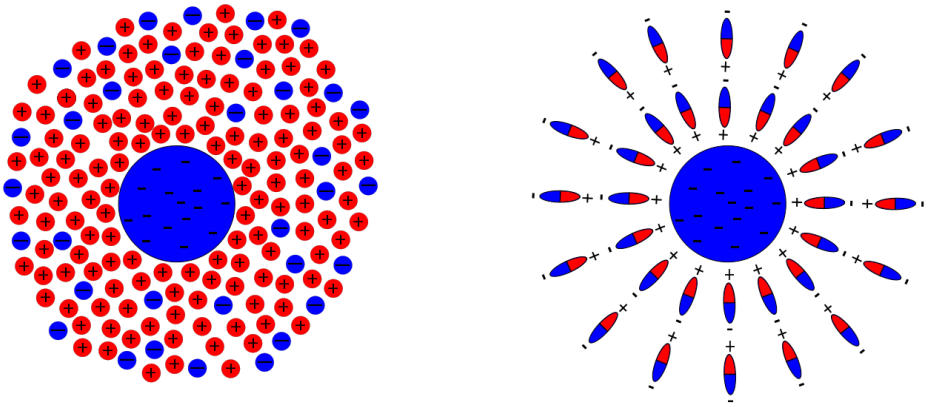

(a) Electrostatic shielding **(b)** Dipole effect

Figure 6.2: 6.2a: A negatively charged source sphere (large blue sphere) is screened by ions in the surrounding fluid. The density of cations (red) are high close to the source sphere and decreases away from the sphere, and opposite for anions (blue).
6.2b: The water molecules are small dipoles, and in the mean they turn one end pointing towards the source center, in the same manner as a compass needle. Although not indicated in the figure, the polarization is assumed equal inside the source sphere.

in the entire volume of the source sphere, implies that the total source charge goes like the sphere radius a to third power. However, it might be desirable that the charge does not increase that rapidly. We can account for this by assuming that the total source charge is placed at the surface of the source sphere instead. The distribution of the charge is assumed to be uniformly over the surface, as above. The free charge of the system is then modified to

$$\rho_f(r) = \begin{cases} 0 & \text{for } r < a \\ \sigma_{f,surf} & \text{for } r = a \\ (n_+ - n_-)e & \text{for } r > a \end{cases} ,$$

where $\sigma_{f,surf}$ is the surface charge density. The source charge Q is then $\sigma_{f,surf} \cdot 4\pi a^2$ which implies that Q increases as the radius a to second power as opposed to third power for the volume charge density. We shall update the electric potential (6.8) in accordance to this adjustment. We keep the total source charge constant, that is

$$\rho_{f,vol} \cdot \frac{4\pi}{3} a^3 = \sigma_{f,surf} \cdot 4\pi a^2 \qquad \Longrightarrow \qquad \rho_{f,vol} = \frac{3}{a}\sigma_{f,surf} \quad . \tag{6.10}$$

On the external domain the solution will not change. Outside the sphere the electric field is experienced as if all charge was placed in the center of the source [17], therefore the solution on this domain is similar for surface charge and volume charge as long as the total charge is kept constant. Hence, it is sufficient to substitute for the surface charge $\sigma_{f,surf}$ in accordance to (6.10) on the external domain.

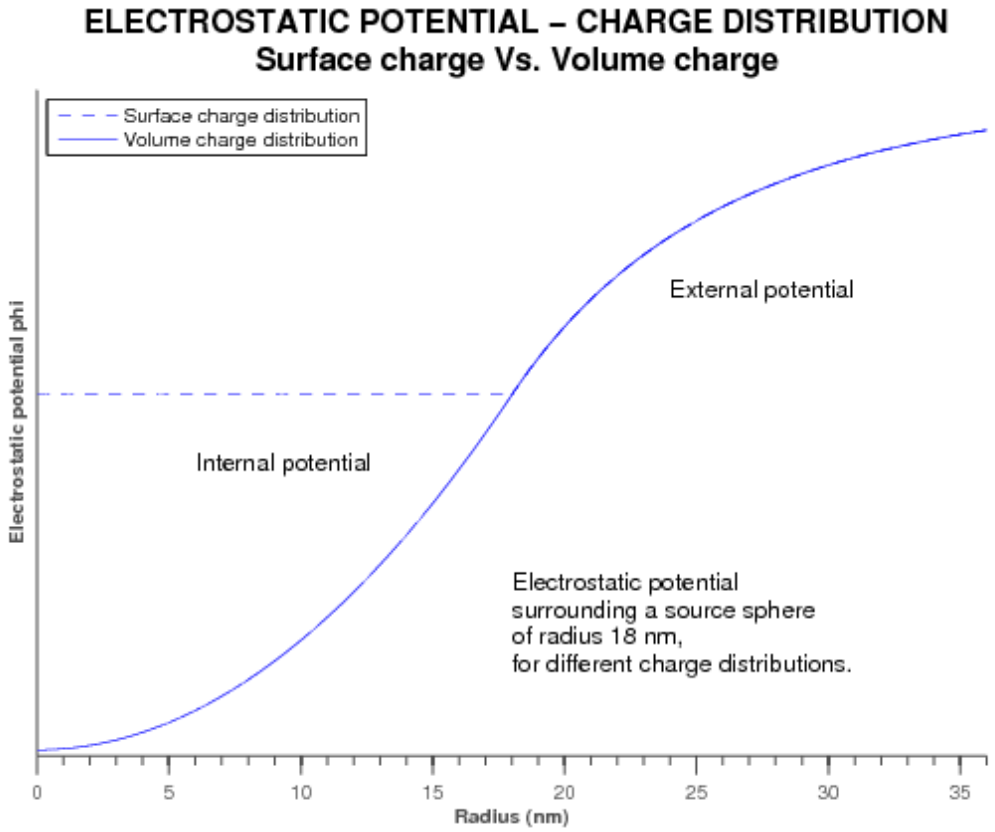

Figure 6.3: The potential surrounding a source sphere with volume charge or surface charge respectively. r = distance from source center.

On the internal domain the free charge is now zero, since the charge is placed at the surface, and the governing equation reduces to the Laplace Equation (6.9) for $r < a$, which was described in the preceding Section 6.3. Together with the boundary condition, that ϕ must be finite as $r \to 0$, this gives that the potential ϕ is constant on the internal domain. A first order matching of the two solutions at the sphere interface $r = a$ determines this constant to be the external value of ϕ as $r \to a^+$. A complete solution for the electric potential induced by a source sphere with surface charge is

$$\phi(r) = \begin{cases} \dfrac{1}{\epsilon_0 \kappa_d} \sigma_{f,surf} \dfrac{a\Lambda_d}{a + \Lambda_d} & \text{for } r < a \\ \dfrac{1}{\epsilon_0 \kappa_d} \sigma_{f,surf} \dfrac{1}{r} \dfrac{a^2 \Lambda_d}{a + \Lambda_d} e^{-\Lambda_d^{-1}(r-a)} & \text{for } r \geq a \end{cases} . \tag{6.11}$$

We have created two plots, see Figure 6.3, to illustrate the difference between the two cases; charge distributed in the entire volume and charge distributed at the surface of the sphere.

6.4.2 Spherical shell charge

As we observe in the plot for surface charge 6.3 the potential is now continuous to first order only. The electric field **E**, which is the gradient of ϕ, is discontinuous at the source sphere surface $r = a$. Since all charge components have a defined three dimensional size, the assumption that all the source charge is placed at the surface of the sphere is clearly nonphysical. We can account for this, and hence make the electric field continuous, by inserting a thin spherical shell of thickness δ at the surface of the source with all the charge distributed inside this shell, see Figure 6.4. Let the charge density in the shell be $\rho_{f,shell}$. The free charge ρ_f is then given as

$$\rho_f(r) = \begin{cases} 0 & \text{for } r \leq a \\ \rho_{f,shell} & \text{for } a < r < a + \delta \\ (n_+ - n_-)e & \text{for } r \geq a + \delta \end{cases} .$$

The density $\rho_{f,shell}$ is obviously a volume density which implies that the governing equation,

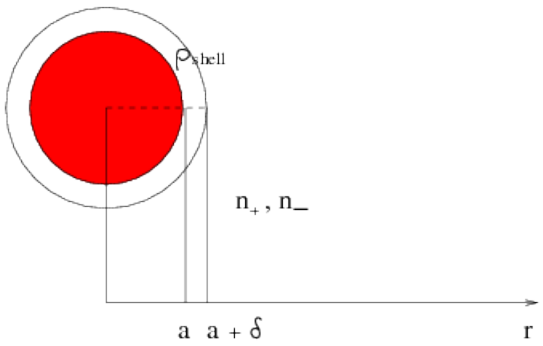

Figure 6.4: The charged spherical shell of thickness δ is surrounded by water and small ions. The free charge of the system changes for $r = a$ and $r = a + \delta$ and the potential must be found on the three domains separately. Inside the source sphere, $0 \leq r < a$, there are no free charges. In the spherical shell, $a < r < a + \delta$, free charge is uniformly distributed $\rho_{f,shell}$. Outside the source, $r > a + \delta$, the free charge is given by the density of anions n_- and cations n_+ times the unit charge e.
r = distance from source center.

and hence the solution for this region $a < r < a + \delta$ is similar as for the internal domain for volume charge described in Section 6.2.1.

On the internal domain $r < a$ the governing equation reduces to the Laplace Equation (6.9) for $r < a$. Together with the boundary condition, that ϕ must be finite as $r \to 0$, this implies that the solution $\phi(r)$ is constant on the internal domain, as for the internal solution for surface charge given in Section 6.4.1.

The governing equation for the external domain is similar as for volume charge, hence the solution ϕ is similar to Equation (6.7). The boundary condition $\phi \to 0$ as $r \to \infty$ implies that the coefficient in front of the positive exponential in that equation is zero. To sum up, we have

$$\phi(r) = \begin{cases} C_1 & \text{for } r < a \\ -\dfrac{1}{6\epsilon_0\kappa_d}\rho_{f,shell}r^2 + \dfrac{C_2}{r} + C_3 & \text{for } a < r < a+\delta \\ C_4\dfrac{1}{r}e^{-\Lambda_d^{-1}r} & \text{for } r \gg a+\delta \end{cases} .$$

In the same manner as we did for volume charge in Section 6.2.3 we require the solution to be continuous to second order, i.e. we require both $r^2\frac{d\phi}{dr}$ and ϕ to be continuous on the entire domain. The external solution is stretched inwards to match at the interface $r = a + \delta$. Continuity is also required at the interface $r = a$. The calculations are left to the Appendix A.4. The resulting solution for the potential ϕ surrounding a source sphere with spherical shell charge density is

$$\phi(r) = \begin{cases} \dfrac{1}{6\epsilon_0\kappa_d}\rho_{f,shell}\left[\dfrac{1}{a+\delta}\left((a+\delta)^3 + 2a^3 + \dfrac{2((a+\delta)^3 - a^3)}{1+(a+\delta)\Lambda_d^{-1}}\right) - 3a^2\right] & \text{for } r < a \\ \dfrac{1}{6\epsilon_0\kappa_d}\rho_{f,shell}\left[\dfrac{1}{a+\delta}\left((a+\delta)^3 + 2a^3 + \dfrac{2((a+\delta)^3 - a^3)}{1+(a+\delta)\Lambda_d^{-1}}\right) - \dfrac{1}{r}(r^3+2a^3)\right] & \text{for } a < r < a+\delta \\ \dfrac{1}{3\epsilon_0\kappa_d}\rho_{f,shell}\left((a+\delta)^3 - a^3\right)\dfrac{1}{1+(a+\delta)\Lambda_d^{-1}}\dfrac{1}{r}e^{-\Lambda_d^{-1}(r-(a+\delta))} & \text{for } r > a+\delta \end{cases} ,$$

which is continuous to second order. The above expression for ϕ is valid for all values of δ since no restrictions have been placed on that parameter. A plot for the potential for different δ is given in Figure 6.5. However, it is a quite complex expression to work with. Therefore, since we only are interested in small δ values, we can first expand the potential (6.4.2) in terms of powers of δ, secondly let $\delta \to 0$ and obtain a zeroth order approximation. It is shown in the Appendix A.4 that the expression then obtained, equals the expression for ϕ with surface charge (6.11) given in Section 6.4.1. Hence, expression (6.11) is a good approximation, mathematically, for the potential ϕ surrounding a source sphere with spherical shell charge density. Thus,We will therefore use this expression in further studies.

6.5 Potential energy

In the preceding sections we have derived an expression for the electric potential ϕ, and hence the electric field $\mathbf{E}$, surrounding a *dressed source sphere*. It was found to be

$$\phi(r) = \begin{cases} \dfrac{1}{4\pi\epsilon_0\kappa_d}Q\dfrac{\Lambda_d}{a+\Lambda_d}\dfrac{1}{a} & \text{for } r < a \\ \dfrac{1}{4\pi\epsilon_0\kappa_d}Q\dfrac{\Lambda_d}{a+\Lambda_d}\dfrac{1}{r}e^{-\Lambda_d^{-1}(r-a)} & \text{for } r \geq a \end{cases} , \tag{6.12}$$

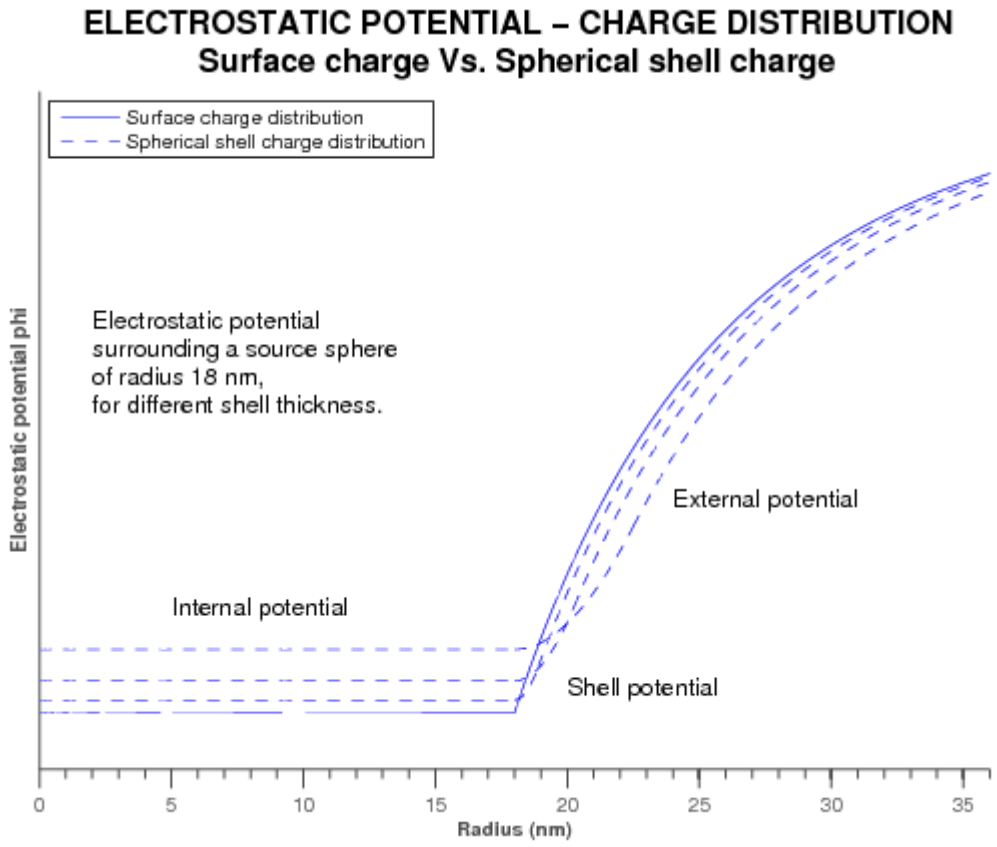

Figure 6.5: The potential surrounding a source sphere of radius $a_2 = 18$ nm, with the free charge distributed in a spherical shell of thickness δ. In the plot δ is set to $a_2/4$, $a_2/8$ and $a_2/20$ respectively.

here expressed by the total source charge Q.

Let us now assume that another, possibly charged, particle enters the domain. Again, in accordance with the notation used in Chapter 3 we will denote this particle as a 1-particle, or simply refer to it as *the enterer*. Subscripts 2 refer to the source sphere. The electric field $\mathbf{E}$ exerts a force on a charged particle, given by

$$\mathbf{F} = q_1 \mathbf{E} \quad ,$$

where q_1 is the particle charge. The force tells us how the particle is affected by the field. However, an entering particle carrying a charge has an *electrostatic potential energy* V_p in the electrostatic potential generated by the source. It might be desirable to study the potential energy V_p rather than the electrostatic force $\mathbf{F}$. The potential energy of the enterer with charge q_1 is

$$V_p(r) = q_1 \phi(r) \quad , \tag{6.13}$$

given that the enterer is a point-like particle. However, if the particle is not point-like and we assume that all its charge is placed on the surface of the particle the expression for the potential energy will modify to

$$V_p = \int \rho_{f,1}(\mathbf{r}) \phi(\mathbf{r}) \, \mathrm{d}\mathbf{r} \qquad , \qquad \rho_{f,1} = \sigma_1 \delta(\mathbf{r} - \mathbf{R} - \mathbf{a_1}) \quad , \tag{6.14}$$

where $\rho_{f,1}$ is the charge density and is given by the Delta function. For a geometric

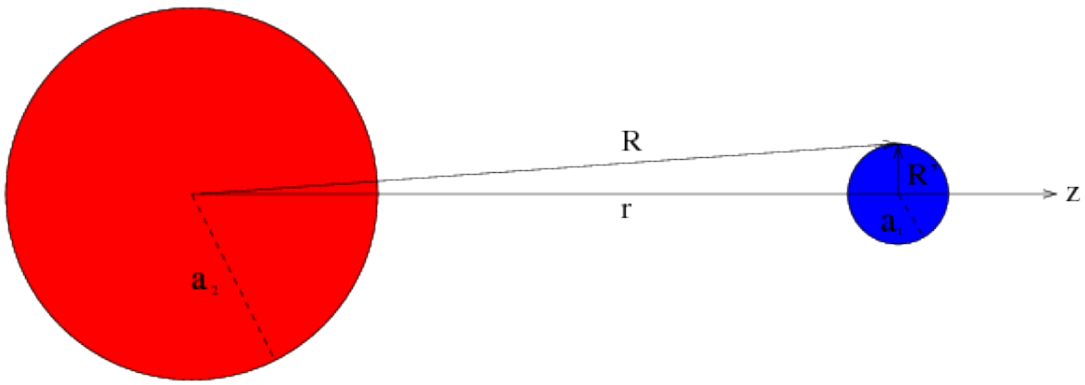

Figure 6.6: A particle with radius a_1 (blue) moves in the electrostatic field surrounding a source sphere of radius a_2 (red). The distance between their centers is r. R is the distance from the source center to an arbitrary point on the surface of the entering particle.
z = distance from the source center.

interpretation of the expressions (6.14) see Figure 6.6. However, as a first attempt, an

expression for the electrostatic potential is obtain by considering the entering particle a point like particle as compared to the source sphere. This approximation is valid whenever the enterer is much smaller than the source sphere, i.e. $a_1 \ll a_2$. The subscripts 2 and 1 refer to the source and the enterer respectively. The potential energy of the entering particle outside the source sphere is then given by (6.13) and is found to be

$$V_p(r) = \frac{1}{4\pi\epsilon_0\kappa_d} Q_2 \frac{\Lambda_d}{a_2 + \Lambda_d} q_1 \frac{1}{r} e^{-\Lambda_d^{-1}(r-a_2)} \quad , \quad r \geq a_2 \quad , \tag{6.15}$$

where q_1 is the total charge of the entering particle.

Chapter 7

Electrostatic Interaction Model Results and Comparison with Experimental Data

In the preceding chapter we obtained an expression for the electrostatic potential ϕ surrounding a source sphere. We also obtained an expression for the electrostatic potential energy V_p of an additional particle entering the domain. The motivation for deriving these expressions is to apply them to our physiological system, and then, hopefully, be able to investigate electrostatic properties of the interstitium. In the present chapter we aim to study how certain interstitial properties, such as ionic strength and pH-value, affect possibly charged macromolecules entering the interstitial domain.

7.1 Model simplifications

In most cases, to be able to model a physical system several properties of the system must be omitted, or at least simplified. Our aim is to use a simplified model to study some of the properties of our physical system. Results obtained based on simplifying assumptions will hopefully show *qualitative* similarities to real-life studies. In the following section the chosen model simplifications are presented, and justified. The assumptions are presented point by point.

7.1.1 GAG

The interstitial matrix consists of several components, mainly collagen fibers and glycosaminoglycans, or GAGs. GAGs are strongly negatively charged in the interstitium, and thereby possess local electric fields around GAG molecules. The present study will focus on proteins interacting with GAGs, and will use a single idealized protein-GAG interaction as a model.

The interstitial fluid surrounds the GAG molecules, and the fluid composition will

affect the electric potential. A description of glycosaminoglycans is given in Chapter 2. They exist in the interstitium as long chained molecules (hyaluronans) or as large branched GAG and protein combinations (proteoglycans). However, the quartenary structure of the molecules is not known exactly. To be able to model these molecules we assume that they take on the shape of a sphere:

- Spherical shape
- Internal ions are neglected

One could think that the long polysaccharide chains curl up and take on the shape of a sphere, see Figure 7.1. This assumption implies that the model GAG sphere also contains

Figure 7.1: The long GAG molecules are assumed to curl up and take on the shape of a sphere of radius a_2. The effect of small ions inside the sphere on the external electric field, is neglected.

a varying amount of water and small solutes, however, we will assume that the ionic charge contribution to the potential is negligible inside the sphere.

- Solid sphere

For simplicity we make the assumption that the model GAG sphere is impermeable to other macromolecules, i.e. proteins. The hyaluronan molecule is then considered a *solid sphere*. This assumption is especially problematic considering the effect of hydration. We will return to this later.

- Surface charge (negative)

We will also assume that the negative charge held by hyaluronan is uniformly distributed on the surface of the sphere. In the previous chapter, however, we showed that it is not how the charge is *distributed* in the sphere but the *total* charge held by the sphere that affects the potential outside the sphere.

- No overlapping potentials

We will assume that the different GAG molecules are placed far away from each other, sufficient to make us able to look at a single sphere and the corresponding potential without considering effects of overlapping potentials.

- Spherical symmetry

A spherical symmetry of the electric field is justified by the above assumptions.

- Fixed in space

Since the large glycosaminoglycan molecules are entrapped in the structural matrix in the interstitium, we regard them as fixed in space.

7.1.2 Proteins

The quartenary structure of proteins are well known in general. The proteins considered in this thesis are all globular proteins with a well defined hydrodynamic radius. It is therefore a reasonable assumption to model the proteins as spheres.

- Globular proteins → spherical shape
- Surface charge (negative)

A possible net charge on the proteins is again assumed to be placed on the surface of the protein. I addition to neutral proteins, we restrict ourselves to look at proteins of negative polarity.

- Solid sphere

The proteins will also be considered as solid spheres.

7.1.3 Energy

We further assume a thermodynamic equilibrium of the fluid. This implies that the velocity distribution for the molecules tend to the Maxwellian. It can be shown that the mean velocity squared is then $\overline{v^2} = 3\frac{\kappa T}{m}$, where T is the temperature in the fluid, m is the mass of the molecule and κ is the Boltzmann constant [13]. Hence, the mean kinetic energy of a molecule in a fluid at temperature T is found to be

$$\overline{E_k} = \frac{1}{2}m\overline{v^2} = \frac{3}{2}\kappa T \quad .$$

This energy is often referred to as a *thermal energy*.

- Proteins enter the electric field domain with thermal energy: $E_k = \frac{3}{2}\kappa T$
- Ion interactions are neglected

The square root of the mean square velocity is denoted thermal velocity v_{th}. It depends on the mass m, i.e. $v_{th} = \sqrt{\frac{3\kappa T}{m}}$. This implies especially that ions and water molecules move around in the fluid at a much higher velocity than proteins, which are much larger molecules, in the mean. However, we will neglect ion interactions since they happen on a much shorter timescale and therefore reach an equilibrium state much faster than the proteins.

- Energy transfer is neglected

At a single GAG-protein encounter, at most a fraction $\frac{m_1}{m_2}$ of the kinetic energies involved can be transferred [15], where m_1 is the mass of a protein and m_2 is the mass of a GAG. Therefore, if we assume that the GAG molecules are much heavier than the proteins, i.e. $m_2 \gg m_1$, we may neglect the energy transfer between the GAG and the protein.

- Head-on velocity

We assume for simplicity that the velocity is pointing towards the center of the GAG.

7.1.4 Excluded volume

In our single GAG-protein model we will calculate the *excluded volume*. This volume is the volume of which the center of the protein is unable to move in, additional to the volume of the GAG sphere. See Figure 7.2a.

The assumptions made in previous sections imply that the protein is always excluded from a certain fraction of the total volume due to its size a_1. This excluded volume is referred to as *steric exclusion*. If the distance from which the protein is repelled is bigger than the sum of the GAG and protein radii, i.e. a_2+a_1, then the excluded volume additional to the steric exclusion is referred to as *electrostatic exclusion*. See Figure 7.2b.

7.1.5 Hydration

The model GAG spheres contain a various amount of fluid, as described above. When the tissue is hydrated the total fluid volume in the interstitium increases. This is assumed to imply an increased amount of fluid also inside the GAG sphere. Therefore, we attempt to model the effect of hydration by increasing the radius of a GAG sphere. See Figure 7.3.

- Hydration leads to a larger GAG sphere

From Equation (6.12) in Chapter 6 we observe how an increased model sphere radius a_2 affects the electric potential surrounding it. The internal potential decreases and the exponential damping of the external potential decreases. We have created a plot to illustrate this, see Figure 7.4.

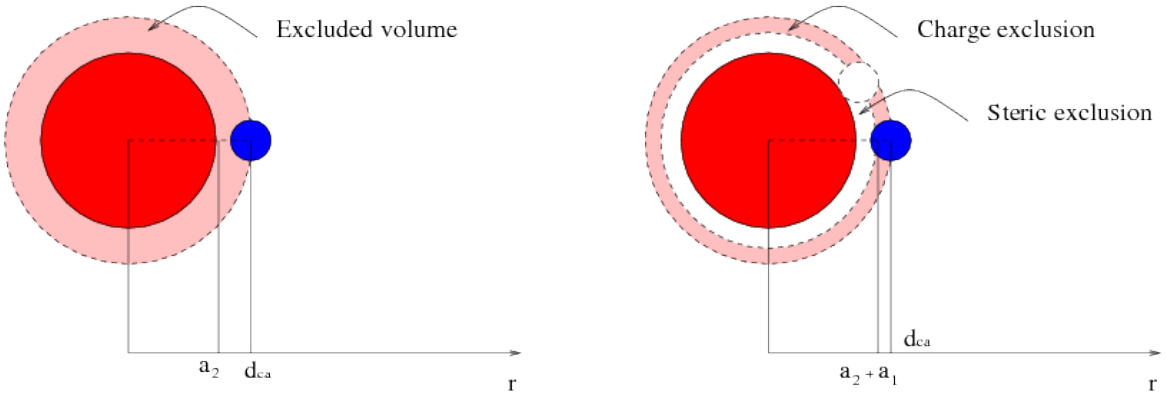

(a) Exclusion **(b)** Steric and electrostatic exclusion

Figure 7.2: A protein (blue) is repelled at a certain distance outside the GAG (red). This distance d_{ca} is called the distance of closest approach.
r = distance from center of GAG.
a_2 = radius of GAG.
a_1 = radius of protein.
7.2a: The excluded volume outside a GAG sphere is indicated in pink.
7.2b: Steric exclusion (white) is due to the molecular size of the protein. Additional exclusion is due to possible molecular charge of the protein, and is referred to as electrostatic exclusion (pink).

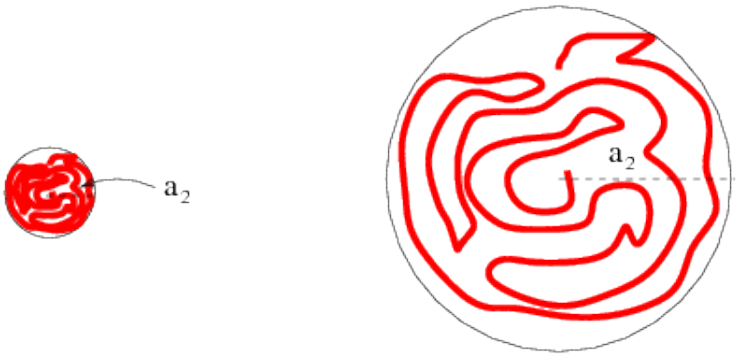

Figure 7.3: The GAG sphere increases in size as more fluid (water and small ions) enter the sphere. This process is referred to as hydration. In the model the total GAG charge is kept constant during hydration. A hydrated GAG sphere is seen to the right.
a_2 = radius of GAG.

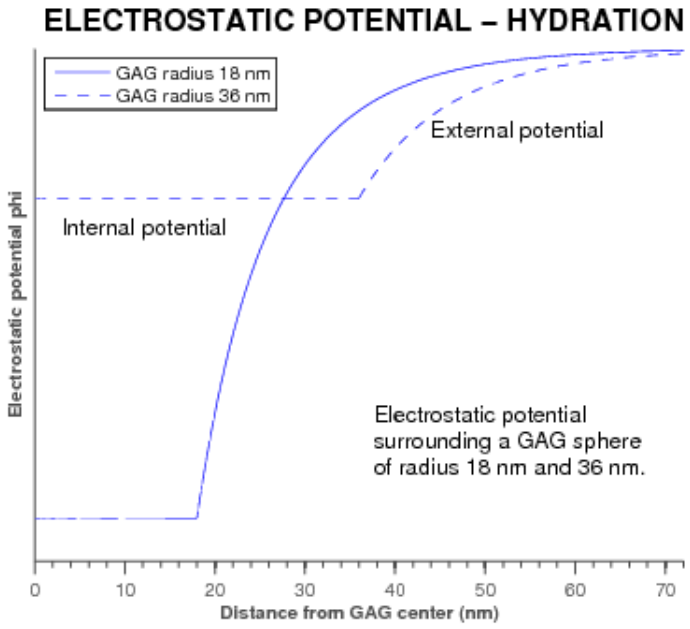

Figure 7.4: The electrostatic potential varies with the radius of the GAG sphere (hydration). The blue curve represents a more hydrated GAG sphere than the red curve. We observe that outside the GAG, the potential is weaker for the hydrated sphere.

7.2 Model equation

In this section we will study a single GAG-protein system, see Figure 7.5. The system

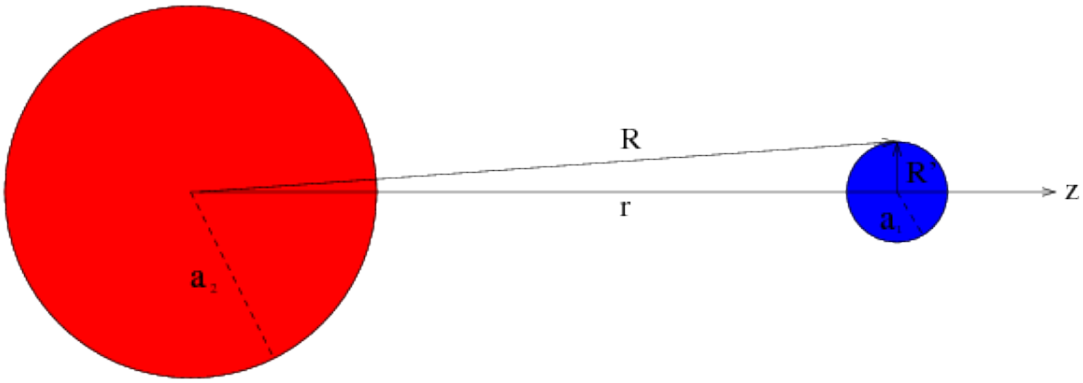

Figure 7.5: A protein with radius a_1 (blue) moves in the electrostatic field surrounding a GAG sphere of radius a_2 (red). The distance between their centers is r, and R is the distance from the source center to an arbitrary point on the protein surface. (The figure is a reproduction of Figure 6.6 in Chapter 6).
z = distance from GAG center.

considered is a GAG sphere fixed in space and a protein which enters the domain with an initial kinetic energy

$$E_{k,init} = \frac{3}{2}\kappa T \quad . \tag{7.1}$$

The protein will experience a force due to the electric field, $\mathbf{F} = q_1\mathbf{E}$, where q_1 is the protein charge. The force is repulsive since the protein charge and GAG charge both are negative, and is obviously zero if the protein is neutral. The magnitude of the force increases as the protein approaches the GAG. This also means that the kinetic energy of the protein is transformed into potential energy. We may use the principle of conservation of energy to calculate how close to the GAG the protein is able to reach[1].

The distance from the GAG center at which the protein is repelled is known as the *distance of closest approach* d_{ca} and is a fundamental length in plasma physics [2], together with the Debye length (6.6). In a plasma[3] the Debye length is much greater than the

[1]This approach is somewhat similar to an approach made in Tanenbaum's Plasma Physics [18] on the derivation of the scattering angle for a particle interaction.

[2]The distance of closest approach is defined e.g. in Tanenbaum's Plasma Physics [18].

[3]Note that a plasma in this context is not a physiological plasma. Definitions of a physical plasma is found in many books on plasma physics, see e.g. Delcroix' Plasma Physics[13].

distance of closest approach, however, in our medium one might expect them to be of more comparable sizes since the temperature is significantly lower. Since we have neglected the energy transfer between protein and GAG, conservation of energy in the protein-GAG system leads to conservation of energy for the protein alone.

$$E_k(r) + V_p(r) = E_{total} \quad , \quad \forall r \quad .$$

In the previous Chapter 6 we obtained an expression for the potential energy of a protein. This was found to be

$$V_p(r) = \frac{1}{4\pi\epsilon_0\kappa_d} Q_2 \frac{\Lambda_d}{a_2 + \Lambda_d} q_1 \frac{1}{r} e^{-\Lambda_d^{-1}(r-a_2)} \quad , \quad r \geq a_2 \quad .$$

We are then able to calculate how close the particle can approach the GAG before it is repelled. For a given q_1 we find which r that solves

$$V_p(r) - E_{k,init} = 0 \quad .$$

If the equation has a solution for $r > a_2 + a_1$, i.e. the protein is repelled before it collides with the solid GAG sphere, this solution is the distance of closest approach d_{ca} for the protein-GAG system. If the equation does not have a solution on this domain, e.g. if the protein charge q_1 is zero, it is assumed that the protein hits the GAG sphere and is repelled at distance $r = a_2 + a_1$.

$$d_{ca} : \begin{cases} \frac{1}{4\pi\epsilon_0\kappa_d} Q_2 \frac{\Lambda_d}{a_2 + \Lambda_d} q_1 \frac{1}{r} e^{-\Lambda_d^{-1}(r-a_2)} - \frac{3}{2}\kappa T = 0 & \text{if solution exist for} \quad r > a_2 + a_1 \\ a_2 + a_1 & \text{else} \end{cases} . \tag{7.2}$$

Several parameters in the equation will affect the d_{ca} computed, e.g. protein charge q_1, GAG size and charge a_2, Q_2 and Debye length Λ_d. Equation (7.2) will be the model equation for our study.

7.3 Charge effects

In addition to the protein charge q_1 and the GAG radius a_2, several parameters affect the solution to the above Equation (7.2). In the following section we will focus on the effect of two specific parameters, namely the ionic density and the pH-value of the fluid. Equation (7.2) will be our model equation for this study.

Test proteins

For our study we have created a set of illustrative proteins of varying size and charge, see Table 7.1. Hopefully this set will capture a relevant span in protein size and charge. The proteins are referred to as *test particles*. The charge is given in unit charges, i.e. number of electron charges.

	radius a_1 (nm)	charge q_1 (e)
Small	1.5	-2.5
	1.5	-12.5
	1.5	-25
Medium	4.5	-2.5
	4.5	-12.5
	4.5	-25
Large	7.5	-2.5
	7.5	-12.5
	7.5	-25

Table 7.1: Radius and charge for test particles.

7.3.1 Ionic density n_0

In Chapter 6 we briefly showed how the Debye length (6.6) varied with the number density for ions n_0. We recall the Debye length

$$\Lambda_d^2 = \frac{\epsilon_0 \kappa_d \kappa T}{2 n_0 e^2} \quad . \tag{7.3}$$

An increased number density gives a shorter Debye length which implies a stronger shielding of the GAG charge. For instance if the number density is increased by a factor 10, this corresponds to a decrease of the Debye length by a factor $\frac{1}{3}$, approximately.

When we derived the expression for the Debye length in Chapter 6, it was assumed that the number density of cations n_+ and anions n_- were approximately equal at a distance sufficiently far away from the GAG. Thus, the ionic number density n_0 included in the expression (7.3) is the density of both cations and anions as they are assumed equal, $n_+ = n_- = n_0$.

In medical terms ionic density, or ionic strength, is given in milli Moles per liter, $\frac{\text{mmol}}{\text{L}}$. This easily adopts to our number density by multiplication with Avogrado's number, N_A, which is the number of molecules in 1 mole.

$$n_0 \quad \left(\frac{1}{\text{m}^3}\right) \quad = \quad \text{ionic strength} \quad \left(\frac{\text{mmol}}{\text{L}}\right) \cdot N_A \quad \left(\frac{1}{\text{mol}}\right) \quad .$$

In the interstitium we assume normal value for ionic strength is 150 $\frac{\text{mmol}}{\text{L}}$. An interval for variation of the ionic density, hopefully relevant for physiological data, is suggested to be

$$\text{ionic strength} \quad \in \quad \left[50, 500\right] \frac{\text{mmol}}{\text{L}} \quad . \tag{7.4}$$

7.3.2 pH-value

One may intuitively assume that the pH-value also affects the d_{ca}. It is not, however, intuitive to understand how it is affected. In Chapter 2 the GAG molecules were described.

They are large molecules built up of amino sugar units that contain carboxcylic acid groups. These acid groups will dissociate into protons (H^+) and negatively charged carboxylate groups (A^-) as the pH increases. It is therefore assumed that glycosaminoglycans follow the general acid-base equilibrium

$$HA \quad \rightleftharpoons \quad H^+ \quad + \quad A^- \quad . \tag{7.5}$$

According to Le Chatelier's Principle, if the equilibrium is disturbed, e.g. an increase in the H^+-density, it shifts to the left to counteract the disturbance. The pH-value is a measure of the number of H^+ ions present in a fluid volume,

$$\mathrm{pH} = -\log[H^+] \quad .$$

Hence, as the pH value in the fluid drops, the number of H^+ ions increases, and the equilibrium 7.5 is shifted to the left. This implies that the total GAG charge decreases as the pH value drops.

At physiological pH, i.e. pH 7.4, all the acid groups on a GAG are negatively charged [5]. Furthermore, we assume that GAGs are neutral at pH around 4.5.

In the model GAG all the charge is placed at the surface of the GAG sphere. Free hydrogen ions H^+ in the fluid move around much faster than heavier molecules, and they 'bombard' the surface of the GAG molecules. Since an increased H^+-density implies a decreased GAG charge Q_2, it is assumed that the GAG charge is negative proportional to the net flux of hydrogen ions on the GAG surface, i.e. $Q_2 \sim -10^{-\mathrm{pH}}$. Together these assumptions relates the total GAG charge and the pH value as

$$Q_2(pH) = Q_{2,max}\left[\frac{1-10^{-(pH-4.5)}}{1-10^{-(7.4-4.5)}}\right] \quad , \tag{7.6}$$

where $Q_{2,max}$ is the GAG charge at $pH = 7.4$ (fully charged). We will assume that $Q_{2,max} = 50000$. In Figure 7.6 it is shown how the GAG charge varies with pH.

The normal value for pH is obviously set to physiological pH, which is 7.4. We let the pH vary from 4.5, where hyaluronans are neutral, to physiological pH, i.e.

$$\mathrm{pH} \quad \in \quad \Big[4.5, 7.4\Big] \quad . \tag{7.7}$$

Remark

It is assumed that the GAGs are fully charged at pH 7.4*. However, it might be the case that they are fully charged at a lower pH value, for instance at pH* 6 *or* 7*. A further increase in the pH towards pH* 7.4 *will not affect the charge, and the GAG charge curve in Figure 7.6 will thus be steeper.*

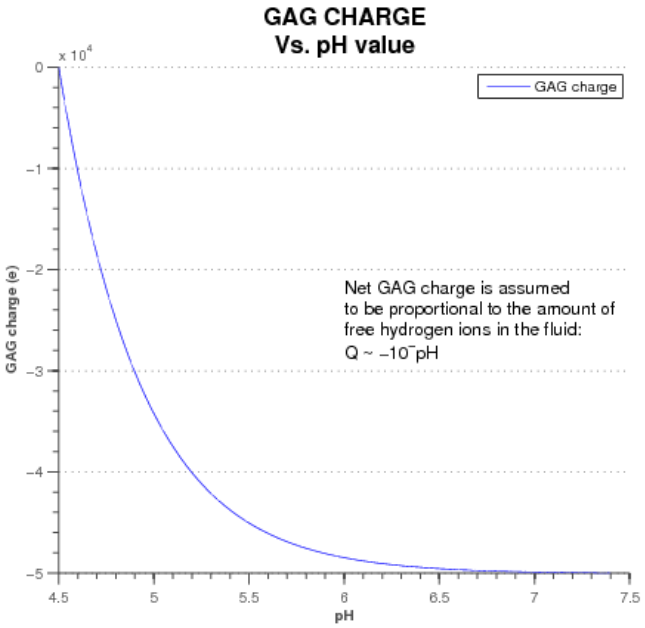

Figure 7.6: The GAG charge varies with pH, and is assumed to follow Equation (7.6). At physiological pH, i.e. $pH = 7.4$, the GAG is fully charged, which is assumed to be 50000 negative unit charges. As pH drops the GAG charge decreases in accordance with Le Chatelier's Principle. At $pH = 4.5$ the GAGs are neutral.

7.4 Results

The distance of closest approach d_{ca} is computed from Equation 7.2[4]. The result is related to the effective protein radius $a_{1,eff}$. If the excluded volume of a protein coincides with the steric excluded volume of a larger sphere, then the *effective radius* of the protein equals the radius of the larger sphere, i.e. $a_{1,eff} = d_{ca} - a_2$, see Figure 7.7. It follows that the

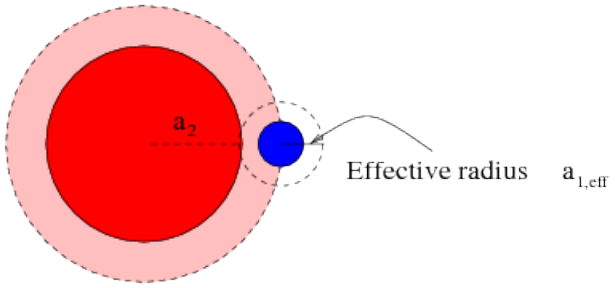

Figure 7.7: The excluded volume of the protein (blue) coincides with the steric excluded volume of a larger sphere (dotted). Thus, the effective radius of the protein $a_{1,eff}$ equals the radius of the larger sphere.
a_2 = radius of GAG.

effective radius is greater than or equal to the real protein radius.

In this section the result of our electrostatic study is presented.

[4]The model is implemented in Matlab.

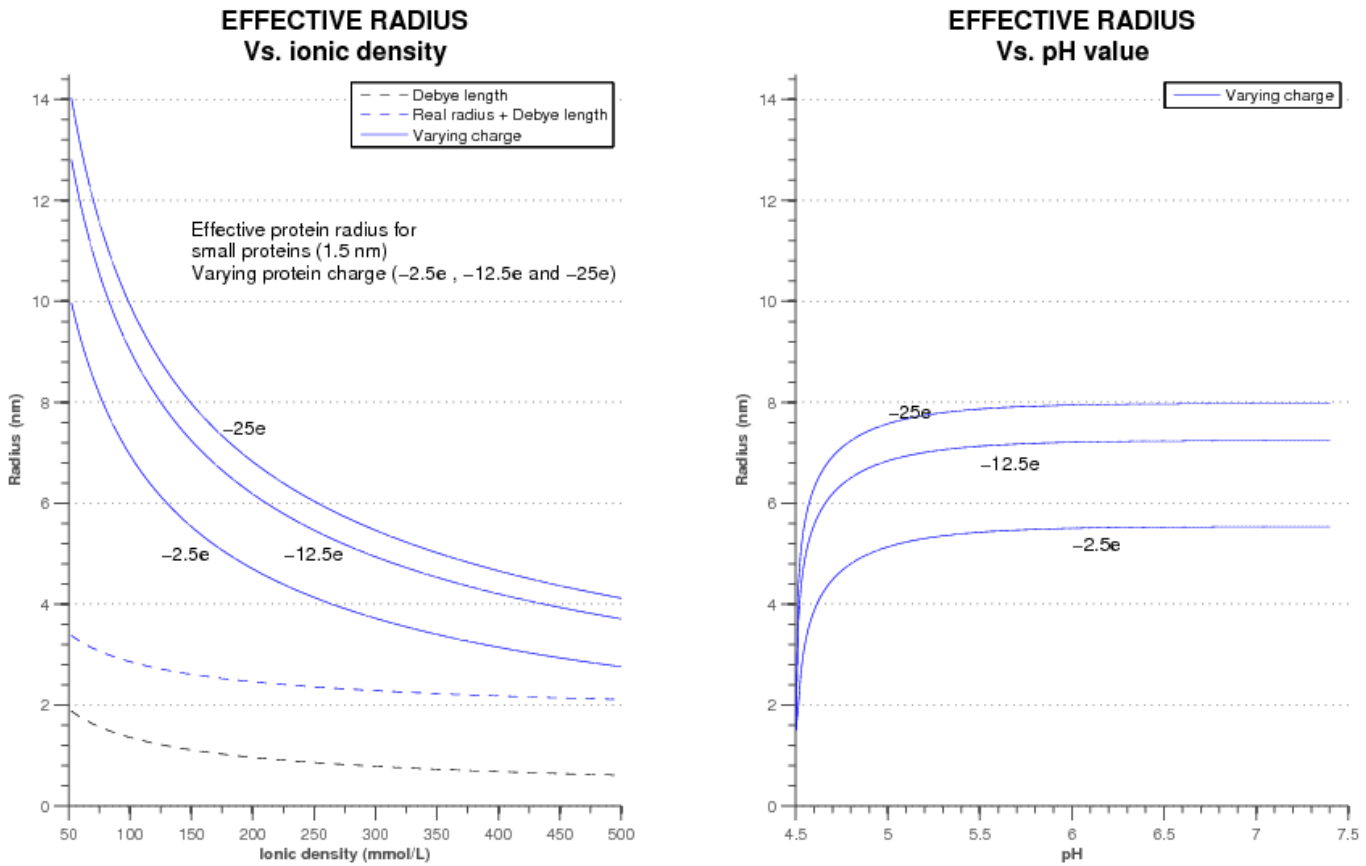

Figure 7.8: The electrostatic exclusion effect is studied for small test particles ($a_1 = 1.5$ nm) of varying charge ($q_1 = -2.5e, -12.5e, -25e$). The effective radius $a_{1,eff}$ is computed for varying ionic density in the left plot, and for varying pH in the right plot. The Debye length Λ_d varies with the ionic density, seen in the left plot. In addition, the Debye length is added to the radius of the test particles $a_1 + \Lambda_d$ and indicated in the plot.

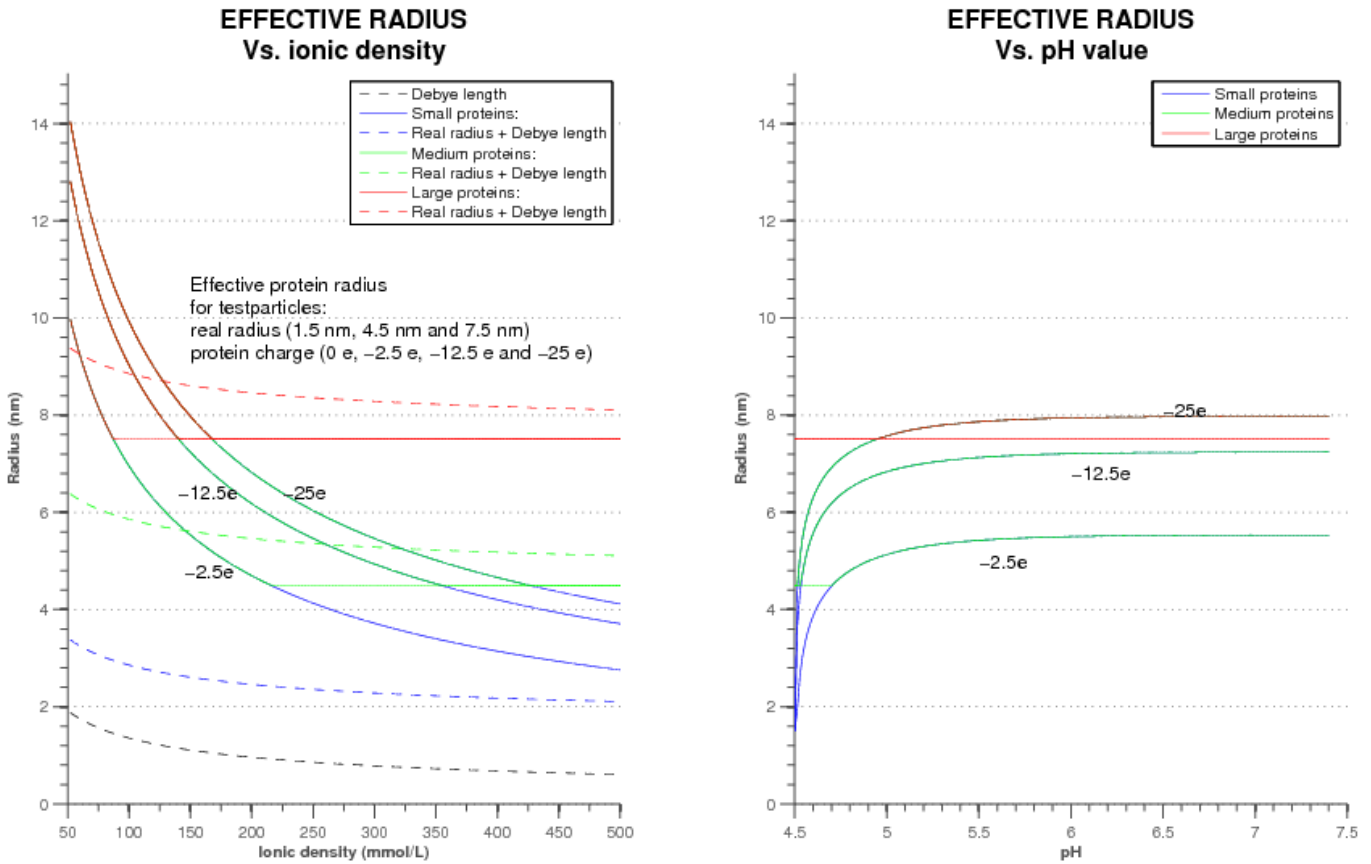

Figure 7.9: The electrostatic exclusion effect is studied for all test particles (a_1 = 1.5 nm, 4.5 nm, 7.5 nm) of varying charge ($q_1 = -2.5e, -12.5e, -25e$). The effective radius $a_{1,eff}$ is computed for varying ionic density in the left plot, and for varying pH in the right plot. The Debye length Λ_d varies with the ionic density, seen in the left plot. In addition, the Debye length is added to the radius of the test particles $a_1 + \Lambda_d$ and indicated in the plot.

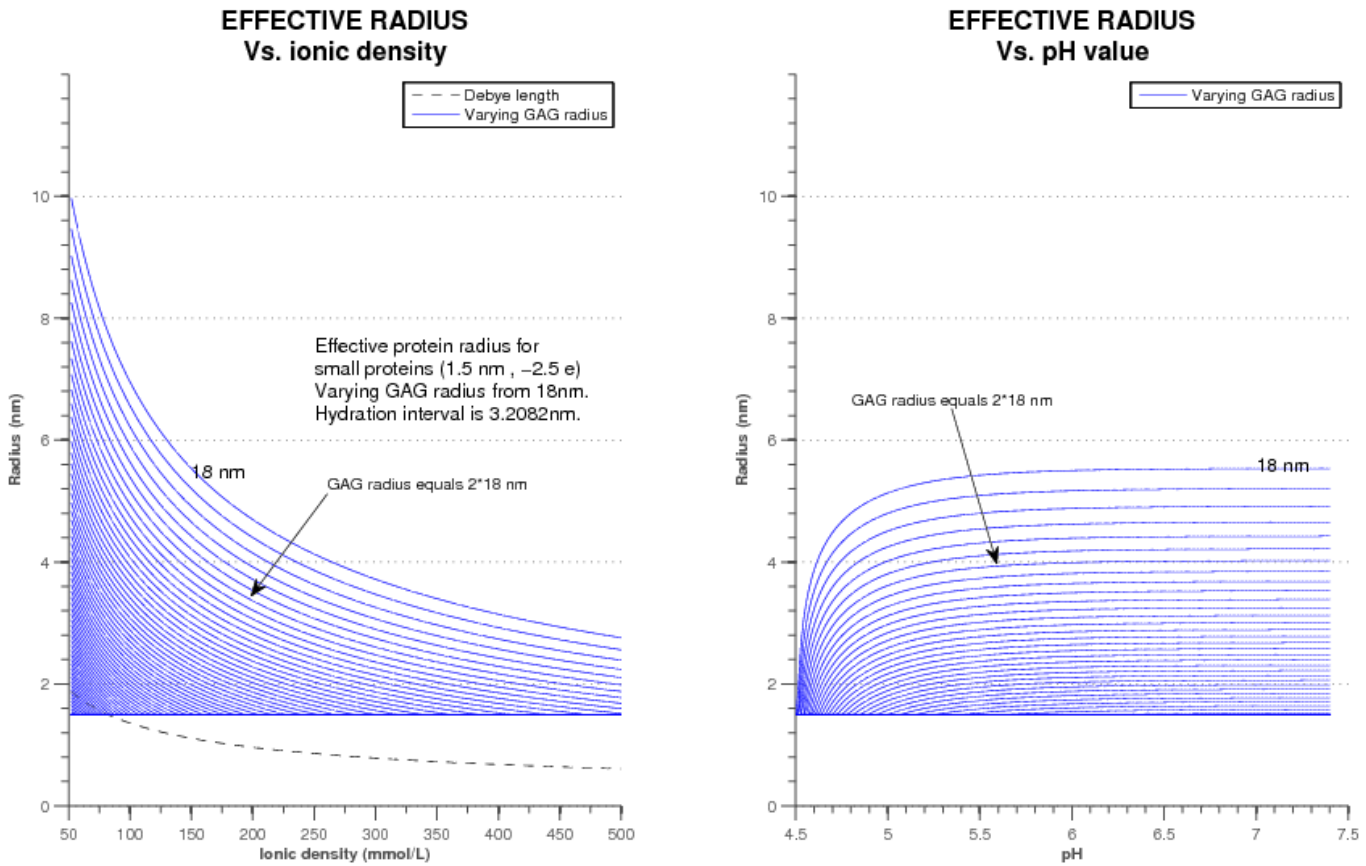

Figure 7.10: The electrostatic exclusion effect is studied for small ($a_1 = 1.5$ nm), weakly charged ($q_1 = -2.5e$) test particles. The effective radius $a_{1,eff}$ is computed for varying ionic density in the left plot, and for varying pH in the right plot. The Debye length Λ_d varies with the ionic density, seen in the left plot. In addition, in both plots the effective radius is computed for several different GAG radii.

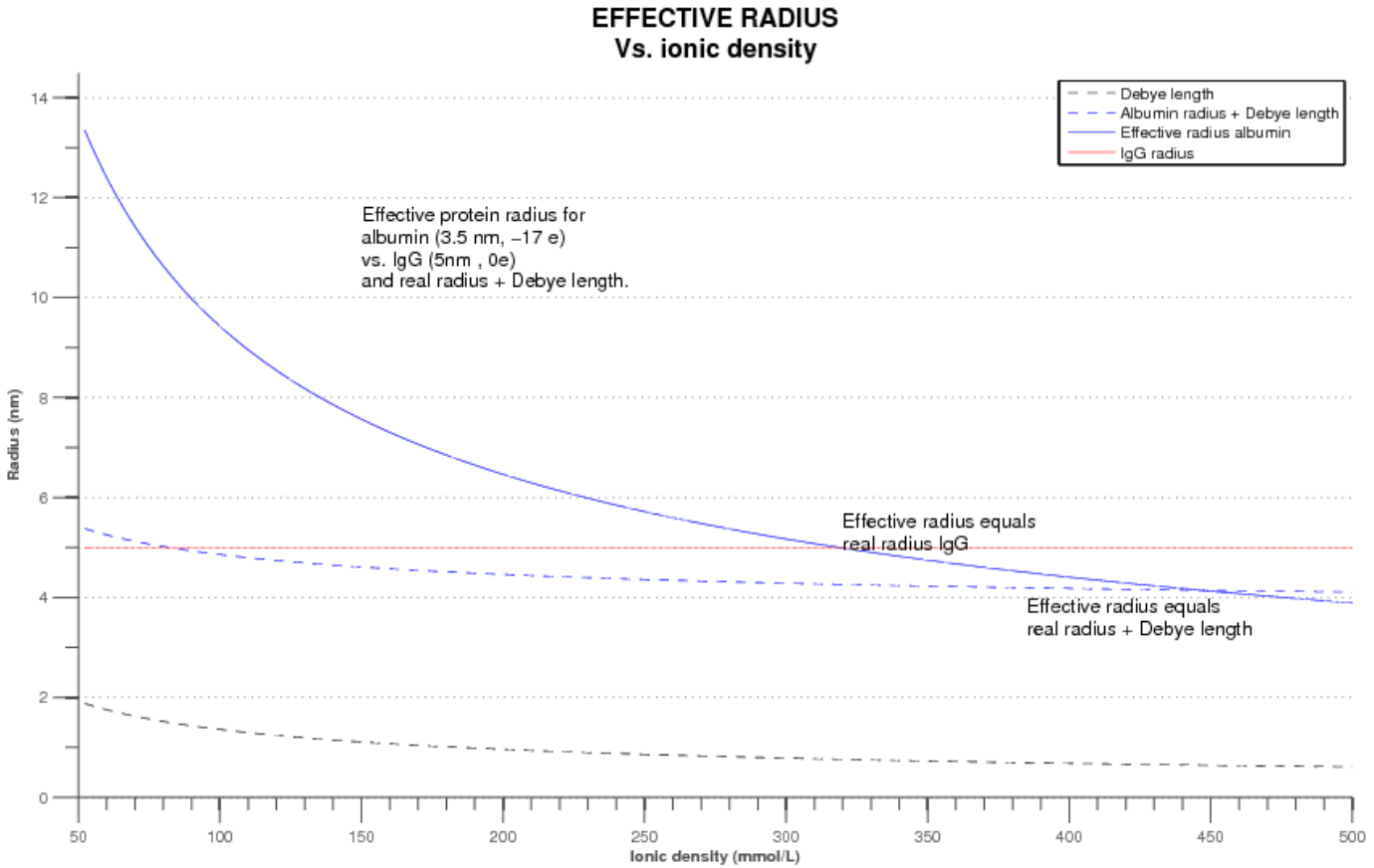

Figure 7.11: The electrostatic exclusion effect is studied for albumin-like test particle ($a_1 = 3.5$ nm, $q_1 = -17e$). The effective radius $a_{1,eff}$ is computed for varying ionic density. The radius of an neutral IgG-like test particle ($a_1 = 5$ nm, $q_1 = 0e$) is indicated. In addition, the Debye length is added to the albumin radius $a_1 + \Lambda_d$ and indicated in the plot.

Following observations are made:

Effective radius $a_{1,eff}$ increases with protein charge:
When a test particle is charged it is excluded from an additional volume surrounding the GAG sphere. This is observed in both Figure 7.8 and 7.9. Strongly charged test particles have a larger effective radius than weakly charged test particles. However, the difference between weakly and moderately charged test particles are larger than the difference between moderate and strongly charged test particles.

Increased ionic density → Decreased effective radius:
We clearly observe in all four plots that as the ionic density increases, the effective radius for charged test particles decreases. For large test particles we observe in Figure 7.9 that when the ionic density is sufficiently high, the effective radius equals the real radius, which implies that the electrostatic effect vanishes.

Effective radius not sensitive to pH-changes:
We observe in all four plots that as the pH drops from physiological pH, i.e. 7.4, there are no significant variations in effective radius until the pH reaches around 5.5. Our model for how the total GAG charge relates to the pH value (7.6) might not be entirely correct. However, it is realistic to believe that the relation may be similar to our model. As briefly mentioned in the remark, it is possible that GAGs are fully charged at lower pH values than 7.4. This would give an even steeper curve than in our plots. Thus, these results might imply that the exclusion effect is not affected by pH variations around physiological pH.

Electrostatic exclusion is less dominant for larger proteins:
The protein size was neglected in the derivation of our model Equation (7.2). Therefore, as long as there is an additional electrostatic exclusion, this exclusion is equal for test particles with equal charge. However, larger test particles will have a larger *steric* exclusion, and it follows that the relative excluded volume due to the particle charge is smaller for large test particles. In Figure 7.9 we observe that for certain values of ionic density or pH, large test particles are not repelled due to their charge (flat curves), i.e. the electrostatic exclusion effect vanishes. Due to their size they are hindered to come close enough to the GAG for the electrostatic exclusion effect to apply.

Hydrated GAG decreases the effective radius:
We observe in Figure 7.10 that as the GAG radius increases the effective radius $a_{1,eff}$ decreases. Outside the GAG sphere proteins experience the electric field as if all GAG charge was placed in the center of the GAG. An increased GAG radius gives a weaker electrostatic field outside the GAG, and thus, the distance of closest approach d_{ca}, and hence the effective radius, decreases. We observe that if the GAG radius is sufficiently large, the electrostatic exclusion effect vanishes.

Protein radius + Debye length = not sufficient!:

An increased ionic density implies a decreased Debye length, i.e. a greater shielding of the GAG charges. The Debye length Λ_d is indicated in the left plots of all the Figures. One might think that adding the Debye length to the protein radius is sufficient to account for the electrostatic exclusion. We observe in the left plot of Figure 7.8 that the effective radius follows the Debye length approach for varying ionic densities, however, is in general larger. In addition the effective radius varies with the protein charge. Thus, this may indicate that adding the Debye length to the real radius, to account for electrostatic exclusion, is not sufficient. A more thorough evaluation might be needed.

Albumin vs. IgG:

There is obtained experimental data on exclusion effects on albumin in the article by Wiig et al. [1] (and in other articles, see references within). In this article it is also observed that the exclusion effect for neutral IgG coincides with that of albumin [5]. In view of these findings we have calculated the effective radius for an albumin-like test particle in Figure 7.11. We observe that around normal values for ionic strength ($150\,\frac{\text{mmol}}{\text{L}}$) the effective radius of albumin is larger than the real radius of IgG. Since this result is relevant only for protein exclusion due to GAGs and not collagenes, we can not conclude that our estimation coincides with experimental findings.
We also observe that adding the Debye length to the albumin radius might not be sufficient to account for electrostatic exclusion.

[5] Both albumin and IgG (Immunoglobulin G) are proteins which occur naturally in the body.

Remarks

In our model we have considered a charged protein moving in the electrostatic field governed by a charged GAG, where the GAG charge is shielded by ions in the surrounding fluid. Therefore, the GAG is referred to as a dressed source sphere, as described in Chapter 6. We have not, however, taken into account a similar effect to the protein. The protein charge might be surrounded by a similar polarization cloud as the GAG. The effect of dressed proteins has not been studied in this thesis, however, such a study might result in a correction of the distance of closest approach d_{ca}, and hence the effective protein radius. It is likely to assume that a correction, due to a dressed protein effect, will give a reduction in the effective radius. GAGs are assumed to be almost immobilized in the interstitium while proteins move more freely, and the attendant polarization cloud to a protein might be affected by the protein motion. Thus, it is difficult to answer how relevant the dressed protein effect is.

We may account for the electrostatic exclusion effect on a microscopic level in the set of solute equations derived in Chapter 4, and hence in the compartment model derived in Chapter 5. The protein size d_1 appear in the solute equations through the collision frequencies obtained in Chapter 3. In this chapter we have shown that negatively charged proteins may interact with the GAGs as if they have a larger effective radius. Therefore, a correction in the protein-matrix collision frequency $\nu_{1\to 2}$ is needed. However, the collagen molecules, which are the main contributor to the interstitial matrix, are net neutral molecules. This might imply that additional refinements are needed in our set of equations from Chapter 4.

In Chapter 8 this set of solute equations is expanded to account for solute interactions with the GAG molecules specifically. Thus, the electrostatic exclusion might be accounted for by replacing the protein size d_1, in the protein-GAG collision frequency, with the effective radius $2 \cdot a_{1,eff}$. Such corrections may be evaluated, however, has not been a part of the present thesis.

Chapter 8

Extended Fluid- and Compartment Model

The compartment model obtained in Chapter 5 was derived without considering the electrostatic properties of the interstitial system. In this chapter we will introduce additional information into the Model (5.17), based on the electrostatic properties of the interstitium. We need to expand the set of Equations (4.27) derived in Chapter 4. Additional equations is needed to account for both charged components in the interstitial matrix, and also anions and cations in the interstitial fluid. We follow the expansions up to compartment level in an attempt to see where and how electrostatic properties influence the compartment model.

8.1 Expansion of the system equations

In the following section we will expand the set of Equations (4.27) step by step, to obtain a set of equations which also account for electrostatic effects. This set of equations apply for a system of fixed macromolecules 2, solute 1 and background solvent s.

8.1.1 Charged components of the matrix

The first expansion is straight forward. We will account for the charged components of the interstitial matrix by simply add parameters d_3 and n_3 where ever d_2 and n_2 appear in the equations. This correspond to a splitting of the macromolecules into one charged component 3 and one uncharged component 2. The two Equations of motion in (4.27) then reads

$$\begin{aligned}\rho_1\left[\frac{\partial \mathbf{U}_1}{\partial t}+\mathbf{U}_1\cdot\nabla\mathbf{U}_1\right] &= n_1\mathbf{F}_1-\nabla\cdot\left(1+\frac{2\pi}{3}d_1^3n_1\chi_{11}\right)\mathbf{P}_1-\sum_{j=2}^{3}\nu_{1j,c}\rho_1\mathbf{U}_1\\ &\quad-\sum_{j=2}^{3}\frac{2\pi}{3}\left(\frac{d_1+d_j}{2}\right)^3\nabla(n_1\kappa T n_j\chi_{1j})-\rho_1\nu_{1s,c}(\mathbf{U}_1-\mathbf{U}_s)\quad ,\end{aligned} \tag{8.1}$$

$$\rho_s\left[\frac{\partial \mathbf{U}_s}{\partial t} + \mathbf{U}_s \cdot \nabla \mathbf{U}_s\right] = n_s\mathbf{F}_s - \nabla p_s + \nabla \cdot \mu\left[\nabla \mathbf{U}_s + (\nabla \mathbf{U}_s)^T - \frac{2}{3}\nabla \cdot \mathbf{U}_s\mathbf{I}\right] - \rho_s\nu_{s1,c}(\mathbf{U}_s - \mathbf{U}_1) - \sum_{j=2}^{3}\rho_s\nu_{sj,c}\mathbf{U}_s \quad . \tag{8.2}$$

8.1.2 Cations and anions

The interstitial fluid contains small charged solutes, i.e. ions, which we already have discussed in Chapter 6 and 7. We will include equations for (monovalent) anions and cations. The equations are deduced in a similar manner as for the solute (1-particles) in Chapter 4. The subscript i refers to ions.

Assumptions

In the same manner as we did for the solute in Chapter 4, we must account for interactions between ions and other components in the fluid.

1. other ions, i-particles

The collisions i-particles do with other i-particles is accounted for. The dense ii-effects will be neglected since the ions are small, almost point-like particles, and d_i is assumed neglegible.

2. structural matrix components, 2- and 3-particles

The ions interact with the fixed components of the matrix. This gives rise to an expanded pressure term in the equation of motion, and furthermore, $i2$- and $i3$ friction terms.

3. background solvent, s-particles

Interactions between ions and background solvent s is assumed to give rise to a is friction drag term in the equation of motion. In addition, this term must be added to the equation of motion for the solvent in accordance with Newton's third law of motion.

4. solute, 1-particles

It is assumed that 1-particles may have a charge q_1. However, we neglect interactions between 1-particles and ions on a collisional level, and assume that interactions take place only when 1-particles are charged. In that case the interactions are considered to be via the electric field.

In accordance with Chapter 6 the electric field $\mathbf{E}$ is given by

$$\nabla \cdot \mathbf{E}(\mathbf{r}, t) = \frac{1}{\epsilon_0\kappa_d}\left(\sum_{i=an,cat} q_i n_i(\mathbf{r}, t) + q_1 n_1(\mathbf{r}, t) + q_3 n_3(\mathbf{r}, t)\right) \quad , \tag{8.3}$$

where n_i are the ionic densities, n_1 and n_3 are the density of 1-particles and charged matrix components respectively, and q_i, q_1 and q_3 are the respective molecular charges. The equation also include the permittivity in vacuum, ϵ_0, and the dielectric constant, κ_d.

Expanded set of equations

For the ions we then have a continuity equation and an equation of motion, for both anions and cations, giving four new equations. The equation of motion for the solvent and 1-particles are modified in accordance with the above assumptions. The expanded set of equations is found to be

$$
\begin{aligned}
&\frac{\partial \rho_1}{\partial t} + \nabla \cdot (\rho_1 \mathbf{U}_1) = 0 \quad , \\
&\rho_1 \left[\frac{\partial \mathbf{U}_1}{\partial t} + \mathbf{U}_1 \cdot \nabla \mathbf{U}_1 \right] = n_1 \mathbf{F}_1 + n_1 q_1 \mathbf{E} - \nabla \cdot \left(1 + \frac{2\pi}{3} d_1^3 n_1 \chi_{11} \right) \mathbf{P}_1 - \sum_{j=2}^{3} \nu_{1j} \rho_1 \mathbf{U}_1 \\
&\qquad - \sum_{j=2}^{3} \frac{2\pi}{3} \left(\frac{d_1 + d_j}{2} \right)^3 \nabla (n_1 \kappa T n_j \chi_{1j}) - \rho_1 \nu_{1s} (\mathbf{U}_1 - \mathbf{U}_s) \quad , \\
&\frac{\partial \rho_s}{\partial t} + \nabla \cdot (\rho_s \mathbf{U}_s) = 0 \quad , \\
&\rho_s \left[\frac{\partial \mathbf{U}_s}{\partial t} + \mathbf{U}_s \cdot \nabla \mathbf{U}_s \right] = n_s \mathbf{F}_s - \nabla p_s + \nabla \cdot \mu \left[\nabla \mathbf{U}_s + (\nabla \mathbf{U}_s)^T - \frac{2}{3} \nabla \cdot \mathbf{U}_s \mathbf{I} \right] \\
&\qquad - \rho_s \nu_{s1} (\mathbf{U}_s - \mathbf{U}_1) - \sum_i \rho_s \nu_{si} (\mathbf{U}_s - \mathbf{U}_i) - \sum_{j=2}^{3} \rho_s \nu_{sj} \mathbf{U}_s \quad , \\
&\frac{\partial \rho_i}{\partial t} + \nabla \cdot (\rho_i \mathbf{U}_i) = 0 \qquad , \qquad i = an, cat \quad , \\
&\rho_i \left[\frac{\partial \mathbf{U}_i}{\partial t} + \mathbf{U}_i \cdot \nabla \mathbf{U}_i \right] = n_i \mathbf{F}_i + n_i q_i \mathbf{E} - \nabla \cdot \mathbf{P}_i - \sum_{j=2}^{3} \nu_{ij} \rho_i \mathbf{U}_i \\
&\qquad - \sum_{j=2}^{3} \frac{2\pi}{3} \left(\frac{d_j}{2} \right)^3 \nabla (n_i \kappa T n_j \chi_{ij}) - \rho_i \nu_{is} (\mathbf{U}_i - \mathbf{U}_s) \qquad , \qquad i = an, cat \quad ,
\end{aligned}
\tag{8.4}
$$

In the above equation, $\mathbf{F}_i$ is now any force additional to $q_i \mathbf{E}$. The electric field $\mathbf{E}$ is given by Equation (8.3).

8.2 Expansion of the compartment model

We will now expand the compartment model derived in Chapter 5. The set of equations derived in the previous section is used for this purpose.

8.2.1 Model adaptation

We keep the compartment structure from the compartment model in Chapter 5. However, the new set of equations makes us able to account for electrostatic properties in the fluid system on both a microscopic and a macroscopic level. The fluid composition is expanded to also include ions and charged components of the matrix, see Figure 8.1.

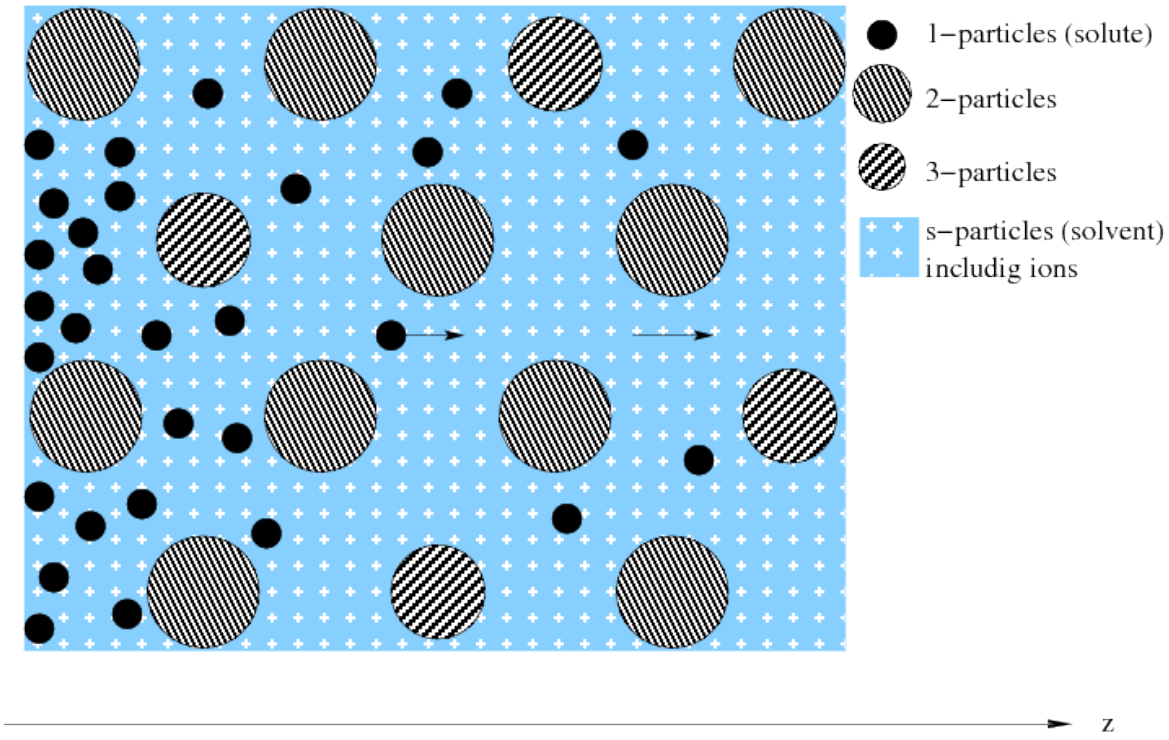

Figure 8.1: The interstitial compartment is composed of fixed macromolecules (lightly shaded), moving macromolecules or solute (black) and a solvent (light blue), as in Chapter 5. The composition is further expanded to also include charged fixed macromolecules (shaded) and small charged solutes (not indicated in the figure). The large solute interacts with both the solvent, small charged solutes and the fixed macromolecules, which account for the interstitial matrix. z = flow direction.

8.2.2 Membrane fluxes

We will not go into detail in the evaluation of the new fluxes, since this was done thoroughly in Chapter 5. However, additional assumptions regarding the electrostatic properties are needed before the fluxes can be evaluated.

- External forces additional to $q\mathbf{E}$ are absent.
- Fixed negative charges uniformly distributed in the capillary wall may give rise to a macroscopic electric field
- Electric field is directed in the z-direction
- No x- and y-dependency in the electric field
- $\mathbf{E} = -\nabla\phi$

The dominating external forces of the system is assumed to be electrostatic forces, possibly due to fixed charges in the capillary wall. This assumption is inspired by work done by Deen et al. [3]. In this article Deen et al. studied fixed charges in the capillary membrane in kidneys, and how they affected fluid filtration through the membrane.

The above assumptions imply an electric field to take the form

$$\mathbf{E} = -\frac{d}{dz}\phi\mathbf{e}_z \quad .$$

The resulting fluxes are

$$\begin{aligned}
J_s &= -K\left[\frac{d}{dz}\left(P - \sigma_1\Pi_1 - \sum_i \sigma_i\Pi_i\right) + R\frac{d\phi}{dz}\right] \quad , \\
J_1 &= \frac{1}{m_1}\frac{1}{\sum_{j=2}^{3}\nu_{1j} + \nu_{1s}} n_1 q_1 \frac{d\phi}{dz} - \frac{1}{m_1}\frac{1}{\sum_{j=2}^{3}\nu_{1j} + \nu_{1s}}\kappa T\frac{d}{dz}(X_1 n_1) \\
&\quad + n_1\frac{\nu_{1s}}{\sum_{j=2}^{3}\nu_{1j} + \nu_{1s}} J_s \quad , \\
J_i &= \frac{1}{m_i}\frac{1}{\sum_{j=2}^{3}\nu_{ij} + \nu_{is}} n_i q_i \frac{d\phi}{dz} - \frac{1}{m_i}\frac{1}{\sum_{j=2}^{3}\nu_{ij} + \nu_{is}}\kappa T\frac{d}{dz}(X_i n_i) \\
&\quad + n_i\frac{\nu_{is}}{\sum_{j=2}^{3}\nu_{ij} + \nu_{is}} J_s \qquad , \qquad i = an, cat \quad ,
\end{aligned}$$

where we have

$$
\begin{aligned}
K &= \frac{1}{\left(1 - \frac{\nu_{s1}}{\sum_{j=2}^{3}\nu_{sj}+\sum_i \nu_{si}+\nu_{s1}} \cdot \frac{\nu_{1s}}{\sum_{j=2}^{3}\nu_{1j}+\nu_{1s}} - \sum_i \frac{\nu_{s1}}{\sum_{j=2}^{3}\nu_{sj}+\sum_i \nu_{si}+\nu_{s1}} \cdot \frac{\nu_{is}}{\sum_{j=2}^{3}\nu_{ij}+\nu_{is}}\right)} \\
&\quad \frac{1}{\rho_s}\frac{1}{\sum_{j=2}^{3}\nu_{sj} + \sum_i \nu_{si} + \nu_{s1}} \quad , \\
\sigma_1 &= \frac{\sum_{j=2}^{3}\nu_{1j}}{\sum_{j=2}^{3}\nu_{1j} + \nu_{1s}} \quad , \\
\sigma_i &= \frac{\sum_{j=2}^{3}\nu_{ij}}{\sum_{j=2}^{3}\nu_{ij} + \nu_{is}} \qquad , \qquad i = an, cat \quad , \\
R &= (1-\sigma_1)n_1 q_1 + \sum_i (1-\sigma_i) n_i q_i \quad , \\
X_1 &= 1 + \frac{2\pi}{3} d_1^3 n_1 \chi_{11} + \sum_{j=2}^{3} \frac{2\pi}{3}\left(\frac{d_1+d_j}{2}\right)^3 n_j \chi_{1j} \quad , \\
X_i &= 1 + \sum_{j=2}^{3} \frac{2\pi}{3}\left(\frac{d_j}{2}\right)^3 n_j \chi_{ij} \quad , \\
\Pi_1 &= \kappa T X_1 n_1 \quad , \\
\Pi_i &= \kappa T X_i n_i \qquad , \qquad i = an, cat \quad , \\
P &= p_s + \Pi_1 + \sum_i \Pi_i \quad .
\end{aligned}
$$

The parameter K is a *local filtration coefficient*. The collision frequencies ν_{1j} and ν_{ij}, which appear in K, are given in accordance with (3.4) in Chapter 3. Additional 'collision frequencies' appearing in K represent the magnitude of a friction force, described in Chapter 4 Section 4.5. ρ_s is the mass density for the solvent.

The parameters σ_1 and σ_i are *reflection coefficients*, and R is an *electrostatic reflection coefficient*. The number densities n_1 and n_i, and the molecular charges q_1 and q_i, all appear in R.

The steric factors X_i for ions correspond to the steric factor X_1 for the solute, which was described in Chapter 5. They are functions of molecular sizes and number densities.

The pressures Π_1 and Π_i are the partial pressures of the solute and ion components respectively, and are osmotic like pressures. κ is the Boltzmann constant and T is the temperature. The pressure P is the sum of all the partial pressures, i.e. the total pressure of the fluid as a whole.

When evaluating the fluxes through the pores we apply the same assumptions as we did in Chapter 5. This imply again that all parameters which include properties of the interstitial matrix, i.e. 2- and 3-parameters, is modified to *pore wall parameters*. Furthermore, we assume a linear drop in the electric potential over the capillary membrane, i.e. $\frac{d\phi}{dz} \approx \frac{1}{l}\Delta\phi$, where l is the membrane thickness.

8.2.3 An expanded compartment Model

A complete expanded compartment model can then be presented.

$$
\begin{aligned}
\frac{d}{dt}V &= K'_{cap,m}\Big[\Delta_{cap,m}P - \sigma_{1,cap,m}\kappa T\Delta_{cap,m}(X_1 n_1) \\
&\quad - \sum_i \sigma_{i,cap,m}\kappa T\Delta_{cap,m}(X_i n_i) + R_{cap,m}\Delta_{cap,m}\phi\Big] \\
&\quad - K'_{ly,m}\Delta_{ly,m}P \quad , \\
\frac{d}{dt}M_1 &= \left(\frac{1}{\nu_{1pw}+\nu_{1s}}\frac{S}{l}\right)_{cap,m}\Big[q_1\overline{n}_{1,cap,m}\Delta_{cap,m}\phi + \kappa T\Delta_{cap,m}(X_1 n_1)\Big] \\
&\quad + m_1\overline{n}_{1,cap,m}(1-\sigma_{1,cap,m})(J_{sz}S)_{in} - m_1\overline{n}_{1,ly,m}(J_sS)_{out} \quad , \\
\frac{d}{dt}M_i &= \left(\frac{1}{\nu_{ipw}+\nu_{is}}\frac{S}{l}\right)_{cap,m}\Big[q_i\overline{n}_{i,cap,m}\Delta_{cap,m}\phi + \kappa T\Delta_{cap,m}(X_i n_i)\Big] \\
&\quad + m_i\overline{n}_{i,cap,m}(1-\sigma_{i,cap,m})(J_{sz}S)_{in} - m_i\overline{n}_{i,ly,m}(J_sS)_{out} \qquad , \qquad i = an, cat \\
m_1 n_{1,int} &= \frac{M_1}{V} \\
m_i n_{i,int} &= \frac{M_i}{V} \qquad , \qquad i = an, cat \\
P_{int} &= F(V) \quad ,
\end{aligned}
\tag{8.5}
$$

for the following 8 unknowns.

$n_{1,int}$			Interstitial solute density
$n_{i,int}$	,	$i = an, cat$	Interstitial ionic density
P_{int}			Interstitial hydrostatic pressure
$M_{1,int}$			Total interstitial solute content
$M_{i,int}$	,	$i = an, cat$	Total interstitial ionic content
V_{int}			Total interstitial fluid volume

The parameter $K'_m = \left(\frac{KS}{l}\right)_m$ is a filtration coefficient for the membrane, where S is the total membrane surface and l is the membrane thickness. The operator Δ_m is the difference operator over the membrane, e.g. $\Delta_{cap,m}P = P_{cap} - P_{int}$ and $\Delta_{ly,m}P = P_{int} - P_{ly}$.

Remark

If fixed charges in the capillary membrane restrict the transport of one type of ions relative to the other, or if one type of ions in any other way is favored relative to the other, this would cause an imbalance in the ionic densities, and hence an ambipolar electric field is governed over the membrane. The ambipolar field will counteract the imbalance in such a way that there are no net transport of ionic charge through the membrane. This effect is called ambipolar diffusion, and is described e.g. in [18]. Thus, if we neglect the transport of charged solutes, this implies that we have

$$J_{an} = J_{cat} \quad .$$

The two compartment equations for the ions may then be used to provide one common compartment equation and one equation for the electrostatic potential differences over the membrane $\Delta\phi$. The potential difference found is then the sum of the potential due to the fixed charges and the ambipolar field. In the Appendix A.6 there is given an example on how to derive a potential difference over a capillary membrane due to fixed charges in the membrane.

Chapter 9

Conclusion and Further Work

9.1 Conclusions

The origin for this thesis was the paper by Wiig et al. [1]. This paper is a study of exclusion phenomena in the interstitium, with emphasis on charge effects. It was quickly established that mathematical modeling of the system could be of good use, and hopefully gain additional information to the study.

The combination of microscopic and macroscopic effects in the problem lead to an approach of solute equations as the governing equations for the system. The complexity of the system became obvious after starting the work on deriving these solute equations. It was decided that, in stead of a detailed study, we should make a general modeling approach and aim to obtain an overall view of different effects which might come into force. In this thesis we have thus obtained a general platform for studying transport of solutes through the interstitium. Throughout the process it has been necessary to make several simplifying assumptions, in order to proceed. It has been possible, and indeed tempting, to dive into specific problem areas throughout the process.

Due to the interdisciplinary nature of the problem, we saw it as our task to present our work in such a way that it may come in useful within areas of research other than Applied Mathematics. Thus, a lot of time and effort has been put into the construction of the thesis, and the presentation of the different subjects which are treated.

The compartment model obtained in this thesis is based on solute equations derived from a microscopic level, and it thus contains microscopic information. Effects on a microscopic level may therefore be followed on a compartment level.

The electrostatic model study performed in this thesis, provides useful observations regarding electrostatic exclusion phenomena. One might think that the electrostatic exclusion effects may be accounted for by adding the Debye length Λ_d to the protein radius. The Debye length has thus been regarded an important parameter. Our study suggests that an evaluation of the distance of closest approach d_{ca}, and hence the effective radius, for

each protein might be necessary for a more accurate approach. For relevant ionic densities and pH, the d_{ca} found in our study, and hence the effective radius $a_{1,eff}$, is of the same size order as the protein radius and the Debye length $a_1 + \Lambda_d$. Allthough other interaction effects may come into force simultaneously, the difference between the two approaches is significant and may be possible to study in experiments.

9.2 Further works

Dressed protein: In our electrostatic model in Chapter 7, a possible shielding effect on the protein is not taken into account. This might affect the distance of closest approach d_{ca}, and hence the effective radius. It is likely that such an effect, if relevant in size, would lead to a decrease in the effective protein radius.

Effect of ions and polarization inside GAG: In the derivation of the electrostatic potential, to be used in the electrostatic model, several simplifying assumptions are made. Inside the source sphere (GAG) the polarization effect (dielectric constant κ_d) is assumed equal to the surrounding fluid. In addition the effect of small ions inside the GAG sphere is neglected. Both simplifications may be further studied.

Macroscopic electrostatic model: Our electrostatic model study may provide an estimation of the effective protein radius, and it might be used to calculate the excluded volume due to glycosaminoglycans. In physiological experiments the total excluded volume is measured, i.e. excluded volume due to both collagenes and GAGs. Thus, a macroscopic model, based on our electrostatic model, that estimates the total excluded volume might be derived.

Macromolecular crowding: In the paper by Wiig et al. [1] it is found that the relative charge contribution to the excluded volume, decreases as the tissue is dehydrated. Thus, effects of overlapping domains of the electrostatic field might come into force. In our model this has not been accounted for.

In Chapter 3 dense gas corrections due to shielding were added to the collision frequency. When the density in a gas increases, particle collisions are increasingly shielded (interrupted) by other particles. The shielding may be interpreted as a loss of efficiency in the collisional transfer at each encounter. This might affect the electrostatic interaction between charged particles, and hence the electrostatic exclusion effect. In addition, since our solute equations contain collision frequencies for interactions between solute and matrix molecules, and since dehydration, or macromolecular crowding of the interstitium, might be represented by an increased density of matrix molecules in our model, it follows that the shielding effect is an interesting property for further studies.

The polarization effect mentioned above may also be further studied in light of macromolecular crowding. There might be a decrease of the polarization effect during dehydration of the tissue. As described in Chapter 6 this would lead to a decrease in the Debye length, which further implies a reduced electrostatic exclusion.

Refine compartment model → simulations: The compartment model obtained in Chapter 5, and further expanded in Chapter 8, may be applied for numerical simulations of interstitial flow. The model is based on several simplifications, which might be refined.

Pore flow/Membrane transport: Our set of solute and solvent equations governing the interstitial flow is assumed to also apply for pore flow through the membranes. This was simply done by removing all terms due to matrix interactions, and add similar term due to pore wall interactions. This process should have been studied more thoroughly.

Expand Starling model to Plasma Leak model: Our compartment model was derived in accordance with the Starling model from the paper by Bert et al. [2]. In this paper there are presented two models; the Starling model and the Plasma Leak model. Whereas the Plasma Leak model accounts for flux variations along the capillary membrane, and thus is a more complex model, these variations are neglected in the Starling model. The Plasma Leak model was found to provide more accurate simulation predictions. Thus, our set of equations may be used to derive a similar compartment model.

Ambipolar field: In Chapter 8 a macroscopic electrostatic field due to fixed charges in the capillary membrane was included in the compartment model. This work was inspired by a paper by Deen et al. [3] on solute transport through a charged capillary membrane in kidneys. A charged capillary membrane might favor the transport of one polarity of small charged solutes (ions), and thus lead to an imbalance in the ionic concentrations. As the imbalance increases an ambipolar field is build up across the capillary membrane, which will affect the transport of charged solutes in such a way that the imbalance is evened out. This was only briefly mentioned in Chapter 8, and should be studied in more details.

Appendix A

A.1 First and second order velocity moments of the Boltzmann equation

Equation of motion - first order moment

First order velocity moment of the Boltzmann equation is obtained multiplying the velocity $\mathbf{v}$ into the equation and integrate over the velocity space. We integrate the Boltzmann Equation (4.6) term by term.

$$\int \mathbf{v}\frac{\partial f}{\partial t}\,\mathrm{d}\mathbf{v} = \frac{\partial}{\partial t}\int \mathbf{v}f\,\mathrm{d}\mathbf{v} = \frac{\partial}{\partial t}(n\mathbf{U}) \quad , \tag{A.1}$$

$$\begin{aligned}\int \mathbf{v}\left(\mathbf{v}\cdot\frac{\partial f}{\partial \mathbf{r}}\right)\mathrm{d}\mathbf{v} &= \int \mathbf{v}\frac{\partial}{\partial \mathbf{r}}\cdot(\mathbf{v}f)\,\mathrm{d}\mathbf{v} = \frac{\partial}{\partial \mathbf{r}}\cdot\int \mathbf{v}\mathbf{v}f\,\mathrm{d}\mathbf{v} \\ &= \frac{\partial}{\partial \mathbf{r}}\cdot\int\Big[(\mathbf{v}-\mathbf{U})(\mathbf{v}-\mathbf{U}) + \mathbf{v}\mathbf{U} + \mathbf{U}\mathbf{v} - \mathbf{U}\mathbf{U}\Big]f\,\mathrm{d}\mathbf{v} \\ &= \frac{\partial}{\partial \mathbf{r}}\cdot\Big[\frac{1}{m}\mathbf{P} + n\mathbf{U}\mathbf{U} + n\mathbf{U}\mathbf{U} - n\mathbf{U}\mathbf{U}\Big] = \frac{1}{m}\nabla\cdot\mathbf{P} + \nabla\cdot(n\mathbf{U}\mathbf{U}) \quad ,\end{aligned} \tag{A.2}$$

$$\begin{aligned}\int \mathbf{v}\left(\frac{\mathbf{F}}{m}\cdot\frac{\partial f}{\partial \mathbf{v}}\right)\mathrm{d}\mathbf{v} &= \int v_j\left(\frac{F_i}{m}\frac{\partial f}{\partial v_i}\right)\mathrm{d}\mathbf{v}\mathbf{e}_j = \frac{F_i}{m}\int v_j\left(\frac{\partial f}{\partial v_i}\right)\mathrm{d}\mathbf{v}\mathbf{e}_j \\ &= \frac{F_i}{m}\delta_{ij}n\mathbf{e}_j = -\frac{1}{m}n\mathbf{F} \quad ,\end{aligned} \tag{A.3}$$

$$\int \mathbf{v}\nu_c(f_M - f)\,\mathrm{d}\mathbf{v} = \nu_c\int \mathbf{v}(f_M - f)\,\mathrm{d}\mathbf{v} = \nu_c(n\mathbf{U} - n\mathbf{U}) = 0 \quad , \tag{A.4}$$

where ∇ is the spatial del operator and δ_{ij} is the Kronecker delta, see Section A.5. In the force term computation (A.3) we have applied integration by parts.

Temperature equation - second order moment

We now multiply $(\mathbf{v}-\mathbf{U})^2$ into the Boltzmann Equation (4.6) and perform the velocity integration. This corresponds to the trace of the tensor $(\mathbf{v}-\mathbf{U})(\mathbf{v}-\mathbf{U})$, and thus is the trace of the second order moment. We integrate the Boltzmann Equation (4.6) term by term.

$$\begin{aligned}
&\int (\mathbf{v}-\mathbf{U})^2 \frac{\partial f}{\partial t}\,\mathrm{d}\mathbf{v} = \frac{\partial}{\partial t}\int (\mathbf{v}-\mathbf{U})^2 f\,\mathrm{d}\mathbf{v} + 2\int f(\mathbf{v}-\mathbf{U})\cdot\frac{\partial \mathbf{U}}{\partial t}\,\mathrm{d}\mathbf{v} \\
&\quad = \frac{\partial}{\partial t}(\frac{1}{m}3n\kappa T) + 2\int f(\mathbf{v}-\mathbf{U})\,\mathrm{d}\mathbf{v}\cdot\frac{\partial \mathbf{U}}{\partial t} = \frac{1}{m}\frac{\partial}{\partial t}(3n\kappa T) \quad , \qquad \text{(A.5)} \\
&\int (\mathbf{v}-\mathbf{U})^2\left(\mathbf{v}\cdot\frac{\partial f}{\partial \mathbf{r}}\right)\mathrm{d}\mathbf{v} = \int (\mathbf{v}-\mathbf{U})^2\frac{\partial}{\partial \mathbf{r}}\cdot\left(\mathbf{v}f\right)\mathrm{d}\mathbf{v} \\
&\quad = \int \frac{\partial}{\partial \mathbf{r}}\cdot\left((\mathbf{v}-\mathbf{U})^2\mathbf{v}f\right)\mathrm{d}\mathbf{v} - \int \frac{\partial}{\partial \mathbf{r}}(\mathbf{v}-\mathbf{U})^2\cdot\mathbf{v}f)\,\mathrm{d}\mathbf{v} \\
&\quad = \frac{\partial}{\partial \mathbf{r}}\cdot\int (\mathbf{v}-\mathbf{U})^2\mathbf{v}f\,\mathrm{d}\mathbf{v} + 2\int \mathbf{v}\cdot\frac{\partial \mathbf{U}}{\partial \mathbf{r}}\cdot(\mathbf{v}-\mathbf{U})f\,\mathrm{d}\mathbf{v} \\
&\quad = \frac{\partial}{\partial \mathbf{r}}\cdot\int (\mathbf{v}-\mathbf{U})^2(\mathbf{v}-\mathbf{U})f\,\mathrm{d}\mathbf{v} + \frac{\partial}{\partial \mathbf{r}}\cdot\int (\mathbf{v}-\mathbf{U})^2\mathbf{U}f\,\mathrm{d}\mathbf{v} \\
&\qquad + 2\int (\mathbf{v}-\mathbf{U})\cdot\frac{\partial \mathbf{U}}{\partial \mathbf{r}}\cdot(\mathbf{v}-\mathbf{U})f\,\mathrm{d}\mathbf{v} + 2\int \mathbf{U}\cdot\frac{\partial \mathbf{U}}{\partial \mathbf{r}}\cdot(\mathbf{v}-\mathbf{U})f\,\mathrm{d}\mathbf{v} \\
&\quad = \nabla\cdot\left(\frac{2}{m}\mathbf{q}\right) + \nabla\cdot\left(\frac{3n\kappa}{m}T\mathbf{U}\right) + \frac{2}{m}\mathbf{P}\colon\nabla\mathbf{U} + \mathbf{U}\cdot\nabla\mathbf{U}(n\mathbf{U}-n\mathbf{U}) \\
&\quad = \frac{2}{m}\nabla\cdot\mathbf{q} + \frac{1}{m}3n\kappa T\nabla\cdot\mathbf{U} + \frac{1}{m}\mathbf{U}\cdot\nabla(3n\kappa T) + \frac{2}{m}\mathbf{P}\colon\nabla\mathbf{U} \quad , \qquad \text{(A.6)} \\
&\int (\mathbf{v}-\mathbf{U})^2\left(\frac{\mathbf{F}}{m}\cdot\frac{\partial f}{\partial \mathbf{v}}\right)\mathrm{d}\mathbf{v} = \int (\mathbf{v}-\mathbf{U})^2\frac{\partial}{\partial \mathbf{v}}\cdot\left(\frac{\mathbf{F}}{m}f\right)\mathrm{d}\mathbf{v} \\
&\quad = \int \frac{\partial}{\partial \mathbf{v}}\cdot\left[(\mathbf{v}-\mathbf{U})^2\frac{\mathbf{F}}{m}f\right]\mathrm{d}\mathbf{v} - 2\int (\mathbf{v}-\mathbf{U})\cdot\frac{\mathbf{F}}{m}f\,\mathrm{d}\mathbf{v} \\
&\quad = \int\limits_{\Sigma_\mathbf{v}} (\mathbf{v}-\mathbf{U})^2\frac{\mathbf{F}}{m}f\cdot\,\mathrm{d}S_\mathbf{v} - 2\int (\mathbf{v}-\mathbf{U})f\,\mathrm{d}\mathbf{v}\cdot\frac{\mathbf{F}}{m} = 0 \quad , \qquad \text{(A.7)} \\
&\int (\mathbf{v}-\mathbf{U})^2\nu_c(f_M - f)\,\mathrm{d}\mathbf{v} = \nu_c\left[\frac{3n\kappa}{m}T - \frac{3n\kappa}{m}T\right] = 0 \quad , \qquad \text{(A.8)}
\end{aligned}$$

where ∇ is the spatial del operator.

A.2 Velocity moments of the Boltzmann equation - corrections for multicomponent fluid and dense gas effects

Multicomponent fluid

The velocity moments of zeroth and first order for the additional term in Boltzmann Equation (4.21) is computed.

$$\int m_i \nu_{ij} (f_{ij,M} - f_i)\,\mathrm{d}\mathbf{v}_i = m_i \nu_{ij} \int (f_{ij,M} - f_i)\,\mathrm{d}\mathbf{v}_i = m_i \nu_{ij}(n_i - n_i) = 0 \quad , \tag{A.9}$$

$$\begin{aligned}\int m_i \mathbf{v}_i \nu_{ij} (f_{ij,M} - f_i)\,\mathrm{d}\mathbf{v}_i &= m_i \nu_{ij} \int \mathbf{v}_i (f_{ij,M} - f_i)\,\mathrm{d}\mathbf{v}_i \\ &= m_i \nu_{ij} \left[\int (\mathbf{v}_i - \mathbf{U}_j) f_{ij,M}\,\mathrm{d}\mathbf{v}_i + \int \mathbf{U}_j f_{ij,M}\,\mathrm{d}\mathbf{v}_i - m_i \nu_{ij} \int \mathbf{v}_i f_i\,\mathrm{d}\mathbf{v}_i \right] \\ &= m_i \nu_{ij}(0 + n_i \mathbf{U}_j - n_i \mathbf{U}_i) = \nu_{ij} \rho_i (\mathbf{U_j} - \mathbf{U_i}) \quad .\end{aligned} \tag{A.10}$$

Dense gas effects

There are included correction terms in the Boltzmann Equation (4.15), first for a one component fluid. Velocity moments of zeroth, first and second order are computed.

$$\begin{aligned}
&\int m\frac{\partial}{\partial \mathbf{r}}\cdot\left[\frac{2\pi}{3}d^3n\chi(\mathbf{U}f_M-\mathbf{v}f)\right]\mathrm{d}\mathbf{v} = m\nabla\cdot\left[\frac{2\pi}{3}d^3n\chi\int \mathbf{U}f_M-\mathbf{v}f\,\mathrm{d}\mathbf{v}\right]\\
&\quad = m\nabla\cdot\left[\frac{2\pi}{3}d^3n\chi(n\mathbf{U}-n\mathbf{U})\right]=0 \quad , \qquad \text{(A.11)}\\
&\int m\mathbf{v}\frac{\partial}{\partial \mathbf{r}}\cdot\left[\frac{2\pi}{3}d^3n\chi(\mathbf{U}f_M-\mathbf{v}f)\right]\mathrm{d}\mathbf{v} = m\nabla\cdot\left[\frac{2\pi}{3}d^3n\chi\int(\mathbf{U}f_M-\mathbf{v}f)\mathbf{v}\,\mathrm{d}\mathbf{v}\right]\\
&\quad = m\nabla\cdot\left[\frac{2\pi}{3}d^3n\chi\Big(\int \mathbf{U}f_M\mathbf{v}\,\mathrm{d}\mathbf{v}-\int(\mathbf{v}-\mathbf{U})(\mathbf{v}-\mathbf{U})f+\mathbf{v}\mathbf{U}f+\mathbf{U}\mathbf{v}f-\mathbf{U}\mathbf{U}f\,\mathrm{d}\mathbf{v}\Big)\right]\\
&\quad = m\nabla\cdot\left[\frac{2\pi}{3}d^3n\chi\Big(n\mathbf{U}\mathbf{U}-(\int \mathbf{v}-\mathbf{U})(\mathbf{v}-\mathbf{U})f\,\mathrm{d}\mathbf{v}+n\mathbf{U}\mathbf{U}+n\mathbf{U}\mathbf{U}-n\mathbf{U}\mathbf{U}\Big)\right]\\
&\quad = -m\nabla\cdot\left[\frac{2\pi}{3}d^3n\chi\int \mathbf{v}-\mathbf{U})(\mathbf{v}-\mathbf{U})f\,\mathrm{d}\mathbf{v}\right]=-\nabla\cdot\left[\frac{2\pi}{3}d^3n\chi\mathbf{P}\right] \quad , \qquad \text{(A.12)}\\
&\int \frac{m}{2}(\mathbf{v}-\mathbf{U})^2\frac{\partial}{\partial \mathbf{r}}\cdot\left[\frac{2\pi}{3}d^3n\chi(\mathbf{U}f_M-\mathbf{v}f)\right]\mathrm{d}\mathbf{v} =\\
&\quad = \nabla\cdot\left[\frac{2\pi}{3}d^3n\chi\int \frac{m}{2}(\mathbf{v}-\mathbf{U})^2(\mathbf{U}f_M-\mathbf{v}f)\,\mathrm{d}\mathbf{v}\right]\\
&\qquad -\int\frac{\partial}{\partial \mathbf{r}}\left(\frac{m}{2}(\mathbf{v}-\mathbf{U})^2\right)\cdot\left[\frac{2\pi}{3}d^3n\chi(\mathbf{U}f_M-\mathbf{v}f)\right]\mathrm{d}\mathbf{v}\\
&\quad = \nabla\cdot\left[\frac{2\pi}{3}d^3n\chi\Big(\int \frac{m}{2}(\mathbf{v}-\mathbf{U})^2\mathbf{U}f_M\,\mathrm{d}\mathbf{v}-\int\frac{m}{2}(\mathbf{v}-\mathbf{U})^2(\mathbf{v}-\mathbf{U})f\,\mathrm{d}\mathbf{v}-\int\frac{m}{2}(\mathbf{v}-\mathbf{U})^2\mathbf{U}f\,\mathrm{d}\mathbf{v}\Big)\right]\\
&\qquad +\int\left(m(\mathbf{v}-\mathbf{U})\cdot\frac{\partial\mathbf{U}}{\partial \mathbf{r}}\right)\cdot\left[\frac{2\pi}{3}d^3n\chi\big(\mathbf{U}f_M-(\mathbf{v}-\mathbf{U}+\mathbf{U})f\big)\right]\mathrm{d}\mathbf{v}\\
&\quad = \nabla\cdot\left[\frac{2\pi}{3}d^3n\chi\Big(\frac{3}{2}n\kappa T\mathbf{U}-\mathbf{q}-\frac{3}{2}n\kappa T\mathbf{U}\Big)\right]\\
&\qquad +\int m\left[\frac{2\pi}{3}d^3n\chi\right]\mathbf{U}(\mathbf{v}-\mathbf{U})\colon\frac{\partial\mathbf{U}}{\partial \mathbf{r}}f_M\,\mathrm{d}\mathbf{v}-\int m\left[\frac{2\pi}{3}d^3n\chi\right](\mathbf{v}-\mathbf{U})(\mathbf{v}-\mathbf{U})\colon\frac{\partial\mathbf{U}}{\partial \mathbf{r}}f\,\mathrm{d}\mathbf{v}\\
&\qquad -\int m\left[\frac{2\pi}{3}d^3n\chi\right]\mathbf{U}(\mathbf{v}-\mathbf{U})\colon\frac{\partial\mathbf{U}}{\partial \mathbf{r}}f\,\mathrm{d}\mathbf{v}\\
&\quad = -\nabla\cdot\left(\frac{2\pi}{3}d^3n\chi\mathbf{q}\right)-\frac{2\pi}{3}d^3n\chi\mathbf{P}\colon\nabla\mathbf{U} \quad . \qquad \text{(A.13)}
\end{aligned}$$

Additional dense gas correction term for multicomponent fluid:

$$\begin{aligned}
&\int m_i \frac{\partial}{\partial \mathbf{r}} \cdot \left[\frac{2\pi}{3} \left(\frac{d_i + d_j}{2} \right)^3 n_j \chi_{ij} \mathbf{v}_i f_{ij,M} \right] \mathrm{d}\mathbf{v}_i = m_i \nabla \cdot \left[\frac{2\pi}{3} \left(\frac{d_i + d_j}{2} \right)^3 n_j \chi_{ij} \int \mathbf{v}_i f_{ij,M} \, \mathrm{d}\mathbf{v}_i \right] \\
&\quad = m_i \nabla \cdot \left[\frac{2\pi}{3} \left(\frac{d_i + d_j}{2} \right)^3 n_j \chi_{ij} \left(\int (\mathbf{v}_i - \mathbf{U}_j) f_{ij,M} \, \mathrm{d}\mathbf{v}_i + \int \mathbf{U}_j f_{ij,M} \, \mathrm{d}\mathbf{v}_i \right) \right] \\
&\quad = m_i \nabla \cdot \left[\frac{2\pi}{3} \left(\frac{d_i + d_j}{2} \right)^3 n_j \chi_{ij} \left(0 + n_i \mathbf{U}_j \right) \right] \\
&\quad = m_i \frac{2\pi}{3} \left(\frac{d_i + d_j}{2} \right)^3 \nabla \cdot \left[n_j \chi_{ij} n_i \mathbf{U}_j \right] = 0 \quad , \qquad \text{(A.14)}
\end{aligned}$$

given that $\mathbf{U}_j = 0$.

$$\begin{aligned}
&\int m_i \mathbf{v}_i \frac{\partial}{\partial \mathbf{r}} \cdot \left[\frac{2\pi}{3} \left(\frac{d_i + d_j}{2} \right)^3 n_j \chi_{ij} \mathbf{v}_i f_{ij,M} \right] \mathrm{d}\mathbf{v}_i \\
&\quad = m_i \nabla \cdot \left[\frac{2\pi}{3} \left(\frac{d_i + d_j}{2} \right)^3 n_j \chi_{ij} \int \mathbf{v}_i \mathbf{v}_i f_{ij,M} \, \mathrm{d}\mathbf{v}_i \right] \\
&\quad = m_i \nabla \cdot \left[\frac{2\pi}{3} \left(\frac{d_i + d_j}{2} \right)^3 n_j \chi_{ij} \int \left((\mathbf{v}_i - \mathbf{U}_j)(\mathbf{v}_i - \mathbf{U}_j) + \mathbf{v}_i \mathbf{U}_j + \mathbf{U}_j \mathbf{v}_i - \mathbf{U}_j \mathbf{U}_j \right) f_{ij,M} \, \mathrm{d}\mathbf{v}_i \right] \\
&\quad = m_i \nabla \cdot \left[\frac{2\pi}{3} \left(\frac{d_i + d_j}{2} \right)^3 n_j \chi_{ij} \left(\frac{1}{m_i} 3 n_i \kappa T \mathbf{I} + n_i \mathbf{U}_j \mathbf{U}_j + n_i \mathbf{U}_j \mathbf{U}_j - n_i \mathbf{U}_j \mathbf{U}_j \right) \right] \\
&\quad = \nabla \cdot \left[\frac{2\pi}{3} \left(\frac{d_i + d_j}{2} \right)^3 n_j \chi_{ij} 3 n_i \kappa T \mathbf{I} + n_i \mathbf{U}_j \mathbf{U}_j \right) \Big] \\
&\quad = -\frac{2\pi}{3} \left(\frac{d_i + d_j}{2} \right)^3 \nabla (n_i \kappa T n_j \chi_{ij}) \quad , \qquad \text{(A.15)}
\end{aligned}$$

given that $\mathbf{U}_j = 0$.

A.3 Derivation of the Boltzmann distribution from equation of motion

An equation of motion for ions was deduced in Chapter 8. If we consider a system of ions and solvent, i.e. no hindrance particles, and if we neglect all outer forces acting on the ions other than the electric force, the equation of motion reduces to

$$\rho_i \left[\frac{\partial \mathbf{U_i}}{\partial t} + \mathbf{U_i} \cdot \nabla \mathbf{U_i} \right] = n_i q_i \mathbf{E} - \nabla \cdot \mathbf{P_i} - \nu_{ij,c} \rho_i (\mathbf{U_i} - \mathbf{U_s}) \quad , \quad i = an, cat \quad .$$

The subscript i refers to either anions or cations. When the fluid is in local thermodynamic equilibrium one assumes that the dominating forces are the pressure force and the electric force, and that the dominating part of the pressure tensor $\mathbf{P_i}$ is $n_i \kappa T \mathbf{I}$, i.e. thermal pressure [13]. If we in addition assume that the acceleration term on the left is small and negligible we are left with a force balance

$$\kappa T \nabla n_i = -n_i q_i \nabla \phi \quad ,$$

where we have made use of $\mathbf{E} = -\nabla \phi$, shown in Chapter 6. The equation is a simple first order DE with solution

$$n_i = n_{i,0} e^{-\frac{q_i}{\kappa T} \phi} \quad , \quad i = an, cat \quad , \tag{A.16}$$

where $n_{i,0}$ is taken to be the ionic density where $\phi = 0$. The above expression is known as the *Boltzmann distribution*, and it relates the ionic density to the electric potential.

A.4 Electrostatic potential - spherical shell model

The solutions for an electric potential surrounding a charged spherical shell on separate domains are found to be

$$\phi(r) = \begin{cases} C_1 & \text{for } r < a \\ -\dfrac{1}{6\epsilon_0\kappa_d}\rho_{f,shell}r^2 + \dfrac{C_2}{r} + C_3 & \text{for } a < r < a+\delta \\ C_4\dfrac{1}{r}e^{-\Lambda_d^{-1}r} & \text{for } r \gg a+\delta \end{cases} , \tag{A.17}$$

$$r^2\frac{d\phi}{dr} = \begin{cases} 0 & \text{for } r < a \\ -\dfrac{1}{3\epsilon_0\kappa_d}\rho_{f,shell}r^3 - C_2 & \text{for } a < r < a+\delta \\ -C_4(1+r\Lambda_d^{-1})e^{-\Lambda_d^{-1}r} & \text{for } r \gg a+\delta \end{cases} . \tag{A.18}$$

The solutions is matched to second order at the two interfaces $r = a$ and $r = a + \delta$.

1. $r^2\dfrac{d\phi}{dr}$ continuous at $r = a$:

$$\lim_{r\to a^-} r^2\frac{d\phi}{dr} = \lim_{r\to a^+} r^2\frac{d\phi}{dr} \quad \Rightarrow$$
$$C_2 = -\frac{1}{3\epsilon_0\kappa_d}\rho_{f,shell}a^3 \quad .$$

2. ϕ continuous in $r = a$:

$$\lim_{r\to a^-} \phi(r) = \lim_{r\to a^+} \phi(r) \quad \Rightarrow$$
$$C_1 = -\frac{1}{2\epsilon_0\kappa_d}\rho_{f,shell}a^2 + C_3 \quad .$$

3. $r^2\dfrac{d\phi}{dr}$ is streched inwards to match in $r = a + \delta$:

$$\lim_{r\to(a+\delta)^-} r^2\frac{d\phi}{dr} = \lim_{r\to(a+\delta)^+} r^2\frac{d\phi}{dr} \quad \Rightarrow$$
$$-\frac{1}{3\epsilon_0\kappa_d}\rho_{f,shell}(a+\delta)^3 - C_2 = -C_4(1+(a+\delta)\Lambda_d^{-1})e^{-\Lambda_d^{-1}(a+\delta)} \quad \Rightarrow$$
$$C_4 = \frac{1}{3\epsilon_0\kappa_d}\rho_{f,shell}\left((a+\delta)^3 - a^3\right)\frac{1}{1+(a+\delta)\Lambda_d^{-1}}e^{\Lambda_d^{-1}(a+\delta)} \quad .$$

4. ϕ is streched inwards to match in $r = a + \delta$:

$$\begin{aligned}
&\lim_{r\to(a+\delta)^-}\phi(r) = \lim_{r\to(a+\delta)^+}\phi(r) \quad \Rightarrow \\
&-\frac{1}{6\epsilon_0\kappa_d}\rho_{f,shell}(a+\delta)^2 + \frac{C_2}{a+\delta} + C_3 = \lim_{r\to a+\delta^+} C_4\frac{1}{a+\delta}e^{-\Lambda_d^{-1}(a+\delta)} \quad \Rightarrow \\
&C_3 = \frac{1}{6\epsilon_0\kappa_d}\rho_{f,shell}\frac{1}{a+\delta}\left((a+\delta)^3 + 2a^3 + \frac{2((a+\delta)^3 - a^3)}{1+(a+\delta)\Lambda_d^{-1}}\right) \quad , \\
&C_1 = \frac{1}{6\epsilon_0\kappa_d}\rho_{f,shell}\left[\frac{1}{a+\delta}\left((a+\delta)^3 + 2a^3 + \frac{2((a+\delta)^3 - a^3)}{1+(a+\delta)\Lambda_d^{-1}}\right) - 3a^2\right] \quad .
\end{aligned}$$

The coefficients goes into the expression (A.17) and we obtain

$$\phi(r) = \begin{cases}
\frac{1}{6\epsilon_0\kappa_d}\rho_{f,shell}\left[\frac{1}{a+\delta}\left((a+\delta)^3 + 2a^3 + \frac{2((a+\delta)^3 - a^3)}{1+(a+\delta)\Lambda_d^{-1}}\right) - 3a^2\right] & \text{for } r < a \\
\frac{1}{6\epsilon_0\kappa_d}\rho_{f,shell}\left[\frac{1}{a+\delta}\left((a+\delta)^3 + 2a^3 + \frac{2((a+\delta)^3 - a^3)}{1+(a+\delta)\Lambda_d^{-1}}\right) - \frac{1}{r}(r^3 + 2a^3)\right] & \text{for } a < r < a+\delta \\
\frac{1}{3\epsilon_0\kappa_d}\rho_{f,shell}\left((a+\delta)^3 - a^3\right)\frac{1}{1+(a+\delta)\Lambda_d^{-1}}\frac{1}{r}e^{-\Lambda_d^{-1}(r-(a+\delta))} & \text{for } r > a+\delta
\end{cases} \quad . \tag{A.19}$$

We now expand the obtained expressions in terms of powers of δ. We make use of the following relations:

$$\begin{aligned}
&\frac{1}{a+\delta} \sim \frac{1}{a}\left[1 - \frac{\delta}{a} + \mathcal{O}(\delta^2)\right] \quad , \\
&\frac{1}{(a+\delta)^2} \sim \frac{1}{a^2}\left[1 - 2\frac{\delta}{a} + \mathcal{O}(\delta^2)\right] \quad , \\
&\frac{1}{1+(a+\delta)\Lambda_d^{-1}} \sim \frac{1}{1+a\Lambda_d^{-1}}\left[1 - \frac{\delta\Lambda_d^{-1}}{1+a\Lambda_d^{-1}} + \mathcal{O}(\delta^2)\right] \quad , \\
&e^{\Lambda_d^{-1}(r-(a+\delta))} \sim e^{\Lambda_d^{-1}(r-a)}\left[1 - \Lambda_d^{-1}\delta + \mathcal{O}(\delta^2)\right] \quad .
\end{aligned}$$

We also make use of a change in the coordinates for $a < r < a + \delta$. We set $r = a + \delta x$ where $0 < x < 1$. This result in the following expansion for ϕ

$$\phi(r) = \begin{cases}
\frac{1}{\epsilon_0\kappa_d}\rho_{f,shell}\delta a\frac{1}{1+a\Lambda_d^{-1}} + \mathcal{O}(\delta^2) & \text{for } r < a \\
\frac{1}{\epsilon_0\kappa_d}\rho_{f,shell}\delta a\frac{1}{1+a\Lambda_d^{-1}} + \mathcal{O}(\delta^2) & \text{for } 0 < x < 1 \quad (a < r < a+\delta) \\
\frac{1}{\epsilon_0\kappa_d}\rho_{f,shell}\delta a\frac{1}{1+a\Lambda_d^{-1}}\frac{a}{r}e^{-\Lambda_d^{-1}(r-a)} + \mathcal{O}(\delta^2) & \text{for } r \geq a+\delta
\end{cases} \quad , \tag{A.20}$$

which is discontinuous to first order. However, the above expression may be a good approximation for the electric potential for small δ.

The free charge for the entire domain is a stepfunction of r, i.e.

$$\rho_f = \begin{cases}
0 & \text{for } r < a \\
\rho_{f,shell} & \text{for } a < r < a+\delta \\
0 & \text{for } r \geq a+\delta
\end{cases} \quad .$$

Thus, to conserve the total charge of the GAG we must require that

$$\lim_{\delta \to 0}(\delta \rho_{f,shell}) = \sigma_{f,surf} \quad , \tag{A.21}$$

where $\sigma_{f,surf}$ is the surface charge density. If we now let $\delta \to 0$ we are left with

$$\phi(r) = \begin{cases} \dfrac{1}{\epsilon_0 \kappa_d} \sigma_{f,surf} a \dfrac{1}{1 + a\Lambda_d^{-1}} & \text{for } r < a \\ \dfrac{1}{\epsilon_0 \kappa_d} \sigma_{f,surf} a \dfrac{1}{1 + a\Lambda_d^{-1}} \dfrac{a}{r} e^{-\Lambda_d^{-1}(r-a)} & \text{for } r \geq a \end{cases} \quad , \tag{A.22}$$

which may approximate the electric potential surrounding charged spherical shells, whenever the shell is sufficiently thin, i.e. δ is sufficiently small.

This derivation has been done in an attempt to explain the 'nonphysical' behaviour of the electric field due to placing all the charge at the surface of a GAG.

A.5 Kronecker Delta

The Kronecker Delta is defined as [19]

$$\delta_{ij} = \begin{cases} 1 & \text{if } i = j \\ 0 & \text{if } i \neq j \end{cases} \quad . \tag{A.23}$$

A.6 Electrostatic potential for a cylindrical geometry - potential difference

In Chapter 6 various solutions for the electric potential is obtained in a spherical geometry. In this section a solution is obtained for a cylindrical geometry. The derivation is similar as in previous attempts, however, the governing equation changes in cylindrical coordinates. Since the derivation have been described thoroughly in Chapter 6, we will omit details in the following derivation.

We consider a charged cylinder where the charge is uniformly distributed in a cylindrical shell outside the cylinder. See Figure A.1. The charged cylinder is placed in the same fluid

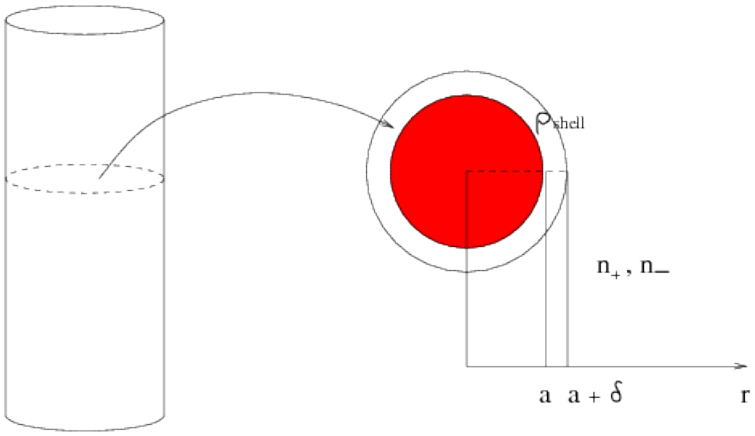

Figure A.1: The charged cylindrical shell of thickness δ is surrounded by water and small ions. The free charge of the system changes for $r = a$ and $r = a + \delta$ and the potential must be found on the three domains separately. Inside the cylinder, $0 \leq r < a$, there are no free charges. In the cylindrical shell, $a < r < a + \delta$, free charge is uniformly distributed $\rho_{f,shell}$. Outside the source shell, $r > a + \delta$, the free charge is given by the density of anions n_- and cations n_+ times the unit charge e.

as in previous attempts, water and ions. With the Laplace operator written in cylindrical coordinates, the governing equation for the three different domains are given as

$$\begin{cases} \frac{1}{r}\frac{d}{dr}\left(r\frac{d}{dr}\phi\right) = 0 & \text{for } r < a \\ \frac{1}{r}\frac{d}{dr}\left(r\frac{d}{dr}\phi\right) = -\frac{1}{\epsilon_0\kappa_d}\rho_{f,shell} & \text{for } a < r < a + \delta \\ \frac{1}{r}\frac{d}{dr}\left(r\frac{d}{dr}\phi\right) = \frac{1}{\Lambda_d^2}\phi & \text{for } r \gg a + \delta \end{cases} . \tag{A.24}$$

It is a straight forward procedure to solve the equation on the two internal domains, $r < a$ and $a \leq r \leq a + \delta$. However, it is not straight forward to obtain a solution on the external

domain, $r > a+\delta$. Here the solution can be written as a linear combination of two modified Bessel functions. Often cylindrical geometries generate this type of solutions, and they are therefore also known as cylinder functions. To sum up we have

$$\phi(r) = \begin{cases} C_1 \ln r + C_2 & \text{for } r < a \\ -\dfrac{1}{4\epsilon_0\kappa_d}\rho_{f,shell} r^2 + C_3 \ln r + C_4 & \text{for } a < r < a+\delta \\ C_5 \mathrm{BesselI}_0(\dfrac{1}{\Lambda_d} r) + C_6 \mathrm{BesselK}_0(\dfrac{1}{\Lambda_d} r) & \text{for } r \gg a+\delta \end{cases} \quad . \tag{A.25}$$

The nature of the Bessel functions can briefly be described as one having a singularity at the origin (BesselK) and one having a singularity at infinity (BesselI). We use the same boundary and matching conditions as for spherical coordinates. Therefore, to avoid the potential to diverge for large r we must require that C_5 is zero. To avoid the potential to diverge at the origin we must in the same manner require that C_1 is zero.

To be able to match the solution at the two boundaries $r = a$ and $r = a+\delta$ we approximate the BesselK function by its first order asymptotic expansion, valid for arguments less than 1, i.e. $r \gg \Lambda_d$:

$$\mathrm{BesselK}_0 \sim \frac{1}{2}\sqrt{2\pi}\sqrt{\frac{\Lambda_d}{r}} e^{-\Lambda_d^{-1} r} + \mathcal{O}(\frac{1}{r^{\frac{3}{2}}} e^{-r}) \quad . \tag{A.26}$$

After completion of the four matching conditions we are left with

$$\phi(r) = \begin{cases} \dfrac{1}{4\epsilon_0\kappa_d}\rho_{f,shell}\left[2\dfrac{\Lambda_d}{a+\delta}\Big((a+\delta)^2 - a^2\Big) + (a+\delta)^2 - a^2 - 2a^2\Big(\ln(a+\delta) - \ln a\Big)\right] & \text{for } r < a \\ \dfrac{1}{4\epsilon_0\kappa_d}\rho_{f,shell}\left[2\dfrac{\Lambda_d}{a+\delta}\Big((a+\delta)^2 - a^2\Big) + (a+\delta)^2 - r^2 - 2a^2\Big(\ln(a+\delta) - \ln r\Big)\right] & \text{for } a < r < a+\delta \\ \dfrac{1}{4\epsilon_0\kappa_d}\rho_{f,shell}\left[2\dfrac{\Lambda_d}{\sqrt{r(a+\delta)}}\Big((a+\delta)^2 - a^2\Big)\right] e^{-\Lambda_d^{-1}(r-(a+\delta))} & \text{for } r > a+\delta \end{cases} \quad , \tag{A.27}$$

which is valid if $a + \delta \gg \Lambda_d$.

It follows that the potential difference over a cylindrical shell of thickness δ is

$$\Delta\phi = \phi(a+\delta) - \phi(a) = -\frac{1}{4\epsilon_0\kappa_d}\rho_{f,shell}\left[(a+\delta)^2 - a^2 - 2a^2\Big(\ln(a+\delta) - \ln a\Big)\right] \quad . \tag{A.28}$$

Appendix B

Nomenclature

Symbol	Description
ν	Collision frequency
$\mathbf{v}$	Particle velocity
d	Diameter
n	number density
V	Volume
χ	Steric factor (microscopic level)
f	Distribution function
f_M	Maxwell distribution
$\mathbf{F}$	Forces
m	Particle mass
ρ	Mass density
$\mathbf{U}$	Velocity field
$\mathbf{P}$	Pressure tensor
p	Scalar pressure
T	Temperature
κ	Boltzmann's constant
$\mathbf{q}$	Heat flux vector
μ	Viscosity
S	Surface
M	Mass
J	Flux
X	Steric factor (macroscopic level)
P	Hydrostatic pressure
Π	Osmotic pressure
K	Local filtration coefficient
σ	Reflection coefficient
K'	Filtration coefficient
l	length

$\mathbf{D}$	Displacement field
ρ_f	Free charge density
$\mathbf{E}$	Electric field
Q, q	Charge
ϵ_0	Permittivity in vacuum
κ_d	Dielectric constant
ϕ	Electrostatic potential
e	Elementary charge
a	radius of a sphere
Λ_d	Debye length
δ	Shell thickness
σ	Surface charge density
V_p	Potential energy
E_k	Kinetic energy
d_{ca}	Distance of closest approach
N_A	Avogrado's number
R	Electrostatic reflection coefficient

Subscripts

Symbol	Description
1	1-particles
2	2-particles
3	3-particles
s	s-particles (solvent)
$+, cat$	cation
$-, an$	anion
vol	volume
$surf$	surface
$shell$	spherical shell
$1 \rightarrow 2, 12$	1- to 2-particle (collisions)
pw	Pore wall
int	Interstitium
cap	Capillary
ly	Lymph
AV	Available
E	Excluded
0	Reference value
eff	Effective

Bibliography

[1] Helge Wiig, Christina Gyenge, Per Ole Iversen, Donald Gullberg, and Olav Tenstad. The Role of the Extracellular Matrix in Tissue Distribution of Macromolecules in Normal and Pathological Tissue: Potential Therapeutic Consequences. *Microcirculation*, 15(4):283–296, 2008.

[2] Joel L. Bert, Bruce D. Bowen, and Rolf K. Reed. Microvascular Exchange and Interstitial Volume Regulation in the Rat: Model Validation. *Am. J. Physiology*, 254:H384–H399, 1988.

[3] William M. Deen, Behrooz Satvat, and James M. Jamieson. Theoretical Model for Glomerular Filtration of Charged Solutes. *Am J. Physiology*, 238:F126–F139, 1980.

[4] K. Aukland and R. K. Reed. Interstitial-Lymphatic Mechanisms in the Control of Extracellular Fluid Volume. *Physiological Reviews*, 73(1):1–78, 1993.

[5] D. L. Nelson and M. M. Cox. *Lehninger Principles of Biochemistry, 5th ed.* W.H. Freeman and Co, New York, 2006. ISBN 0-321-27000-2.

[6] Wayne D. Comper and Torvard C. Laurent. Physiological Function of Connective Tissue Polysaccharides. *Physiological Reviews*, 58(1):255–315, 1978.

[7] Harris J. Granger, Glen A. Laine, George E. Barnes, and Ruth E. Lewis. Dynamics and Control of Transmicrovascular Fluid Exchange. *In: Edema (Staub, N. C., Taylor, A. E., Eds.), Raven Press*, pages 189–228, 1984.

[8] S. Chapman and T. G. Cowling. *The Mathematical Theory of Non-Uniform Gases, 3rd ed.* Cambridge University Press, 1970. Library of Congress Catalog Card Number 70-77285.

[9] G. Schmidt. *Physics of high temperature plasmas, 2nd ed.* Academic Press, 1979. ISBN 0-12-626660-3.

[10] D. Kincaid and W. Cheney. *Numerical Analysis. Mathematics of Scientific Computing, 3rd ed.* Brooks/Cole, 2002. ISBN 0-534-38905-8.

[11] S. Succi. *The Lattice Boltzmann Equation for Fluid Dynamics and Beyond.* Clarendon Press, Oxford, 2001. ISBN 0-19-850398-9.

[12] P. L. Bhatnagar, E. P. Gross, and M. Krook. A Model for Collision Processes in Gases. I. Small Amplitude Processes in Charged and Neutral One-Component Systems. *Physical Review*, 94(3):511–525, 1954.

[13] J. L. Delcroix. *Plasma Physics*. John Wiley & Sons Ltd, 1965. Library of Congress Catalog Card Number 65-16997.

[14] Li-Shi Luo. Unified Theory of the Lattice Boltzmann Models for Nonideal Gases. *Physical Review Letters*, 81(8):1618–1621, 1998.

[15] D. C. Montgomery and D. A. Tidman. *Plasma Kinetic Theory*. McGraw-Hill Book Company, 1964. Library of Congress Catalog Card Number 63-23536 42851.

[16] J. Cross. *Electrostatics: Principles, Problems and Applications*. Adam Hilger, 1987. ISBN 0-85274-589-3.

[17] G. L. Pollack and D. R. Stump. *Electromagnetism*. Addison Wesley, 2002. ISBN 0-8053-8567-3.

[18] B. S. Tanenbaum. *Plasma Physics*. McGraw-Hill Book Company, 1967. Library of Congress Catalog Card Number 67-22971 62812.

[19] P. K. Kundu and I. M. Cohen. *Fluid Mechanics, 3rd ed.* Elsevier Academic Press, 2004. ISBN-10: 0-12-178253-0.